

ตัวรับประเภทโทอาคราวันอีเทอร์และอิมิดาโซเดียมเป็นเซ็นเซอร์สำหรับแคตไอออนและแอนไอออน



นางสาว ศรกฤษณ์ มาบำรุง

สถาบันวิทยบริการ

จุฬาลงกรณ์มหาวิทยาลัย

วิทยานิพนธ์นี้เป็นส่วนหนึ่งของการศึกษาตามหลักสูตรปริญญาวิทยาศาสตรมหาบัณฑิต

สาขาวิชาเคมี ภาควิชาเคมี

คณะวิทยาศาสตร์ จุฬาลงกรณ์มหาวิทยาลัย

ปีการศึกษา 2549

ลิขสิทธิ์ของจุฬาลงกรณ์มหาวิทยาลัย

**THIACROWNETHER AND IMIDAZOLIUM RECEPTOR AS SENSOR FOR CATIONS
AND ANIONS**



Miss Sornkrit Marbumrung

สถาบันวิทยบริการ
A Thesis Submitted in Partial Fulfillment of the Requirements
for the Degree of Master of Science Program in Chemistry

Department of Chemistry

Faculty of Science

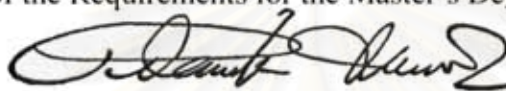
Chulalongkorn University

Academic Year 2006

Copyright of Chulalongkorn University

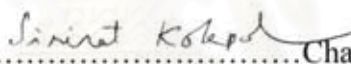
Thesis Title THIAACROWNETHER AND IMIDAZOLIUM
RECEPTOR AS SENSOR FOR CATIONS AND
ANIONS
By Miss Sornkrit Marbumrung
Field of Study Chemistry
Thesis Advisor Assistant Professor Boosayarat Tomapatanaget, Ph.D.
Thesis Co-Advisor Associate Professor Thawatchai Tuntulani, Ph.D.

Accepted by the Faculty of Science, Chulalongkorn University in Partial
Fulfillment of the Requirements for the Master's Degree




.....Dean of the Faculty of Science
(Professor Piamsak Menasveta, Ph.D.)

Thesis Committee



.....Chairman
(Associate Professor Sirirat Kokpol, Ph.D.)



.....Thesis Advisor
(Assistant Professor Boosayarat Tomapatanaget, Ph.D.)



.....Thesis Co-Advisor
(Associate Professor Thawatchai Tuntulani, Ph.D.)



.....Member
(Associate Professor Orawon Chailapakul, Ph.D.)



.....Member
(Assistant Professor Soamwadee Chaianansutcharit, Ph.D.)

ศรกฤษณ์ มาบำรุง: ตัวรับประบาทไทอาคราวน์อีเทอร์และอิมิดาโซเลียมเป็นเซ็นเซอร์สำหรับแคตไอออนและแอนไอออน (THIACROWNETHER AND IMIDAZOLIUM RECEPTOR AS SENSOR FOR CATIONS AND ANIONS) อ. ที่ปรึกษา :ผศ.ดร. บุษยรัตน์ ธรรมพัฒน์กิจ; อ.ที่ปรึกษาร่วม: รศ.ดร. ธวัชชัย ต้นทุลานี; 89 หน้า.

ได้สังเคราะห์พอลิเอธิลีนไกลคอลที่มีอิมิดาโซเลียมและเอไมด์เป็นองค์ประกอบ จากนั้นทำการศึกษาสมบัติการเกิดสารประกอบเชิงซ้อนของลิแกนด์ L กับไอออนชนิดต่างๆ ด้วยเทคนิคทางสเปกโตรสโกปี ได้แก่ โปรตอนนิวเคลียร์แมกเนติกเรโซแนนซ์ (เอ็นเอ็มอาร์) ยูวีวิสลิเบิล และฟลูออเรสเซนซ์ โดยพบว่าเกิดสารประกอบเชิงซ้อนในอัตราส่วน 1:1 และให้ค่าการดูดกลืนแสงสูงสุดที่ 346 นาโนเมตร ผลของแอนไอออนจะทำให้เกิดการเลื่อนของค่าการดูดกลืนแสงสูงสุดไปที่ความยาวคลื่นต่ำลง และลิแกนด์ให้ค่าสเปกตรัมการเปล่งแสงสูงสุดที่ 532 นาโนเมตร โดยทั้งแอนไอออนและแคตไอออนส่งผลให้ความเข้มของสเปกตรัมการคายแสงลดลง ซึ่งการหาค่าคงที่ของสารประกอบเชิงซ้อนทำโดยวิธีการไทเทรตด้วยเทคนิคฟลูออริเมตริกพบว่า ความสามารถในการเกิดสารประกอบเชิงซ้อนกับแอนไอออนเป็นดังนี้ อะซีเตต > ฟลูออไรด์ > ไดไฮโดรเจนฟอสเฟต และในกรณีของแคตไอออน (โลหะแทรนซิชัน) พบว่า ลิแกนด์มีความจำเพาะต่อคอปเปอร์ไอออน นอกจากนี้ได้ทำการศึกษาผลของอะลอสเตอริกของแอนไอออนที่มีผลต่อความสามารถในการจับของลิแกนด์กับโลหะแทรนซิชัน โดยพบว่า เมื่อแอนไอออนจับกับลิแกนด์จะส่งผลให้ความสามารถในการจับกับซิลเวอร์ไอออนของลิแกนด์ดีขึ้น โดยเฉพาะแอนไอออนที่เป็นฟลูออไรด์ และพบว่า แอนไอออนไม่ส่งผลให้การจับของลิแกนด์จับกับคอปเปอร์ดีขึ้น เนื่องจากเกิดไอออนแพร์ระหว่างคอปเปอร์กับแอนไอออน

สถาบันวิทยบริการ จุฬาลงกรณ์มหาวิทยาลัย

ภาควิชา.....เคมี..... ลายมือชื่อนิสิต.....ศรกฤษณ์ มาบำรุง.....
สาขาวิชา.....เคมี..... ลายมือชื่ออาจารย์ที่ปรึกษา.....ผศ.ดร. บุษยรัตน์ ธรรมพัฒน์กิจ.....
ปีการศึกษา.....2549..... ลายมือชื่ออาจารย์ที่ปรึกษาร่วม.....รศ.ดร. ธวัชชัย ต้นทุลานี.....

4772589023 : MAJOR CHEMISTRY.

KEY WORDS: IMIDAZOLE, FLUOROIONOPHORE, DITOPIC RECEPTOR, FLUORIMETRIC TITRATION, QUENCHING

SORNKRIT MARBUMRUNG: THIA-CROWN-ETHER AND IMIDAZOLIUM RECEPTOR AS SENSOR FOR CATIONS AND ANIONS.
 THESIS ADVISOR: ASSIST. PROF. BOOSAYARAT TOMAPATANAGET, Ph.D. THESIS CO-ADVISOR: ASSOC. PROF. THAWATCHAI TUNTULANI, Ph.D. 89 pp.

Acyclic thiacycrown ether derivative containing imidazolium moieties and amide NH protons **L** was synthesized. Complexation studies of ligand **L** with various ions were carried out by ¹H-NMR, UV-Vis, and fluorescent spectroscopy. This receptor also forms 1:1 stoichiometry complexes with anion guest as confirmed by Job's plot. The maximum absorption band of ligand showed at 346 nm and in the presence of various anions, the absorption band shifted hypsochromically. For fluorescence technique, the appearance of the maximum emission band of free ligand showed at 532 nm. Upon the addition of anions, the fluorescent intensity was decreased gradually. The stability constant of ligand **L** measured by fluorimetric titration in acetonitrile displayed the anions binding in order of CH₃CO₂⁻ > F⁻ > H₂PO₄⁻. For cation complexation studies, ligand **L** was found to form a complex with copper ion selectively. Moreover, allosteric studies of transition metal induced anion complexation were carried out by fluorescence technique. Only silver ion showed the positive allosteric effect in term of the enhancement for cation binding properties especially in the presence of F⁻ anion. In contrast, copper ion showed a negative allosteric effect because of ion-pairing.

Department.....Chemistry.....

Field of study...Chemistry.....

Academic year...2006.....

student's signature...*Sornkrit Marbumrung*.....

Advisor's signature...*Boosayarat Tomapatanaget*.....

Co-advisor's signature...*Thawatchai Tuntulani*.....

ACKNOWLEDGEMENTS

The accomplishment of this thesis could not occur without the kindness, personal friendship, encouragement, suggestions, assistance and the extensive supports throughout my master degree career from my thesis advisor, Assist. Prof. Dr. Boosayarat Tomapatanaget. Particular thanks are given to my thesis co-advisor, Assoc. Prof. Dr. Thawatchai Tuntulani for suggestions, assistance and personal friendship. In addition, I would like to thank Assoc. Prof. Dr. Sirirat Kokpol, Assoc. Prof. Dr. Orawon Chailapakul and Assist. Prof. Dr. Soamwadee Chaianansutcharit for their input, interest, valuable suggestions and comments as committee members and thesis examiners.

This thesis would not be successful without kindness and helps of a number of people. First, I am grateful to the Scientific and Technological Research Equipment Center of Chulalongkorn University, particularly, Miss Gamolwan Tumcharean (National Science and Technology Development Agency) for NMR results. I am grateful to Mr. Boontana Wanalerse for elemental analysis data. I would like to express my appreciation to former and the current staffs in the Supramolecular Chemistry Research Unit.

Financial supported by National Science and Technology Development Agency (NSTDA) and the Thailand Research Fund (TRF).

Finally, I would like to express my deepest gratitude to my family for their love, care, kindness, encouragement and other assistance throughout my life.

สถาบันวิทยบริการ
จุฬาลงกรณ์มหาวิทยาลัย

CONTENTS

	Page
Abstract in Thai	iv
Abstract in English	v
Acknowledgements	vi
Contents	vii
List of Abbreviation and Symbols	ix
List of Figures	x
List of Schemes	xiii
List of Tables	xiv
CHAPTER I INTRODUCTION	1
1.1 The important of transition metals and anions.....	1
1.2 Concept of supramolecular chemistry.....	2
1.3 Molecular recognition and molecular receptors.....	3
1.4 Allosteric receptor.....	5
1.5 Anion receptor based on imidazolium groups.....	7
1.6 Chemical sensors (Chemosensors).....	8
1.7 Chromoionophores and fluoroionophores.....	9
1.7.1 Chromoionophores.....	9
1.7.2 Fluoroionophores.....	11
1.8 Design of chromoionophores and fluoroionophores.....	15
1.9 Some characteristics of fluoronoionophores.....	16
1.9.1 Selectivity.....	16
1.10 Objective and the scope of this research.....	17
CHAPTER II EXPERIMENTAL	18
2.1 General procedures.....	18
2.1.1 Analytical instrument.....	18
2.1.2 Materials.....	18
2.2 Synthesis.....	19

	Page
2.2.1 Preparation of tetraethylene glycol ditosylate (1).....	19
2.2.2 Preparation of 1,8-Bis(aminothiophenol) tetraethylene glycol(2)	20
2.2.3 Preparation of 1,8-Bis(2-chloromethylamide) tetraethylene glycol (3).....	21
2.2.4 Preparation of 1,8-Bis(2-methylbenzimidazolium) tetraethylene glycol (4).....	22
2.2.5 Preparation of acyclic thiacycrown ether containing imidazolium and dansyl fluorophore (L).....	23
2.3 Complexation studies of ligand L by ¹ H-NMR titrations.....	24
2.4 Complexation studies of ligand L by UV-Vis titrations.....	26
2.5 Complexation studies of ligand L by fluorescent titrations.....	27
CHAPTER III RESULTS AND DISCUSSION.....	40
3.1 Design concept.....	40
3.2 Synthesis and characterization of acyclic thiacycrown ether derivatives containing imidazolium moieties (L).....	42
3.3 The complexation studies of ligand L.....	46
3.3.1 Anion complexation studies.....	46
3.3.2 Cation complexation studies.....	58
3.3.3 Complexation studies of ligand L in the presence of an anion such as acetate, fluoride and dihydrogen phosphate toward Ag ⁺ and Cu ²⁺	62
CHAPTER IV CONCLUSION.....	72
REFERENCES.....	73
APPENDICES.....	78
VITA.....	89

LIST OF ABBREVIATIONS AND SYMBOLS

A	Absorbance
Ar	Aryl group
°C	Degree Celsius
¹³ C-NMR	Carbon nuclear magnetic resonance
DMF	N, N-dimethylformamide
equiv.	Equivalent
g	Gram
Hz	Hertz
¹ H-NMR	Proton nuclear magnetic resonance
I_F^0	the fluorescence intensity of the solutions containing free ligand L
I_F	the fluorescence intensity of the ligand complexed with guest
<i>J</i>	Coupling constant
mmol	Millimol
mL	Milliliter
M	Molar
M ¹	Per molar
δ	Chemical shift
ppm	Part per million
s, d, t, m	Splitting patterns of ¹ H-NMR (singlet, doublet, triplet, multiplet)
c	complexation

สถาบันวิทยบริการ
จุฬาลงกรณ์มหาวิทยาลัย

LIST OF FIGURES

Figure	Page
1.1 Macrobicyclic ditopic receptor.....	5
1.2 Scheme of metal chelation.....	6
1.3 Allosteric receptor.....	6
1.4 Anion receptor based on imidazolium groups.....	7
1.5 Anion receptor based on imidazolium groups.....	8
1.6 A general concept of chemosensors.....	9
1.7 A chromoionophore which induces blue-shift upon binding with guest	10
1.8 A chromoionophore which induces red-shift upon binding with guest	11
1.9 Principle of PET sensors.....	12
1.10 Example of PET fluorophore.....	13
1.11 Spectral displacements of PCT sensors.....	14
1.12 Principle of cation recognition by fluorescence PCT sensors.....	14
1.13 Example of PCT fluorophore.....	15
3.1 ¹ H-NMR spectrum of L	44
3.2 The mass spectrum of L	45
3.3 The IR spectrum of L	45
3.4 ¹ H-NMR spectra (400 MHz) of L toward various anions.....	47
3.5 Job's plot of the complexation of L $H_2PO_4^-$.....	49
3.6 The absorption and the emission spectra of L in acetonitrile.....	50
3.7 Absorption spectra (9×10^{-5} M) of L toward various anions in acetonitrile.....	51
3.8 The fluorescence spectrum of L (1×10^{-6} M) in acetonitrile upon addition of increasing amounts of $CH_3CO_2^-$ (6.67×10^{-5} M).....	52
3.9 The fluorescence spectrum of L (1×10^{-6} M) in acetonitrile upon addition of increasing amounts of F^- (6.67×10^{-5} M).....	52
3.10 The fluorescence spectrum of L (1×10^{-6} M) in acetonitrile upon addition of increasing amounts of $H_2PO_4^-$ (6.67×10^{-5} M).....	53
3.11 The linear plot between $Y = \{I_F^0 / (I_F - I_F^0)\}$ and $1/[CH_3CO_2^-]$ for the first fluorimetric titration.....	55

Figure	Page
3.12 The linear plot between $Y = \{I_F^0 / (I_F - I_F^0)\}$ and $1/[F^-]$ for the first fluorimetric titration	55
3.13 The linear plot between $Y = \{I_F^0 / (I_F - I_F^0)\}$ and $1/[H_2PO_4^-]$ for the first fluorimetric titration	56
3.14 The propose structure of ligand L induced by anion.....	57
3.15 Absorption spectra (9×10^{-5} M) of L toward various cations in acetonitrile.....	58
3.16 The fluorescence spectrum of L (1×10^{-6} M) in acetonitrile upon addition of increasing amounts of Cu^{2+} (6.67×10^{-5} M).....	59
3.17 The linear plot between $Y = \{I_F^0 / (I_F - I_F^0)\}$ and $1/[Cu^{2+}]$ for the first fluorimetric titration	61
3.18 The propose structure of ligand L induced by transition metal ion	62
3.19 1H -NMR spectra (400 MHz) of $L \cdot CF^-$ with various transition metals in CD_3CN	63
3.20 The fluorescence spectrum of L (1×10^{-6} M) in acetonitrile upon addition of increasing amounts of Ag^+ (6.67×10^{-5} M).....	64
3.21 The fluorescence spectra of $L \cdot CH_3CO_2^-$ (1×10^{-5} M) in acetonitrile upon addition of increasing amounts of cation (a) Ag^+ and (b) Cu^{2+} (6.67×10^{-5} M).....	65
3.22 The fluorescence spectrum of $L \cdot CF^-$ (1×10^{-5} M) in acetonitrile upon addition of increasing amounts of Ag^+ (6.67×10^{-5} M).....	65
3.23 The fluorescence spectra of $L \cdot H_2PO_4^-$ (1×10^{-5} M) in acetonitrile upon addition of increasing amounts of cation (a) Ag^+ and (b) Cu^{2+} (6.67×10^{-5} M).....	66
3.24 The fluorescence spectrum of $L \cdot H_2PO_4^-$ (1×10^{-5} M) in acetonitrile upon addition of increasing amounts of Cu^{2+} (2.67×10^{-4} M).....	67
3.25 The linear plot between $Y = I_F^0 / (I_F - I_F^0)$ and $1/[Ag^+]$ for the first fluorimetric titration of $L \cdot CH_3CO_2^- / Ag^+$	68
3.26 The linear plot between $Y = I_F^0 / (I_F - I_F^0)$ and $1/[Ag^+]$ for the first fluorimetric titration of $L \cdot CF^- / Ag^+$	68

Figure		Page
3.27	The linear plot between $Y = I_F^0 / (I_F - I_F^0)$ and $1/[Ag^+]$ for the first fluorimetric titration of $LCH_2PO_4^-/Ag^+$	69
3.28	The mass spectrum of LCF^-/Ag^+ complexation.....	70
3.29	The propose structure of $LCanion/Ag^+$	71



สถาบันวิทยบริการ
จุฬาลงกรณ์มหาวิทยาลัย

LIST OF SCHEMES

Scheme	Page
3.1 Synthesis pathway of ligand L.....	41



สถาบันวิทยบริการ
จุฬาลงกรณ์มหาวิทยาลัย

LIST OF TABLES

Table	Page
2.1	Amounts of solutions of the anions used to prepare various anion : ligand ratios..... 25
2.2	The concentration of anions that used in anion complexation studies with ligand L and the final ratios of guest:host..... 26
2.3	The concentration of anions that used in anion complexation studies with ligand L and the final ratios of guest:host..... 27
2.4	The concentration of fluoride ion that used in anion complexation studies with ligand L and the final ratios of guest:host..... 28
2.5	The concentration of acetate ion that used in anion complexation studies with ligand L and the final ratios of guest:host..... 29
2.6	The concentration of dihydrogenphosphate ion that used in anion complexation studies with ligand L and the final ratios of guest:host 30
2.7	The concentration of copper ion that used in anion complexation studies with ligand L and the final ratios of guest:host..... 32
2.8	The concentration of silver ion that used in anion complexation studies with ligand L and the final ratios of guest:host..... 33
2.9	The concentration of anions that used in transition metal ion complexation studies with ligand L in the presence of an anion and final ratios of guest:host..... 34
2.10	The concentration of fluoride ion that used in silver ion complexation studies with ligand L in the presence of an anion and final ratios of guest:host..... 35
2.11	The concentration of acetate ion that used in silver ion complexation studies with ligand L in the presence of an anion and final ratios of guest:host..... 36
2.12	The concentration of acetate ion that used in copper ion complexation studies with ligand L in the presence of an anion and final ratios of guest:host..... 37
2.13	The concentration of dihydrogenphosphate ion that used in silver ion complexation studies with ligand L in the presence of an anion and final ratios of guest:host..... 38

Table	Page
2.14 The concentration of dihydrogenphosphate ion that used in copper ion complexation studies with ligand L in the presence of an anion and final ratios of guest:host.....	39
3.1 ¹ H-NMR chemical shift (ppm) for ligand L (in CDCl ₃) in the absence and presence of anions.....	48
3.2 The fluorescence intensity of ligand L upon adding various anions	54
3.3 The stability constants of ligand L towards F ⁻ , H ₂ PO ₄ ⁻ and CH ₃ CO ₂ ⁻	56
3.4 The fluorescence intensity of ligand L upon adding of Cu ²⁺	60
3.5 The stability constants of ligand L towards Ag ⁺	69



สถาบันวิทยบริการ
จุฬาลงกรณ์มหาวิทยาลัย

CHAPTER I

INTRODUCTION

1.1 The importance of Transition Metals and Anions

In the periodic table found that more than 50 percent of all elements are transition metals. There are several common characteristic properties of transition elements: has d-electron subshell, often form colored compounds, can have a variety of different oxidation states, good catalysts and often paramagnetic. Transition metals and anions also play important roles in many fields of chemical and biological process, which can be categorized as follows:

1.1.1 Biologically

Although transition metal ions occur in a trace scale in living bodies but they are indispensable components in oxygen transporters and extensively use of metals such as iron, copper and manganese for activation protein. Iron, the most abundant heavy metallic element in organisms, is a center core of two well-known oxygen carriers, hemoglobin and myoglobin, in warm blood animals. In contrast, arthropods and mollusks use copper containing proteins like hemerythrin and hemocyanin to uptake and transport dioxygen molecules. Some important enzymes have zinc ion as their essential constituents such as carbonic anhydrase and carboxy peptidase. Cobalt found in vitamin B-12 and coenzyme vitamin B-12, acts as a metal core center of reductase and methyl transfer metalloenzymes.[1-2] In addition, 70% of all enzyme substrates are negatively charged. Between 70 and 75 percent of enzymes, substrates and cofactors are anions, very often phosphate residues (as in adenosine triphosphate (ATP), the energy source of life) is a tetraanion at physiological pH. Deoxyribonucleic acid (DNA) is also a polyanion, containing phosphate esters along its ribose backbone. Anions such as sulphate and carboxylate are also found in biochemical systems.

1.1.2 Environmentally

The existence of some transition metal ions in high level can cause harmful pollution such as lead, cadmium, or mercury. Clearly chromium ion, especially in oxidation state VI as in CrO_4^{2-} or $\text{Cr}_2\text{O}_7^{2-}$ from dyes industries, is mentioned as a

server carcinogenic substance. High quantity of Ni^{2+} ion in natural resources is also fatal to human beings. In addition, anions can pose severe pollution problem. Nitrate anions from fertilizers run off agricultural land into the water supply leading to disrupts aquatic life cycles. [3]

1.1.3 Industrially

Many transition complexes, in particular organometallic complexes are utilized as potential catalysts in industrial processes. For example, $\text{Rh}(\text{PPh}_3)\text{Cl}$ or Wilkinson's catalyst, is the good catalyst reagent for hydrogenation process.[4] Pertechnetate anions are a toxic, radioactive by-product of the nuclear power industry.

1.1.4 Medically

More than 80-90% of drugs are organic compounds. Water soluble vanadium complexes like bis(*maltalano*)oxovanadium ($[\text{VO}(\text{malto})_2]$)[5] and VO-Salen were found to be effective insulin mimics. Auranofin, $[\text{Au}(\text{Pet}_3)(\text{ttag})]$ (ttag = tetra-O-acetylthioglucose) and its related gold(I) thiolate compounds have been the primary drugs which used for rheumatoid arthritis treatments.[6] Cisplatin, $[\text{cis-PtNH}_3)_2\text{Cl}_2]$, and its platinum-based derivatives are considered to be drugs against human malicious cancers and for protein repair.[7-8] Anions are of great importance in many disease pathways. Chloride anion is the major extracellular anions. Compounds of fluorine, including sodium fluoride (NaF), stannous fluoride (SnF_2) and sodium MFP, are used in toothpaste to prevent dental cavities. Anion-binding proteins have also been implicated in the mechanism of Alzheimer's disease. [9]

1.2 Concept of Supramolecular chemistry

Supramolecular chemistry becomes one of the most rapidly expanded fields in modern chemistry.[10] The knowledge from this enchanting topic can be applied to enormous diversities of chemical system especially the production of molecular devices and artificial biological systems. The definition of supramolecular chemistry may be expressed in many terms as 'chemistry of molecular assemblies and of the intermolecular bond' or 'chemistry of the non-covalent bond'. Supermolecules consist of two or more species held together by weak intermolecular forces (non-covalent intermolecular bond) such as hydrogen bonding, van der Waals interaction, electrostatic interaction, dipole-dipole interaction or π - π interaction.[11] Construction

of any supermolecule are lead to the three important functions: molecular recognition, translocation and transformation.[12] Indeed, molecular recognition has become characteristics of the language of supramolecular chemistry and has been studied more widely than the others.

1.3 Molecular Recognition and Molecular Receptors

As mentioned above, molecular recognition is defined by the energy and the information involved in the binding and selection of many substrates by a given receptor molecule. It can be implied as the (molecular) storage and (supramolecular) read out of molecular information. High recognition between receptors and substrates was affected by several factors as follows:

- a.) steric complementarity: it depends on shapes and sizes of receptors and substrates;
- b.) interactional complementarities, i.e. presence of complementarity binding sites in the suitable disposition on a substrate and a receptor;
- c.) large contact area between molecules of a receptor and substrates;
- d.) multiple interaction sites due to weak intermolecular interactions;
- e.) strong overall bindings; [10]

Studies of molecular recognition require suitable molecular receptors to specifically interact with many substrates. Molecular receptors are clearly defined as organic structures held by covalent bonds, that are able to bind ionic or molecular substrates by means of intermolecular interactions, leading to an assembly of two or more species. Excellent molecular receptor is one that can bind a particular substrate with high selectivity, high stability and high flexibility.[11] Receptors are divided in two types according to the number of binding site.

1.3.1 Receptors have one binding site.

1.3.1.1 Cation receptors are based on the chemistry of crown ethers, azacrown ether and cryptands. [13]

1.3.1.2 Anion receptors, which can bind with anion by electrostatic interaction and/or hydrogen bonds, or Lewis acid metal ligand interaction. The binding of anions depends on the properties of anions: charge, size, pH, solvation and geometry.

1.3.2 Receptor have two binding sites in the same receptor are referred to as ditopic receptor.

1.3.2.1 Cascade approach: a receptor capable of binding more than one metal cation. The metal ions are then used to form interactions with an anionic guest, co-binding it between them and within the recognition cavity.

1.3.2.2 Binding zwitterions: the recognition units have the correct spatial arrangement to bind both positive and negative charge of the molecule such as amino acids, containing acidic and basic groups.

1.3.2.3 Binding ion pairs: receptors containing two individual recognition units, one for cation and one for anion.

The design of new multisites ion pair receptors that contain covalently linked binding site for both cations and anions is a new area of coordination chemistry. In a ditopic receptor is whether the binding of the cation enhances the binding of the anion, exhibited allosteric cooperative complexation, or *vice versa*. [14-17] In addition, to being a potential selective extraction/membrane transportation reagent for metal salts, these ditopic ligand systems can be tailored to exhibit novel cooperative and allosteric behavior where by the complexation of one charged guest can be influenced, through electrostatic and conformation effect, the subsequent coordination of the pairing ion.

In 2001, two bifunctional receptors **1** and **2** for cooperative complexation of cations and anions were synthesized on the basis of azacrown ether, the amide group as binding sites are illustrated in Figure 1.1. Binding properties of receptors **1** and **2** were studied by using ^1H NMR titration in $\text{DMSO-}d_6$ and X-ray crystallography. They find that **2** is the first example of a ditopic salt-receptor that binds a contact ion pair in solution more strongly than either of the free ions. [18]

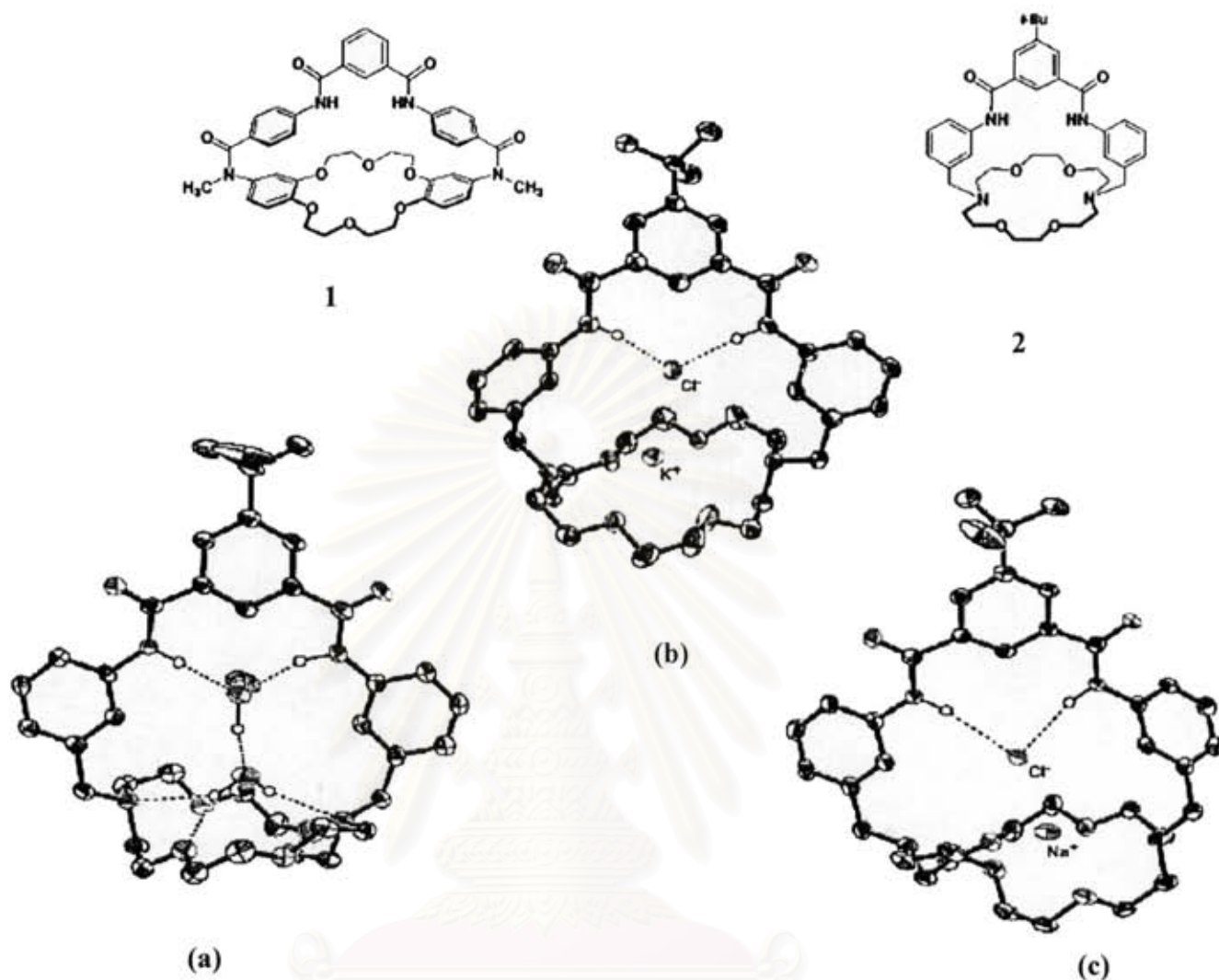


Figure 1.1 Macrobicyclic ditopic receptors 1 and 2 and X-ray crystal structures (a) receptor 2 with a water and methanol in the cavity, (b) one of the two 2·KCl structures found in the unit cell, and (c) 2·NaCl

1.4 Allosteric receptor

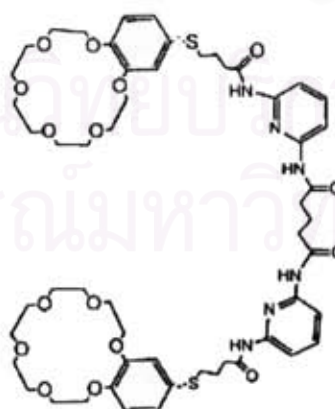
Allosteric interactions between subunits are known as one of the elegant strategies for precisely regulating and controlling the function in biological systems. An allosteric system is one that involves conformation coupling between two or more influences (turn on or off) the binding ability of the second site. This concept is exemplified in Figure 1.2, where one part of the molecule is coordinated to the metal center results in the allosteric organization of a second distance binding site. [19-21]

Cooperative binding is a special case of allostery. It requires the macromolecule that has more than one binding site, since cooperativity results from the interactions between binding sites. If the binding of ligand at one site increases the affinity of the ligand at another site, the macromolecule exhibits positive cooperativity. Conversely, if the binding of ligand at one site decrease the affinity of the ligand at another site, the macromolecule exhibits negative cooperativity. If the ligand binds at each site independently, the binding is non-cooperative.



Figure 1.2 Schematic illustration of allosteric effect of ditopic metal receptor [22]

Nabeshima's bis(crown)-substituted hydrogen-bonding **3** has a moderate affinity for Cl^- and Br^- ions in 4:1 $\text{CDCl}_3/\text{CD}_3\text{CN}$, as detected by NMR spectroscopy.[23] Formation of a 1:1 Cs^+ complex with both crown units organizes the two H-bond-donating 2,6-bis(acylamido)pyridine moieties. This leads to enhance binding constant, 10-fold in the case of Br^- and 45-fold in the case of Cl^- .(Figure 1.3)



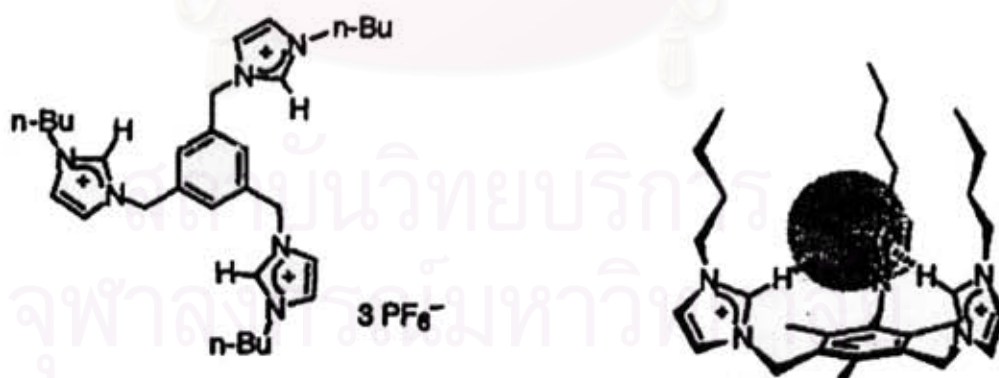
3

Figure 1.3 Allosteric receptor for metal cation and anion [23]

1.5 Anion receptor based on imidazolium groups

The design and synthesis of receptors capable of binding anionic guest is prime importance in supramolecular chemistry, due to its biological, medical, and environmental relevance. The selective binding of anions by host molecules depends upon the size and geometry of anions as well as the host molecule. Receptors that have amide, urea, pyrrole, ammonium, or guanidinium groups as binding sites have been designed for anion recognition. Recently, imidazolium group was an interest to use for anion binding site. Because imidazolium group can make a strong interaction with anions through the $(C-H)^+ \cdots X^-$ type ionic hydrogen bonding involving the dominating charge-charge electrostatic interaction which is contrast to well-known neutral receptors involving typical hydrogen bonding for the anion binding such as amide, pyrrole, urea, etc.

In 1999, Sato et al. have reported receptors with 1,3-disubstituted imidazolium groups, which bind anions by forming $(C-H)^+ \cdots X^-$ ionic hydrogen bonds between the imidazolium rings and the guest anion. These receptors also form 1:1 stoichiometry complexes with the Cl^- anion. The association constants are fairly large ($75000-7200 \text{ dm}^3 \text{ mol}^{-1}$). The magnitude of the chemical shift changes and association constants decrease in the order $Cl^- > Br^- > I^-$, consistent with their relative hydrogen-bonding abilities and surface charge density.[24]



4

Figure 1.4 Anion receptor based on imidazolium groups and possible structure of 4 with halide ion

Pramod S. Pandey and coworkers synthesized bile acid-based cyclic imidazolium receptors **5** and **6**. Receptor **5** has a moderate selectivity for the fluoride ion while receptor **6** shows high selectivity and affinity for the chloride ion. Interestingly, the single crystal X-ray analysis of the complexes of these receptors with bromide ion revealed the participation of the methylenic hydrogens of both the acetyl groups in the hydrogen bond interaction with the bromide ion. The addition of tetrabutylammonium salts to receptors **5** and **6** in CDCl_3 solution, resulted in large downfield chemical shifts of the C-2 protons of the imidazolium/benzimidazolium moieties, which suggested complexation of the anion through $(\text{C-H})^+\cdots\text{X}^-$ ionic hydrogen bonds.[25]

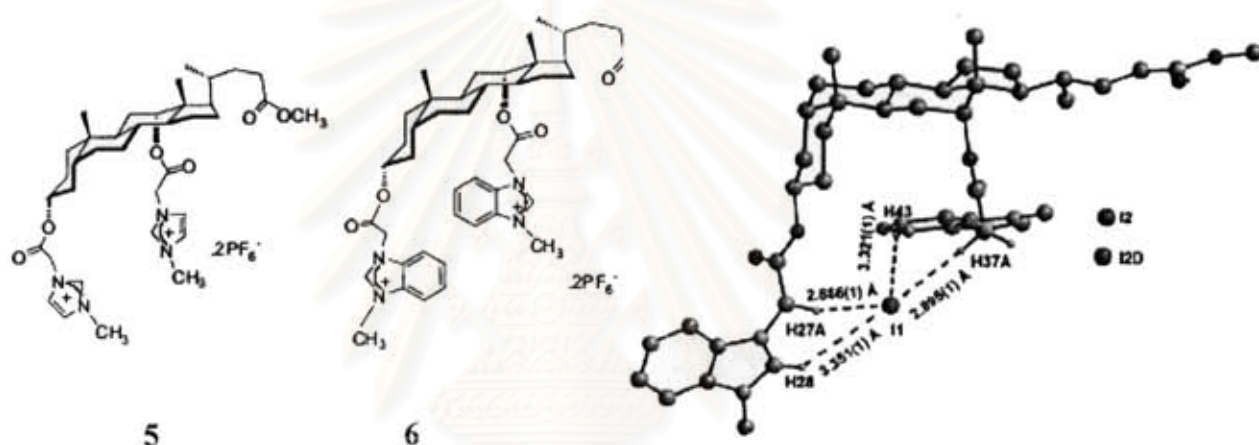


Figure 1.5 Anion receptors based on imidazolium **5** and benzimidazolium **6** and Ball-Stick model of $\text{C}_{45}\text{H}_{60}\text{I}_2\text{N}_4\text{O}_6$ showing $\text{C-H}\cdots\text{I}^-$ interactions

1.6 Chemical sensors (Chemosensors)

A chemosensor can be defined as a molecule able to bind selectively and reversibly the analyte of interest with a concomitant change in the property of the system, such as a redox potential and absorption or luminescence spectra. To obtain the detection of the target analyte, two different procures are needed: molecular recognition and signal transduction. This means that chemosensors have to be built by components able to perform these functions. It usually consists of two molecular units: a receptor or ionophore (able to selectively bind the analyte) and an active unit or a

signaling unit such as a chromophore or a fluorophore (that changes one or more of its properties upon analyte complexation) (Figure 1.6).

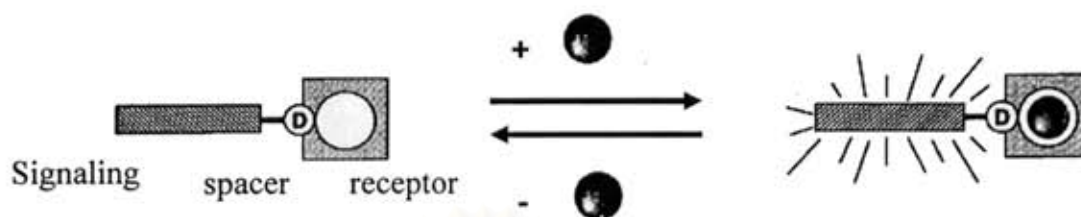


Figure 1.6 A general concept of chemosensors [26]

1.7 Chromoionophores and fluoroionophores

A number of direct sensing schemes have been described using colorimetric and fluorescent chemosensor molecules whose optical properties change upon direct binding of the guest (*chromoionophores* and *fluoroionophores*).

1.7.1 Chromoionophores

Color reactions are popular criteria for the identification and quantitative determination of substances.

In the metal salt complexes of ionophores, the positive cation charge influence the donor heteroatom (O, N, S) and their electronic surrounding by ion-dipole forces. If one of the heteroatoms is a constituent of chromoionophores, the electronic disturbance propagates the whole ($n+\pi$) system. Due to different influences on the ground and photoexcited states by cations, changes occur in the absorption spectra. Similarly, in the case of anions can induced a change of absorption properties of receptor. Basically, the change of color of chromoionophores occurs through two mechanisms. [27-28]

1.7.1.1 hypsochromic shifts (blue shift)

When a chromoionophore contains an electron donor group (often an amino group) conjugated to aromatic ring (electron acceptor), it can complex a cation as well as being a chromophore. The amine nitrogen atoms of the chromoionophore are positively polarized, the excited states are more strongly destabilized by cations than the ground state, therefore, resulting in hypsochromic shifts. (Figure 1.7)

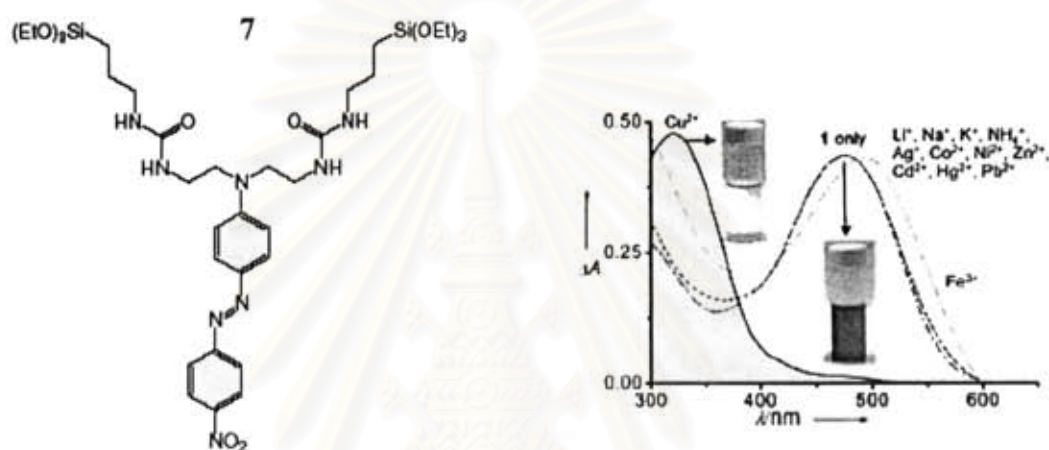


Figure 1.7 UV-Vis spectra of **7** (0.025 mM) in the presence of metal nitrates (5.0 equiv) in acetonitrile

The addition of Cu^{2+} into receptor **7** resulted in the largest hypochromic shift to 320 nm ($\Delta\lambda = 160$ nm), changing its solution color from red to pale-yellow only in acetonitrile.

However, no significant color change was observed upon addition of excess amounts of Li^+ , Na^+ , K^+ , NH_4^+ , Co^{2+} , Cd^{2+} , Pb^{2+} , Zn^{2+} , Hg^{2+} , Fe^{3+} , and Ag^+ , indicating that only Cu^{2+} forms a strong coordination through the donor atoms of **7**. [29]

The chromophores are influenced by these ion-dipole forces, depending on the size and direction of the dipole moment. The more the dipole moment alters during the excitation, the more the absorption band shifts.

1.7.1.2 bathochromic shifts (red shift)

When a chromoionophore contains an electron acceptor, it can give color change upon complexation. Because the donor atom will surely be polarized positively in the ground state, the excited states are more strongly stabilization by binding of guest at the acceptor site, causing bathochromic band shifts (Figure 1.8). The hydrogen-bond interaction between anion and the electron donor of receptor increased the electron density in the donor group (thiourea group). This increase in charge density resulted in the red shift of absorption.[30]

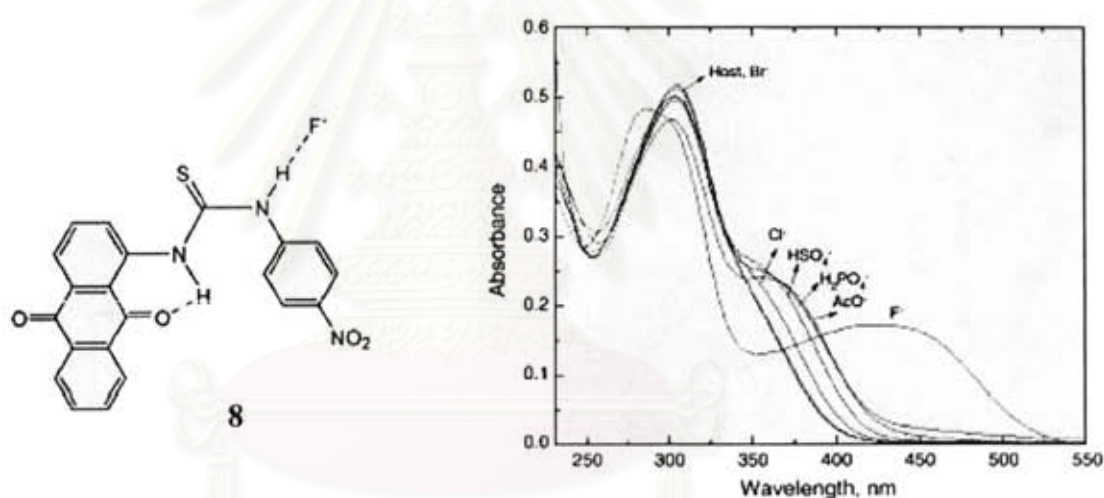


Figure 1.8 Absorption spectra of **8** (5.0×10^{-5} mol.L⁻¹) in the presence and absence of anions in acetonitrile

1.7.2 Fluoroionophores

Fluoroionophores or fluorosensors are generally multi-component systems comprising of a signaling moiety (fluorophore) and a guest-binding site (receptor). The two units are often separated by a space group. The components are chosen such that the communication between the receptor and the fluorophore results in “switching off” of

fluorescence of the system or fluorescence quenching in the absence of a guest. However, in the presence of a guest, the communication between the receptor and fluorophore gets turned-off leading to the recovery of the fluorescence of the system. Thus, the presence of the guest is indicated by a switching-on the fluorescence or fluorescence enhancement [31-33] The origin of the excellent 'off-on' Hg^{2+} sensing analyzed further by Bronson et al. X-ray crystallography of the complex, clearly shows that the metal is only bound by the pair of hydroxyquinolines and not by the diazacrown. So the latter serves two important roles: (a) as a scaffold for the ligating groups and (b) as an intramolecular base to pick up the protons from the phenol upon metal binding. PET from the amines would be inhibited in this way and strong fluorescence of the complex would be tolerated.[34]

1. *Fluorescence PET (Photoinduced Electron Transfer)*; In PET sensors, the metal ion receptor is an electron donor (e.g.amino-containing group) and the fluorophore acts as an electron acceptor. In the analyte-free form, upon excitation by photons the electron of the highest occupied molecular orbital (HOMO) of the fluorophore is promoted to the local lowest unoccupied molecular orbital (LUMO); subsequently, the electron seated on the HOMO of the donor transfers to the HOMO of the fluorophore synergistically (electron transfer), which causes fluorescence quenching.[35] When binding to a target cation, the energy gap between these two HOMO orbitals is changed from positive to negative, so the quenching process does not occur (Figure 1.9).

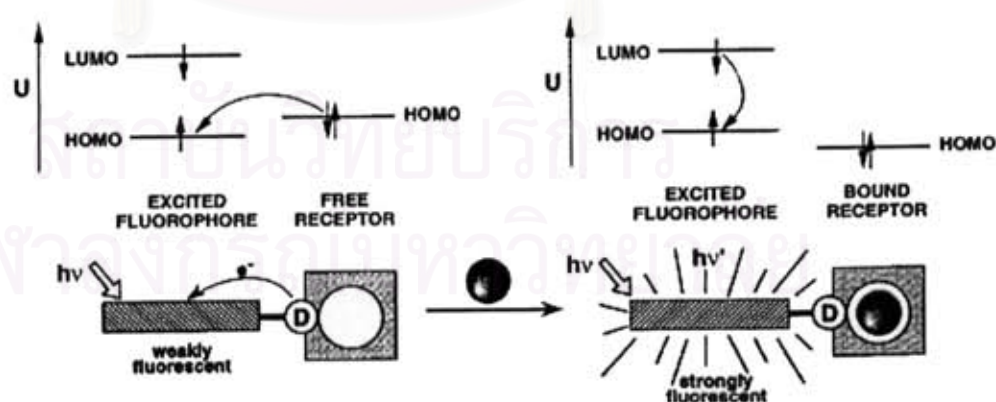


Figure 1.9 Principle of the PET sensor [36]

Fluorescent photoinduced electron-transfer sensors (Figure 1.10) were made from *p*-phenylenediamine-substituted azacrown ether attached with a dansyl group, in which the *p*-phenylenediamine moiety serves as electron donor and the dansyl group acts as the acceptor.[37]

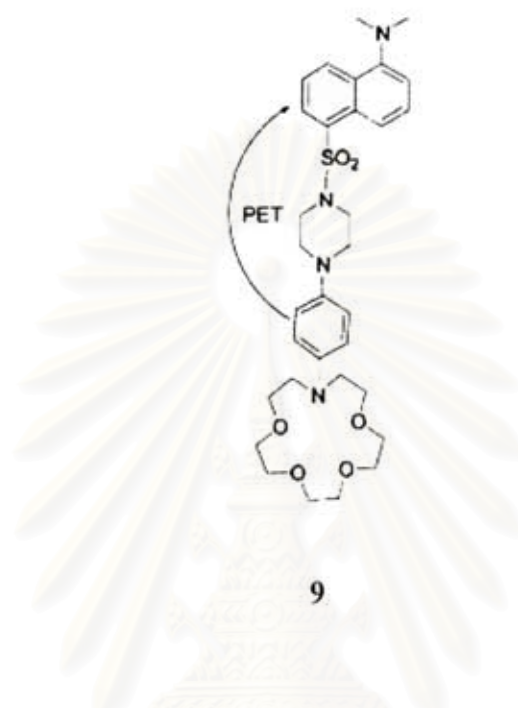


Figure 1.10 Azacrown ether-based PET fluorophore

Another fluorophore design involved *excimer-monomer PET system*. Some fluorophores such as anthracene and pyrene can form an excimer (excited dimer) when an excited molecule come close to another one during the lifetime of excited state, dual fluorescence is then observed with monomer band at shorter wavelength and excimer broad band at longer wavelength. When the proximity of the fluorophore is disturbed, for example by cation binding, the excimer formation is altered and the monomer/ excimer fluorescence intensity ratio is also altered.

2. *Fluorescence PCT (Photoinduced charge transfer)*. In PCT sensors, the fluorophore contains an electron-donating group (usually an amino group) conjugated to an electron-withdrawing group, which undergoes internal charge transfer (ICT) from the donor to the acceptor. [38] The consequent change of the dipole moment leads to a Stokes' shift, which is influenced by the microenvironment of the fluorophore. When the cation interacts with the donor group, the excited state is more

strongly destabilized by the cation than the ground state, and a blue shift of the absorption and emission spectra is expected. Conversely, when the cation interacts with the acceptor group, the excited state is more stabilized by the cation than the ground state, and this leads to a red shift of the absorption and emission spectra.

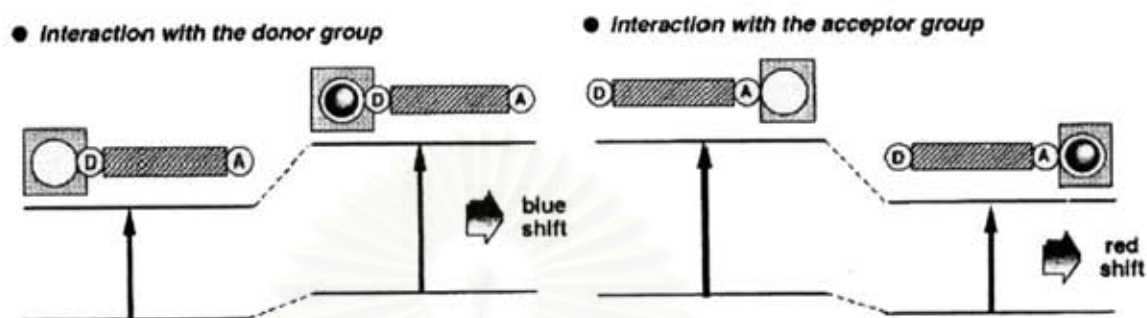


Figure 1.11 Spectral displacements of PCT sensors resulting from interaction of a bound cation with an electron-donating or electron-withdrawing group.

Additionally, the ICT process may be accompanied by an internal rotation between the donor and acceptor leading to a twisted intramolecular charge transfer state, which will influence the fluorescence intensity to some extent. Figure 1.11 show the fluorescence PCT sensor of Zn^{2+} ion.

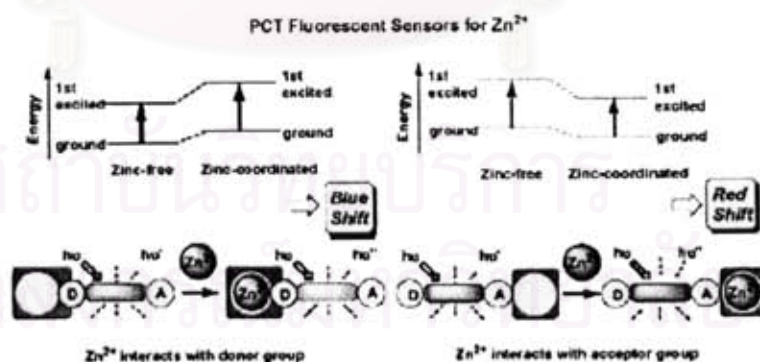


Figure 1.12 Principle of cation recognition by fluorescence PCT sensors [39]

Crown ether **10** is the PCT sensor, when a cation is coordinated with the carbonyl group, the excited state is more stabilized than the ground state so that both

the absorption and emission spectra are red-shifted. The spectral red shifts observed with **10** on addition of cations are shown in Figure 1.12.

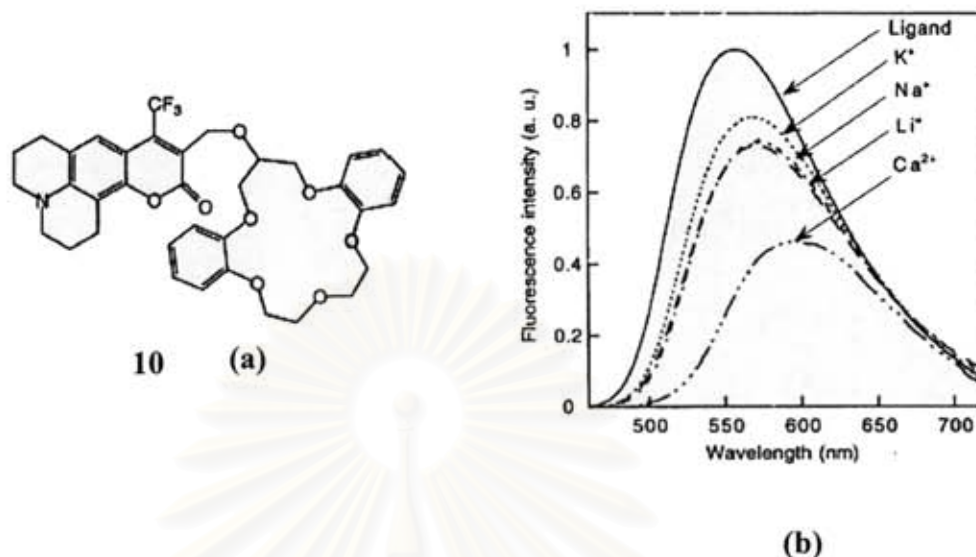


Figure 1.13 (a) A crown ether-based PCT fluoroionophore and (b) fluorescence spectra of **10** and its complexes in acetonitrile [36]

1.8 Design of chromoionophores and fluoroionophores

In order to design a host that will selectively bind a transition metal ion and anion, we use the chelate and macrocyclic effects as well as the concept of complementarity (matching of host and guest and electronic requirements) and crucially, host preorganization.

Having defined parameters such as the required host size, charge, characters of the donor atoms etc. the intellectual process of ligands tailoring can begin. Host-guest interactions occur through binding sites. The type and number of binding sites must be selected in a fashion that is most complementary to the characteristics of the binding sites of the guest. These binding sites must be arranged on an organic framework of suitable size to accommodate the guest. Binding site should be spaced somewhat apart from one another to minimize repulsions between them, but arranged so that can all interact simultaneously with the guest. [40]

The nature of the organic framework of the host itself, whether lipophilic or hydrophilic, plays a fundamental role in a host behavior. This determines the

solubility characteristics of host and its complexes. The part of the signaling unit must be selected suitably.

1.9 Some characteristics of fluoronoionophores.

1.9.1 Selectivity

A selectivity of a receptor is a preference of that receptor towards a guest. This is customarily estimated from a magnitude of a thermodynamic *stability constant* of a receptor-guest or, in more general terms, a ligand-metal complex. For fluoroionophore, the method of obtaining a binding constant is through fluorimetric titration—a measurement of fluorescence intensity at different metal-ligand ratios.[41-43]

The complexation of a metal ion M by a ligand L in solution can be represented by the equilibrium



which is controlled by the stability constant

$$K_s = \frac{[ML]}{[L][M]}$$

where the bracket denotes the concentration of each species in mole per liter.

In fluorimetric titration, the fluorescence intensity of the solutions containing free ligand L (I_F^0) and ligand complexed with metal ion ML (I_F) at the chosen emission wavelength are measured and are related to the initial concentration of the ligand (C_0) by

$$I_F^0 = kaC_0 \quad (1)$$

I_F depend directly on [L] and [ML]

$$I_F = ka[L] + kb[ML] \quad (2)$$

Where k, a and b is a constant

Since $[ML] = C_0 - [L]$

Therefore $I_F - I_F^0 = k(b-a)(C_0 - [L])$ (3)

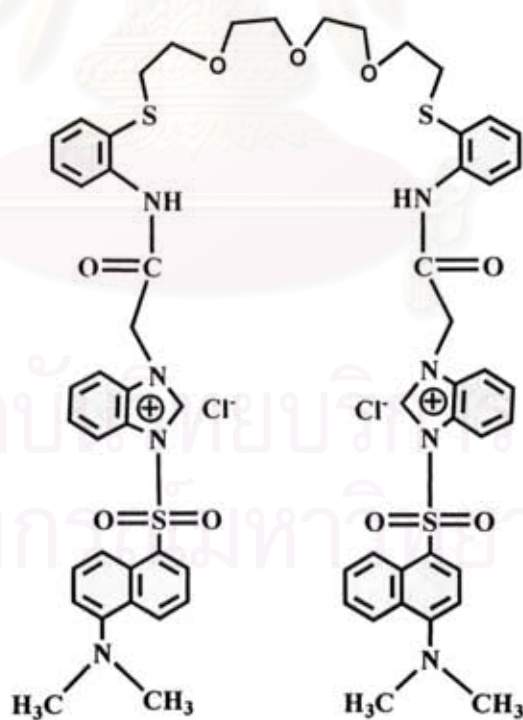
After rearrangement

$$\frac{I_F^0}{I_F - I_F^0} = \left(\frac{a}{b-a} \right) \left(\frac{1}{K_s[M]} + 1 \right) \quad (4)$$

Equation 4 shows that a plot of $I_F^0 / (I_F - I_F^0)$ against $1/[M]$ would be a straight line in which stability constant K_s can be calculated.

1.10 Objective and the scope of this research

The objective of this research is to synthesize acyclic thiacycrown like-ether containing imidazolium and amide groups **L** as sensor for both cations and anions. Complexation studies of ligand **L** with transition metal ions and various anions such as F^- , AcO^- and $H_2PO_4^-$ are investigated by means of fluorescence titration. Furthermore, we also study the effect of F^- , AcO^- and $H_2PO_4^-$ toward cation binding abilities. The target molecules were shown below. The results of this research should give information about the relationship between cavity size and the strength interactions of host and guests. Moreover, to deduce the effect and function of anions, that influences binding abilities of cation binding sites and *vice versa*.



L

CHAPTER II

EXPERIMENTAL SECTION

2.1 General procedures

2.1.1 Analytical instrument

Nuclear magnetic resonance (NMR) spectra were recorded on a Varian 200, 400 and a Bruker DRX 400 MHz nuclear resonance spectrometers. In all cases, samples were dissolved in deuterated chloroform, except ^1H -NMR titrations were dissolved in acetonitrile- d_3 . The chemical shifts were recorded in part per million (ppm) using a residue proton solvents as internal reference. Elemental analysis was carried out on CHNS/O analyzer (Perkin Elmers PE 2400 series II). MALDI-TOF mass spectra were recorded on Bruker Daltonic using doubly recrystallized 2-cyano-4-hydroxy cinnamic acid (CCA) as matrix. Absorption spectra were measured by a Varian Cary 50 UV-Vis spectrophotometer. Fluorescence spectra were performed on Varian spectrofluorometer by personal computer data processing unit. The light source is Cary Eclipse a pulsed xenon lamp and a detector is a photomultiplier tube. IR spectrum of the sample was recorded on a Nicolet Impact 410 FTIR spectrophotometer at room temperature with the potassium bromide (KBr) disk method. The sample was scanned over a range of $500\text{-}4000\text{ cm}^{-1}$ at resolution of 16 cm^{-1} and the number of scan was 32. The measurement was controlled by Omnic software.

2.1.2 Materials

Unless otherwise specified, the solvent and all materials were reagent grades purchased from Fluka, BDH, Aldrich, Carlo erba, Merck or Lab scan and used without further purification. Commercial grade solvents such as acetone, dichloromethane, hexane, methanol and ethyl acetate were purified by distillation before used. Acetonitrile, dimethylformamide and dichloromethane for set up the reaction were

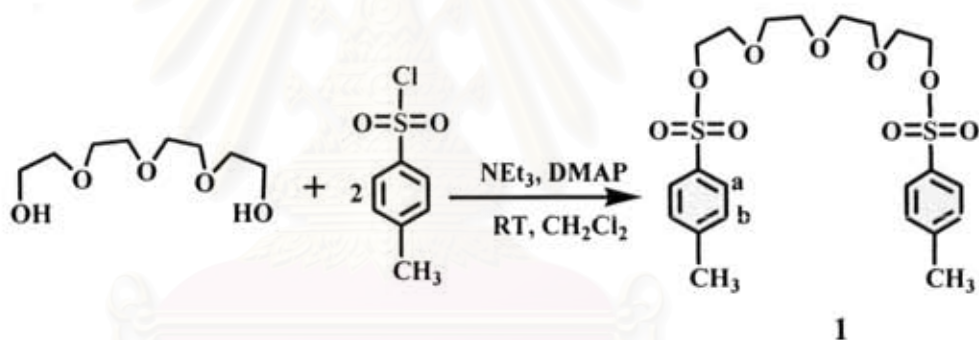
dried over calcium hydride and freshly distilled under nitrogen atmosphere prior to use.

Column chromatography was carried out on silica gel (Kieselgel 60, 0.063-0.200 mm, Merk). Thin layer chromatography (TLC) was performed on silica gel plates (Kieselgel 60, F₂₅₄, 1 mm, Compounds on TLC plates were detected by the UV-light. Acetonitrile fluorescence measurement (AR grade, Lab scan) were dried over calcium hydride and freshly distilled under nitrogen atmosphere prior to use.

All synthesized compounds were characterized by ¹H-NMR spectroscopy, mass spectrometry, IR spectroscopy and elemental analysis.

2.2 Synthesis

2.2.1 Preparation of tetraethylene glycol ditosylate (1)



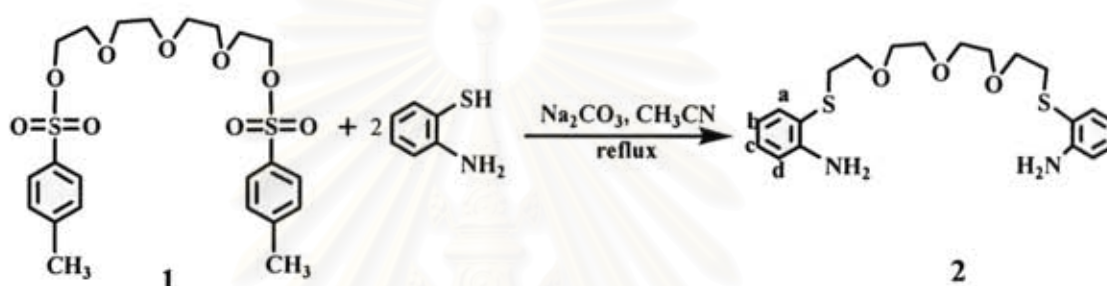
In a 500 mL two-neck round bottom flask equipped with a magnetic bar, tetraethyleneglycol (5.825 g, 0.03 mol), triethylamine (9.107 g, 0.09 mol), a catalytic amount of 4-dimethylaminopyridine (DMAP) and dichloromethane (100 mL) were stirred under nitrogen atmosphere at room temperature for 1 h. Toluene-4-sulfonyl chloride (11.50 g, 0.060 mol) in dichloromethane was added in the reaction at 0° C and stirred overnight. Treated with 3 M hydrochloric acid (200 mL) and extracted with dichloromethane (2 x 20 mL). The organic layer was dried over anhydrous sodium sulphate, filtered and evaporated to dryness in *vacuo*. The residue was purified by column chromatography on a silica gel with a mixture of 10% ethyl acetate and dichloromethane. The product yielded as a clear liquid (8.459 g, 56%).

Characterization data for 1

$^1\text{H-NMR}$ spectrum (400 MHz, CDCl_3): δ (in ppm)

δ 7.72 (d, $J = 8.4$ Hz, 4H, ArH_a), 7.27 (d, $J = 7.6$ Hz, 4H, ArH_b), 4.08 (t, $J = 4.8$ Hz, 4H, $\text{SO}_3\text{CH}_2\text{CH}_2\text{O}$), 3.61 (t, $J = 4.8$ Hz, 12H, $\text{CH}_2\text{OCH}_2\text{CH}_2\text{OCH}_2\text{CH}_2\text{OCH}_2$), 2.36 (s, 6H, ArCH_3).

2.2.2 Preparation of 1,8-Bis(aminothiophenol) tetraethylene glycol (2)



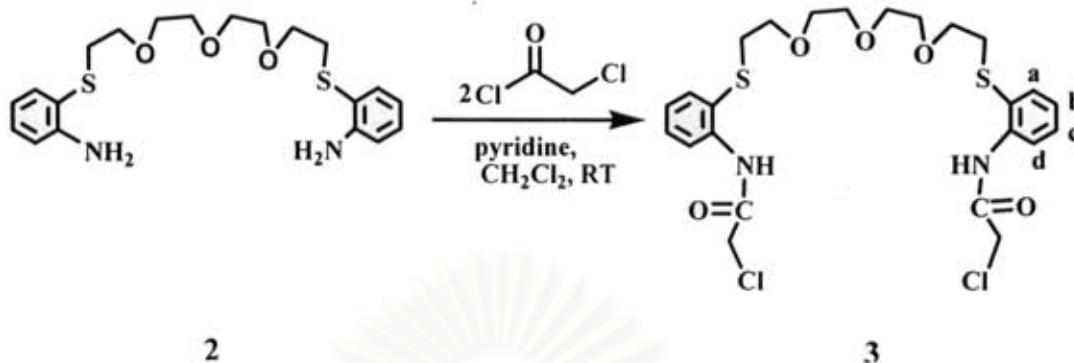
In a 250 mL two-neck round bottom flask equipped with a magnetic bar, 2-aminothiophenol (3.159 g, 0.025 mol), sodium carbonate (5.274 g, 0.050 mol) and acetonitrile (50 mL) were heated at reflux under nitrogen atmosphere for 1 h. Compound 1 (5.044 g, 0.010 mol) in acetonitrile was then added dropwise. The reaction was kept refluxing overnight under nitrogen atmosphere. After reaction mixture was cooled down to room temperature and the solid was filtered, the solvent was removed to dryness under reduced pressure. Compound 2 was purified by column chromatography (SiO_2) using dichloromethane until 15% ethyl acetate as eluent to afford a yellow liquid (2.267 g, 55 %).

Characterization data for 2

$^1\text{H-NMR}$ spectrum (400 MHz, CDCl_3) : δ (in ppm)

δ 7.39 (d, $J = 8$ Hz, 2H, ArH_a), 7.12 (t, $J = 7.6$ Hz, 2H, ArH_c), 6.71 (d, $J = 8.4$ Hz, 2H, ArH_d), 6.67 (t, $J = 7.4$ Hz, 2H, ArH_b), 3.57 (t, $J = 6.6$ Hz, 12H, $\text{CH}_2\text{OCH}_2\text{CH}_2\text{OCH}_2\text{CH}_2\text{OCH}_2$), 2.93 (t, $J = 6.8$ Hz, 4H, $\text{SCH}_2\text{CH}_2\text{O}$).

2.2.3 Preparation of 1,8-Bis(2-chloromethylamide) tetraethylene glycol (3)



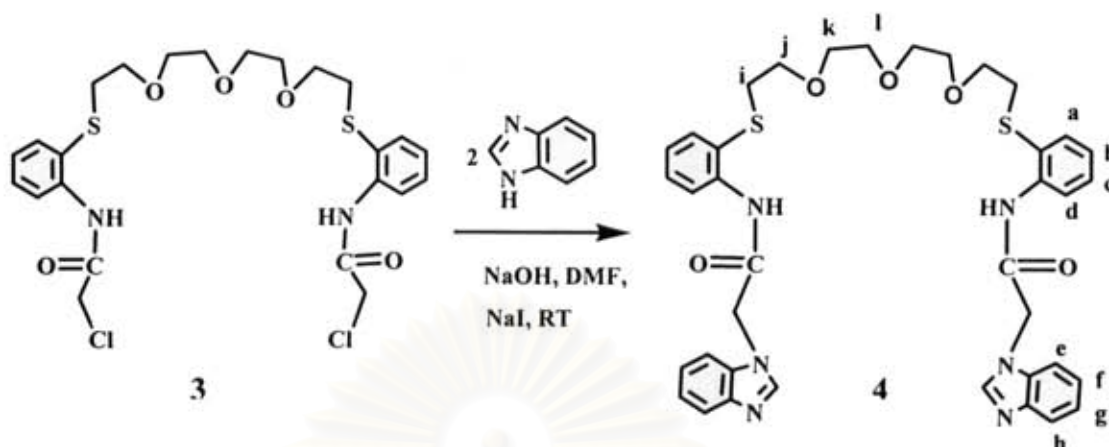
In a 100 mL two-neck round bottom flask equipped with a magnetic bar, compound **2** (1.059 g, 0.0026 mol) and dichloromethane (10 mL) were stirred under nitrogen atmosphere at room temperature for 0.5 h. Pyridine (0.443 g, 0.005) and chloroacetyl chloride (0.596 g, 0.005 mol) were then added in the reaction at 0°C. The mixture reaction was stirred under nitrogen atmosphere for 4 h. After treated with 3 M hydrochloric acid (20 mL), it was extracted with dichloromethane (2 x 20 mL). The organic layer was dried over anhydrous sodium sulphate. The solvent was removed under reduced pressure. The compound **3** was obtained as a gray liquid (1.067 g, 74 %).

Characterization data for **3**

^1H NMR spectrum (400 MHz, CDCl_3) : δ (in ppm)

δ 9.72 (s, 2H, NHAr), 8.40 (d, $J = 8$ Hz, 2H, ArH_a), 7.58 (d, $J = 7.6$ Hz, 2H, ArH_d), 7.35 (t, $J = 8$ Hz, 2H, ArH_c), 7.11 (t, $J = 7.4$ Hz, 2H, ArH_b), 4.25 (s, 4H, ClCH_2CO), 3.56 (t, $J = 6.4$, 12H, $\text{CH}_2\text{OCH}_2\text{CH}_2\text{OCH}_2\text{CH}_2\text{OCH}_2$), 2.96 (t, $J = 6.6$ Hz, 4H, $\text{SCH}_2\text{CH}_2\text{O}$).

2.2.4 Preparation of 1,8-Bis(2-methylbenzimidazolium) tetraethylene glycol (4)



In a 100 mL two-neck round bottom flask equipped with a magnetic bar, sodium hydroxide (0.30 g, 0.0075 mol) and dimethylformamide (DMF) (10 mL) were stirred under nitrogen atmosphere for 0.5 h. Benzimidazole (0.75 g, 0.0064 mol) in DMF was then added in the reaction and further stirred under nitrogen atmosphere for 1 h. Then **3** in DMF was slowly dropped in the reaction and left stirring for 2 days under nitrogen atmosphere. The mixture was filtered and the solvent was removed under reduced pressure. The residue was dissolved in ethyl acetate and placed on a silica gel chromatography column. Compound **4** was purified by column chromatography using ethyl acetate until 10% methanol as eluent. The desired product **4** yielded as a yellow solid (0.91 g, 45%).

Charaterization data for 4

^1H NMR spectrum (400 MHz, CDCl_3): δ (in ppm)

δ 8.88 (s, 2H, CONHAr), 8.30 (d, $J = 8.4$ Hz, 2H, ArH_a), 8.05 (s, 2H, NCHN), 7.82 (t, $J = 3.2$, 2H, ArH_c), 7.40 (m, 4H, ArH_{d,h}), 7.29 (m, 6H, ArH_{b,e,g}), 7.00 (t, $J = 7.4$ Hz, 2H, ArH_f), 5.03 (s, 4H, COCH₂N), 3.45 (d, $J = 4.4$ Hz, 4H, SCH₂CH₂O), 3.39 (m, 4H, OCH₂_kCH₂O), 3.20 (t, $J = 5.8$ Hz, 4H, OCH₂CH₂O), 2.46 (t, $J = 5.8$ Hz, 4H, SCH₂_iCH₂O).

$CH_2OCH_2CH_2OCH_2CH_2OCH_2$), 2.92 (t, $J = 5.8$ Hz, 4H, SCH_2CH_2O), 2.87 (s, 12H, $ArCH_3$).

MALDI-TOF mass spectroscopy : $C_{62}H_{64}Cl_2N_8O_9S_4 [L + H^+]^+$ at $m/z = 1266.77$

2.3 Complexation studies of ligand L by 1H -NMR titrations

2.3.1 Complexation studies of ligand L in the presence of 2 equivalents of tetrabutyl ammonium fluoride with various cations excess.

Typically, a solution of 1×10^{-3} M of a ligand L (0.00063 g, 4.98×10^{-7} mol) in CD_3CN (0.5 mL) was prepared in NMR tube containing 1.2×10^{-6} mol (2 equiv) of tetrabutylammonium fluoride and 3×10^{-6} mol (5 equiv) of metal cation such as Ni^{2+} , Co^{2+} , Cd^{2+} , Cu^{2+} , Ag^+ or Zn^{2+} .

2.3.2 Anion complexation studies of ligand L with fluoride and dihydrogen phosphate

Typically, a solution of 0.001 M of a ligand L (0.00164 g, 1.3×10^{-6} mol) in CD_3CN (0.6 mL) was prepared in NMR tube. A solution of 0.012 M of fluoride and dihydrogen phosphate as tetrabutylammonium salt in CD_3CN (0.25 mL) was prepared in a vial and added directly to the NMR tube by a microsyringe to have guest:host ratios shown in Table 2.1. 1H -NMR spectra were recorded after each addition.

สถาบันวิทยบริการ
จุฬาลงกรณ์มหาวิทยาลัย

Table 2.1 Amounts of solutions of the anions used to prepare various anion:ligand **L** ratios

Ratio of anion : ligand L	Volume anion added(μ L)	[ligand L] M	[anion] M
0.00 : 1.00	0.00	1.00×10^{-3}	0
0.10 : 1.00	5.00	9.92×10^{-4}	9.92×10^{-5}
0.20 : 1.00	5.00	9.84×10^{-4}	1.96×10^{-4}
0.30 : 1.00	5.00	9.76×10^{-4}	2.93×10^{-4}
0.40 : 1.00	5.00	9.68×10^{-4}	3.87×10^{-4}
0.50 : 1.00	5.00	9.60×10^{-4}	4.80×10^{-4}
0.60 : 1.00	5.00	9.52×10^{-4}	5.71×10^{-4}
0.70 : 1.00	5.00	9.45×10^{-4}	6.61×10^{-4}
0.80 : 1.00	5.00	9.37×10^{-4}	7.50×10^{-4}
0.90 : 1.00	5.00	9.30×10^{-4}	8.37×10^{-4}
1.00 : 1.00	5.00	9.23×10^{-4}	9.23×10^{-4}
1.20 : 1.00	10.00	9.09×10^{-4}	1.09×10^{-3}
1.40 : 1.00	10.00	8.95×10^{-4}	1.25×10^{-3}
1.60 : 1.00	10.00	8.82×10^{-4}	1.41×10^{-3}
1.80 : 1.00	10.00	8.70×10^{-4}	1.56×10^{-3}
2.00 : 1.00	10.00	8.57×10^{-4}	1.71×10^{-3}
2.50 : 1.00	25.00	8.27×10^{-4}	2.07×10^{-3}
3.00 : 1.00	25.00	8.00×10^{-4}	2.40×10^{-3}
3.50 : 1.00	25.00	7.74×10^{-4}	2.71×10^{-3}
4.00 : 1.00	25.00	7.50×10^{-4}	3.00×10^{-3}

2.4 Complexation studies of ligand L by UV-vis titrations

2.4.1 Complexation studies of Ligand L with various anions: fluoride, acetate, benzoate, dihydrogen phosphate

Typically, a solution of 9×10^{-5} M of a ligand L in a 0.01 M tetrabutyl ammonium hexafluorophosphate in dried acetonitrile was prepared. A stock solution of 0.025 M of an anion (F^- , BzO^- , AcO^- , $H_2PO_4^-$ as tetrabutylammonium salt) in dried acetonitrile was prepared in a 25 mL volumetric flask.

Absorption spectra of ligand L and anion complexes were recorded from 200-500 nm at ambient temperature. The solution of an anion was added directly to 2.00 mL of 9×10^{-5} M ligand L in a 1-cm quartz cuvette by microburette and stirred for 30 seconds. Absorption spectra were measured after each addition. Table 2.2 shows a concentration of anions in titration experiments.

Table 2.2 The concentration of anions were used in anion complexation studies with ligand L and the final ratios of guest:host

anion	[anion] M	Final guest:host ratios
Fluoride	1.20×10^{-3}	10:1
Benzoate	6.00×10^{-4}	5:1
Acetate	3.60×10^{-3}	30:1
Dihydrogen phosphate	1.20×10^{-2}	100:1

2.5 Complexation studies of ligand L by fluorescent titrations

2.5.1 Complexation studies of Ligand L with various anions : fluoride, acetate, dihydrogen phosphate

Typically, a solution of 1×10^{-6} M of a ligand L in a 0.01 M tetrabutyl ammonium hexafluoro phosphate in dried acetonitrile was prepared by adding 0.1 mL of a stock solution of ligand L (1×10^{-4} M) in a 10 mL volumetric flask. A stock solution of 0.025 M of anion (F^- , AcO^- , $H_2PO_4^-$ as tetrabutylammonium salt) in dried acetonitrile was prepared in a 10 mL volumetric flask.

Fluorescent spectra of ligand L and anion complexes were recorded from 230-700 nm at ambient temperature. The solution of an anion was added directly to 2.00 mL of 1×10^{-6} M ligand L in a 1-cm quartz cuvette by microburette and stirred for 30 seconds. Fluorescent spectra were measured after each addition. Table 2.3 shows a concentration of anions in titration experiments.

Table 2.3 The concentration of anions were used in anion complexation studies with ligand L and the final ratios of guest:host

anion	[anion] M	Final guest:host ratios
Fluoride	6.67×10^{-5}	50:1
Acetate	6.67×10^{-5}	50:1
Dihydrogen phosphate	6.67×10^{-5}	50:1

Table 2.4 The concentration of fluoride ion was used in anion complexation studies with ligand L and the final ratios of guest:host

Point	F/L	[L] mM	[F ⁻] mM	V of F ⁻ (mL)	V total (mL)
1	0.00	1.00×10^{-3}	0	0	2.00
2	0.33	1.00×10^{-3}	3.30×10^{-4}	0.01	2.01
3	0.67	9.90×10^{-4}	6.60×10^{-4}	0.02	2.02
4	1.00	9.90×10^{-4}	9.90×10^{-4}	0.03	2.03
5	1.33	9.80×10^{-4}	1.31×10^{-3}	0.04	2.04
6	1.67	9.80×10^{-4}	1.63×10^{-3}	0.05	2.05
7	2.33	9.70×10^{-4}	2.26×10^{-3}	0.07	2.07
8	3.00	9.60×10^{-4}	2.87×10^{-3}	0.09	2.09
9	3.67	9.50×10^{-4}	3.48×10^{-3}	0.11	2.11
10	4.34	9.40×10^{-4}	4.07×10^{-3}	0.13	2.13
11	5.00	9.30×10^{-4}	4.65×10^{-3}	0.15	2.15
12	7.00	9.00×10^{-4}	6.34×10^{-3}	0.21	2.21
13	9.00	8.80×10^{-4}	7.93×10^{-3}	0.27	2.27
14	11.01	8.60×10^{-4}	9.45×10^{-3}	0.33	2.33
15	13.01	8.40×10^{-4}	1.09×10^{-2}	0.39	2.39
16	15.01	8.20×10^{-4}	1.22×10^{-2}	0.45	2.45
17	18.34	7.80×10^{-4}	1.44×10^{-2}	0.55	2.55
18	21.68	7.50×10^{-4}	1.64×10^{-2}	0.65	2.65
19	25.01	7.30×10^{-4}	1.82×10^{-2}	0.75	2.75
20	28.35	7.00×10^{-4}	1.99×10^{-2}	0.85	2.85
21	31.68	6.80×10^{-4}	2.15×10^{-2}	0.95	2.95
22	38.35	6.30×10^{-4}	2.44×10^{-2}	1.15	3.15
23	45.02	6.00×10^{-4}	2.69×10^{-2}	1.35	3.35
24	51.69	5.60×10^{-4}	2.91×10^{-2}	1.55	3.55

Table 2.5 The concentration of acetate ion was used in anion complexation studies with ligand **L** and the final ratios of guest:host

Point	AcO ⁻ /L	[L] mM	[AcO ⁻] mM	V of AcO ⁻ (mL)	V total (mL)
1	0.00	1.00 x 10 ⁻³	0	0	2.00
2	0.67	9.90 x 10 ⁻⁴	6.60 x 10 ⁻⁴	0.02	2.02
3	1.34	9.80 x 10 ⁻⁴	1.31 x 10 ⁻³	0.04	2.04
4	2.01	9.70 x 10 ⁻⁴	1.95 x 10 ⁻³	0.06	2.06
5	2.68	9.60 x 10 ⁻⁴	2.58 x 10 ⁻³	0.08	2.08
6	3.35	9.50 x 10 ⁻⁴	3.19 x 10 ⁻³	0.10	2.1
7	4.02	9.40 x 10 ⁻⁴	3.79 x 10 ⁻³	0.12	2.12
8	4.69	9.30 x 10 ⁻⁴	4.38 x 10 ⁻³	0.14	2.14
9	5.36	9.30 x 10 ⁻⁴	4.96 x 10 ⁻³	0.16	2.16
10	6.03	9.20 x 10 ⁻⁴	5.53 x 10 ⁻³	0.18	2.18
11	6.70	9.10 x 10 ⁻⁴	6.09 x 10 ⁻³	0.20	2.2
12	8.04	8.90 x 10 ⁻⁴	7.18 x 10 ⁻³	0.24	2.24
13	9.38	8.80 x 10 ⁻⁴	8.23 x 10 ⁻³	0.28	2.28
14	10.72	8.60 x 10 ⁻⁴	9.24 x 10 ⁻³	0.32	2.32
15	12.06	8.50 x 10 ⁻⁴	1.02 x 10 ⁻²	0.36	2.36
16	13.40	8.30 x 10 ⁻⁴	1.12 x 10 ⁻²	0.40	2.40
17	16.75	8.00 x 10 ⁻⁴	1.34 x 10 ⁻²	0.50	2.50
18	20.10	7.70 x 10 ⁻⁴	1.55 x 10 ⁻²	0.60	2.60
19	23.45	7.40 x 10 ⁻⁴	1.74 x 10 ⁻²	0.70	2.70
20	26.80	7.10 x 10 ⁻⁴	1.91 x 10 ⁻²	0.80	2.80
21	30.15	6.90 x 10 ⁻⁴	2.08 x 10 ⁻²	0.90	2.90
22	36.85	6.50 x 10 ⁻⁴	2.38 x 10 ⁻²	1.10	3.10
23	43.55	6.10 x 10 ⁻⁴	2.64 x 10 ⁻²	1.30	3.30
24	50.25	5.70 x 10 ⁻⁴	2.87 x 10 ⁻²	1.50	3.50
25	56.95	5.40 x 10 ⁻⁴	3.08 x 10 ⁻²	1.70	3.70

Table 2.6 The concentration of dihydrogenphosphate ion was used in anion complexation studies with ligand **L** and the final ratios of guest:host

Point	H ₂ PO ₄ ⁻ /L	[L] mM	[H ₂ PO ₄ ⁻] mM	V of H ₂ PO ₄ ⁻ (mL)	V total (mL)
1	0.00	1.00 x 10 ⁻³	0	0	2.00
2	0.67	9.90 x 10 ⁻⁴	6.60 x 10 ⁻⁴	0.02	2.02
3	1.33	9.80 x 10 ⁻⁴	1.31 x 10 ⁻³	0.04	2.04
4	2.00	9.70 x 10 ⁻⁴	1.94 x 10 ⁻³	0.06	2.06
5	2.67	9.60 x 10 ⁻⁴	2.57 x 10 ⁻³	0.08	2.08
6	3.34	9.50 x 10 ⁻⁴	3.18 x 10 ⁻³	0.10	2.10
7	4.67	9.30 x 10 ⁻⁴	4.36 x 10 ⁻³	0.14	2.14
8	6.00	9.20 x 10 ⁻⁴	5.51 x 10 ⁻³	0.18	2.18
9	7.34	9.00 x 10 ⁻⁴	6.61 x 10 ⁻³	0.22	2.22
10	8.67	8.80 x 10 ⁻⁴	7.67 x 10 ⁻³	0.26	2.26
11	10.01	8.70 x 10 ⁻⁴	8.70 x 10 ⁻³	0.30	2.30
12	13.34	8.30 x 10 ⁻⁴	1.11 x 10 ⁻²	0.40	2.40
13	16.68	8.00 x 10 ⁻⁴	1.33 x 10 ⁻²	0.50	2.50
14	20.01	7.70 x 10 ⁻⁴	1.54 x 10 ⁻²	0.60	2.60
15	23.35	7.40 x 10 ⁻⁴	1.73 x 10 ⁻²	0.70	2.70
16	26.68	7.10 x 10 ⁻⁴	1.91 x 10 ⁻²	0.80	2.80
17	33.35	6.70 x 10 ⁻⁴	2.22 x 10 ⁻²	1.00	3.00
18	40.02	6.30 x 10 ⁻⁴	2.50 x 10 ⁻²	1.20	3.20
19	46.69	5.90 x 10 ⁻⁴	2.75 x 10 ⁻²	1.40	3.40
20	53.36	5.60 x 10 ⁻⁴	2.96 x 10 ⁻²	1.60	3.60
21	60.03	5.30 x 10 ⁻⁴	3.16 x 10 ⁻²	1.80	3.80

2.5.2 Complexation studies of Ligand L with transition metal cations : silver and copper

Typically, a solution of 1×10^{-6} M of a ligand L in a 0.01 M tetrabutylammonium hexafluorophosphate in dried acetonitrile was prepared by adding 0.1 mL of a stock solution of ligand L (1×10^{-4} M) in a 10 mL volumetric flask. A stock solution of 0.025 M of a transition metal ion (Cu^{2+} and Ag^+ as nitrate salt) in dried acetonitrile was prepared in a 25 mL volumetric flask.

Fluorescent spectra of ligand L and metal complexes were recorded from 230-700 nm at ambient temperature. The solution of a metal ion was added directly to 2.00 mL of 1×10^{-6} M ligand L in a 1-cm quartz cuvette by microburette and stirred for 30 seconds. Fluorescent spectra were measured after each addition to have guest:host ratios from 0:1 to 50:1.



สถาบันวิทยบริการ
จุฬาลงกรณ์มหาวิทยาลัย

Table 2.7 The concentration of copper ion was used in anion complexation studies with ligand **L** and the final ratios of guest:host

Point	$\text{Cu}^{2+} / \text{L}$	$[\text{L}] \text{ mM}$	$[\text{Cu}^{2+}] \text{ mM}$	V of Cu^{2+} (mL)	V total (mL)
1	0.00	1.00×10^{-3}	0	0	2.00
2	0.67	9.90×10^{-4}	6.60×10^{-4}	0.02	2.02
3	1.33	9.80×10^{-4}	1.31×10^{-3}	0.04	2.04
4	2.00	9.70×10^{-4}	1.94×10^{-3}	0.06	2.06
5	2.67	9.60×10^{-4}	2.57×10^{-3}	0.08	2.08
6	3.34	9.50×10^{-4}	3.18×10^{-3}	0.10	2.10
7	4.00	9.40×10^{-4}	3.78×10^{-3}	0.12	2.12
8	4.67	9.30×10^{-4}	4.36×10^{-3}	0.14	2.14
9	5.34	9.30×10^{-4}	4.94×10^{-3}	0.16	2.16
10	6.00	9.20×10^{-4}	5.51×10^{-3}	0.18	2.18
11	6.67	9.10×10^{-4}	6.06×10^{-3}	0.20	2.20
12	8.00	8.90×10^{-4}	7.15×10^{-3}	0.24	2.24
13	9.34	8.80×10^{-4}	8.19×10^{-3}	0.28	2.28
14	10.67	8.60×10^{-4}	9.20×10^{-3}	0.32	2.32
15	12.01	8.50×10^{-4}	1.02×10^{-2}	0.36	2.36
16	13.34	8.30×10^{-4}	1.11×10^{-2}	0.40	2.40
17	16.01	8.10×10^{-4}	1.29×10^{-2}	0.48	2.48
18	18.68	7.80×10^{-4}	1.46×10^{-2}	0.56	2.56
19	21.34	7.60×10^{-4}	1.62×10^{-2}	0.64	2.64
20	24.01	7.40×10^{-4}	1.77×10^{-2}	0.72	2.72
21	26.68	7.10×10^{-4}	1.91×10^{-2}	0.80	2.80
22	30.02	6.90×10^{-4}	2.07×10^{-2}	0.90	2.90
23	33.35	6.70×10^{-4}	2.22×10^{-2}	1.00	3.00
24	36.69	6.50×10^{-4}	2.37×10^{-2}	1.10	3.10
25	40.02	6.30×10^{-4}	2.50×10^{-2}	1.20	3.20
26	43.36	6.10×10^{-4}	2.63×10^{-2}	1.30	3.30
27	46.69	5.90×10^{-4}	2.75×10^{-2}	1.40	3.40
28	50.03	5.70×10^{-4}	2.86×10^{-2}	1.50	3.50
29	53.36	5.60×10^{-4}	2.96×10^{-2}	1.60	3.60
30	56.70	5.40×10^{-4}	3.06×10^{-2}	1.70	3.70

Table 2.8 The concentration of silver ion was used in anion complexation studies with ligand **L** and the final ratios of guest:host

Point	Ag ⁺ /L	[L] mM	[Ag ⁺] mM	V of M (mL)	V total (mL)
1	0.00	1.00 x 10 ⁻³	0	0	2.00
2	1.33	9.80 x 10 ⁻⁴	1.31 x 10 ⁻³	0.04	2.04
3	2.67	9.60 x 10 ⁻⁴	2.57 x 10 ⁻³	0.08	2.08
4	4.00	9.40 x 10 ⁻⁴	3.78 x 10 ⁻³	0.12	2.12
5	5.34	9.30 x 10 ⁻⁴	4.94 x 10 ⁻³	0.16	2.16
6	6.67	9.10 x 10 ⁻⁴	6.06 x 10 ⁻³	0.20	2.20
7	8.00	8.90 x 10 ⁻⁴	7.15 x 10 ⁻³	0.24	2.24
8	9.34	8.80 x 10 ⁻⁴	8.19 x 10 ⁻³	0.28	2.28
9	10.67	8.60 x 10 ⁻⁴	9.20 x 10 ⁻³	0.32	2.32
10	12.01	8.50 x 10 ⁻⁴	1.02 x 10 ⁻²	0.36	2.36
11	13.34	8.30 x 10 ⁻⁴	1.11 x 10 ⁻²	0.40	2.40
12	15.34	8.10 x 10 ⁻⁴	1.25 x 10 ⁻²	0.46	2.46
13	17.34	7.90 x 10 ⁻⁴	1.38 x 10 ⁻²	0.52	2.52
14	19.34	7.80 x 10 ⁻⁴	1.50 x 10 ⁻²	0.58	2.58
15	21.34	7.60 x 10 ⁻⁴	1.62 x 10 ⁻²	0.64	2.64
16	23.35	7.40 x 10 ⁻⁴	1.73 x 10 ⁻²	0.70	2.70
17	26.01	7.20 x 10 ⁻⁴	1.87 x 10 ⁻²	0.78	2.78
18	28.68	7.00 x 10 ⁻⁴	2.01 x 10 ⁻²	0.86	2.86
19	31.35	6.80 x 10 ⁻⁴	2.13 x 10 ⁻²	0.94	2.94
20	34.02	6.60 x 10 ⁻⁴	2.25 x 10 ⁻²	1.02	3.02
21	36.69	6.50 x 10 ⁻⁴	2.37 x 10 ⁻²	1.10	3.10
22	40.02	6.30 x 10 ⁻⁴	2.50 x 10 ⁻²	1.20	3.20
23	43.36	6.10 x 10 ⁻⁴	2.63 x 10 ⁻²	1.30	3.30
24	46.69	5.90 x 10 ⁻⁴	2.75 x 10 ⁻²	1.40	3.40
25	50.03	5.70 x 10 ⁻⁴	2.86 x 10 ⁻²	1.50	3.50
26	53.36	5.60 x 10 ⁻⁴	2.96 x 10 ⁻²	1.60	3.60
27	56.70	5.40 x 10 ⁻⁴	3.06 x 10 ⁻²	1.70	3.70

2.5.3 Complexation studies of Ligand L in the presence of 5 equivalents of an anion (F^- , AcO^- or $H_2PO_4^-$) with various cations : copper and silver

Typically, A stock solution of anion 1×10^{-6} mol of ligand L (1×10^{-5} M) in a 0.01 M tetrabutylammonium hexafluorophosphate in dried acetonitrile was prepared by adding the solution of an anion 1×10^{-6} mol and 2 mL of a stock solution of ligand L (1×10^{-4} M) in a 20 mL volumetric flask.

Fluorescent spectra of ligand L plus anion and cation complexes were recorded from 230-700 nm at ambient temperature. The solution of a metal ion was added directly to 2.00 mL of 1×10^{-5} M ligand L and anion in a 1-cm quartz cuvette by microburette and stirred for 30 seconds. Fluorescent spectra were measured after adding of a solution of a transition metal ion as nitrate salt in acetonitrile. The concentration of a transition metal ion in supporting electrolyte added gradually in cuvette was shown in the table 2.4.

Table 2.9 The concentration of anions that used in transition metal ion complexation studies with ligand L in the presence of an anion and final ratios of guest:host

anion	[anion] (M)	mole of anion	equivalent anion : ligand	[guest] (M)		guest:host	
				Ag^+	Cu^{2+*}	Ag^+	Cu^{2+}
F^-	5×10^{-5}	1×10^{-6}	5.0	6.67×10^{-5}	6.67×10^{-5}	5:1	5:1
AcO^-	5×10^{-5}	1×10^{-6}	5.0	6.67×10^{-5}	6.67×10^{-5}	5:1	5:1
$H_2PO_4^-$	5×10^{-5}	1×10^{-6}	5.0	6.67×10^{-5}	6.67×10^{-5}	5:1	5:1

* The concentration of Cu^{2+} ions were determined by EDTA titration using merexide as an indicator before used in UV-vis and fluorescent titrations.

Table 2.10 The concentration of fluoride ion was used in silver ion complexation studies with ligand **L** in the presence of an anion and final ratios of guest:host

Point	Ag ⁺ /L	[L+F ⁻] mM	[Ag ⁺] mM	V of M (mL)	V total (mL)
1	0.00	1.00 x 10 ⁻²	0	0	2.00
2	0.07	9.90 x 10 ⁻³	6.60 x 10 ⁻³	0.02	2.02
3	0.13	9.80 x 10 ⁻³	1.31 x 10 ⁻³	0.04	2.04
4	0.20	9.71 x 10 ⁻³	1.94 x 10 ⁻³	0.06	2.06
5	0.27	9.62 x 10 ⁻³	2.57 x 10 ⁻³	0.08	2.08
6	0.33	9.52 x 10 ⁻³	3.18 x 10 ⁻³	0.10	2.10
7	0.40	9.43 x 10 ⁻³	3.78 x 10 ⁻³	0.12	2.12
8	0.47	9.35 x 10 ⁻³	4.36 x 10 ⁻³	0.14	2.14
9	0.53	9.26 x 10 ⁻³	4.94 x 10 ⁻³	0.16	2.16
10	0.60	9.17 x 10 ⁻³	5.51 x 10 ⁻³	0.18	2.18
11	0.67	9.09 x 10 ⁻³	6.06 x 10 ⁻³	0.20	2.20
12	0.80	8.93 x 10 ⁻³	7.15 x 10 ⁻³	0.24	2.24
13	0.93	8.77 x 10 ⁻³	8.19 x 10 ⁻³	0.28	2.28
14	1.07	8.62 x 10 ⁻³	9.20 x 10 ⁻³	0.32	2.32
15	1.20	8.47 x 10 ⁻³	1.02 x 10 ⁻²	0.36	2.36
16	1.33	8.33 x 10 ⁻³	1.12 x 10 ⁻²	0.40	2.40
17	1.60	8.06 x 10 ⁻³	1.29 x 10 ⁻²	0.48	2.48
18	1.87	7.81 x 10 ⁻³	1.46 x 10 ⁻²	0.56	2.56
19	2.13	7.58 x 10 ⁻³	1.62 x 10 ⁻²	0.64	2.64
20	2.40	7.35 x 10 ⁻³	1.77 x 10 ⁻²	0.72	2.72
21	2.67	7.14 x 10 ⁻³	1.91 x 10 ⁻²	0.80	2.80
22	3.00	6.90 x 10 ⁻³	2.07 x 10 ⁻²	0.90	2.90
23	3.34	6.67 x 10 ⁻³	2.22 x 10 ⁻²	1.00	3.00
24	3.67	6.45 x 10 ⁻³	2.37 x 10 ⁻²	1.10	3.10
25	4.00	6.25 x 10 ⁻³	2.50 x 10 ⁻²	1.20	3.20
26	4.34	6.06 x 10 ⁻³	2.63 x 10 ⁻²	1.30	3.30
27	4.67	5.88 x 10 ⁻³	2.75 x 10 ⁻²	1.40	3.40
28	5.00	5.71 x 10 ⁻³	2.86 x 10 ⁻²	1.50	3.50
29	5.34	5.56 x 10 ⁻³	2.96 x 10 ⁻²	1.60	3.60

Table 2.11 The concentration of acetate ion was used in silver ion complexation studies with ligand L in the presence of an anion and final ratios of guest:host

Point	Ag ⁺ /L	[L+AcO ⁻] mM	[Ag ⁺] mM	V of M (mL)	V total (mL)
1	0.00	1 x 10 ⁻²	0	0	2.00
2	0.07	9.90 x 10 ⁻³	6.60 x 10 ⁻⁴	0.02	2.02
3	0.13	9.80 x 10 ⁻³	1.31 x 10 ⁻³	0.04	2.04
4	0.20	9.71 x 10 ⁻³	1.94 x 10 ⁻³	0.06	2.06
5	0.27	9.62 x 10 ⁻³	2.57 x 10 ⁻³	0.08	2.08
6	0.33	9.52 x 10 ⁻³	3.18 x 10 ⁻³	0.10	2.10
7	0.47	9.35 x 10 ⁻³	4.36 x 10 ⁻³	0.14	2.14
8	0.60	9.17 x 10 ⁻³	5.51 x 10 ⁻³	0.18	2.18
9	0.73	9.01 x 10 ⁻³	6.61 x 10 ⁻³	0.22	2.22
10	0.87	8.85 x 10 ⁻³	7.67 x 10 ⁻³	0.26	2.26
11	1.00	8.70 x 10 ⁻³	8.70 x 10 ⁻³	0.30	2.30
12	1.33	8.33 x 10 ⁻³	1.11 x 10 ⁻²	0.40	2.40
13	1.67	8.00 x 10 ⁻³	1.33 x 10 ⁻²	0.50	2.50
14	2.00	7.69 x 10 ⁻³	1.54 x 10 ⁻²	0.60	2.60
15	2.33	7.41 x 10 ⁻³	1.73 x 10 ⁻²	0.70	2.70
16	2.67	7.14 x 10 ⁻³	1.91 x 10 ⁻²	0.80	2.80
17	3.34	6.67 x 10 ⁻³	2.22 x 10 ⁻²	1.00	3.00
18	4.00	6.25 x 10 ⁻³	2.50 x 10 ⁻²	1.20	3.20
19	4.67	5.88 x 10 ⁻³	2.75 x 10 ⁻²	1.40	3.40
20	5.34	5.56 x 10 ⁻³	2.96 x 10 ⁻²	1.60	3.60
21	6.00	5.26 x 10 ⁻³	3.16 x 10 ⁻²	1.80	3.80

จุฬาลงกรณ์มหาวิทยาลัย

Table 2.12 The concentration of acetate ion was used in copper ion complexation studies with ligand **L** in the presence of an anion and final ratios of guest:host

Point	Cu^{2+}/L	$[\text{L}+\text{AcO}^-]$ mM	$[\text{Cu}^{2+}]$ mM	V of M ml	V total ml
1	0.00	1.00×10^{-2}	0	0	2.00
2	0.07	9.90×10^{-3}	6.60×10^{-4}	0.02	2.02
3	0.13	9.80×10^{-3}	1.31×10^{-3}	0.04	2.04
4	0.20	9.71×10^{-3}	1.94×10^{-3}	0.06	2.06
5	0.27	9.62×10^{-3}	2.57×10^{-3}	0.08	2.08
6	0.33	9.52×10^{-3}	3.18×10^{-3}	0.10	2.10
7	0.47	9.35×10^{-3}	4.36×10^{-3}	0.14	2.14
8	0.60	9.17×10^{-3}	5.51×10^{-3}	0.18	2.18
9	0.73	9.01×10^{-3}	6.61×10^{-3}	0.22	2.22
10	0.87	8.85×10^{-3}	7.67×10^{-3}	0.26	2.26
11	1.00	8.70×10^{-3}	8.70×10^{-3}	0.30	2.30
12	1.33	8.33×10^{-3}	1.11×10^{-2}	0.40	2.40
13	1.67	8.00×10^{-3}	1.33×10^{-2}	0.50	2.50
14	2.00	7.69×10^{-3}	1.54×10^{-2}	0.60	2.60
15	2.33	7.41×10^{-3}	1.73×10^{-2}	0.70	2.70
16	2.67	7.14×10^{-3}	1.91×10^{-2}	0.80	2.80
17	3.00	6.90×10^{-3}	2.07×10^{-2}	0.90	2.90
18	3.34	6.67×10^{-3}	2.22×10^{-2}	1.00	3.00
19	3.67	6.45×10^{-3}	2.37×10^{-2}	1.10	3.10
20	4.00	6.25×10^{-3}	2.50×10^{-2}	1.20	3.20
21	4.67	5.88×10^{-3}	2.75×10^{-2}	1.40	3.40
22	5.34	5.56×10^{-3}	2.96×10^{-2}	1.60	3.60
23	6.00	5.26×10^{-3}	3.16×10^{-2}	1.80	3.80

Table 2.13 The concentration of dihydrogenphosphate ion was used in silver ion complexation studies with ligand **L** in the presence of an anion and final ratios of guest:host

Point	Ag ⁺ /L	[L+H ₂ PO ₄ ⁻] mM	[Ag ⁺] mM	V of M (mL)	V total (mL)
1	0.00	1.00 x 10 ⁻²	0	0	2.00
2	0.07	9.90 x 10 ⁻³	6.60 x 10 ⁻³	0.02	2.02
3	0.13	9.80 x 10 ⁻³	1.31 x 10 ⁻³	0.04	2.04
4	0.20	9.71 x 10 ⁻³	1.94 x 10 ⁻³	0.06	2.06
5	0.27	9.62 x 10 ⁻³	2.57 x 10 ⁻³	0.08	2.08
6	0.33	9.52 x 10 ⁻³	3.18 x 10 ⁻³	0.10	2.10
7	0.40	9.43 x 10 ⁻³	3.78 x 10 ⁻³	0.12	2.12
8	0.47	9.35 x 10 ⁻³	4.36 x 10 ⁻³	0.14	2.14
9	0.53	9.26 x 10 ⁻³	4.94 x 10 ⁻³	0.16	2.16
10	0.60	9.17 x 10 ⁻³	5.51 x 10 ⁻³	0.18	2.18
11	0.67	9.09 x 10 ⁻³	6.06 x 10 ⁻³	0.20	2.20
12	0.80	8.93 x 10 ⁻³	7.15 x 10 ⁻³	0.24	2.24
13	0.93	8.77 x 10 ⁻³	8.19 x 10 ⁻³	0.28	2.28
14	1.07	8.62 x 10 ⁻³	9.20 x 10 ⁻³	0.32	2.32
15	1.20	8.47 x 10 ⁻³	1.02 x 10 ⁻²	0.36	2.36
16	1.33	8.33 x 10 ⁻³	1.11 x 10 ⁻²	0.40	2.40
17	1.60	8.06 x 10 ⁻³	1.29 x 10 ⁻²	0.48	2.48
18	1.87	7.81 x 10 ⁻³	1.46 x 10 ⁻²	0.56	2.56
19	2.13	7.58 x 10 ⁻³	1.62 x 10 ⁻²	0.64	2.64
20	2.40	7.35 x 10 ⁻³	1.77 x 10 ⁻²	0.72	2.72
21	2.67	7.14 x 10 ⁻³	1.91 x 10 ⁻²	0.80	2.80
22	3.00	6.90 x 10 ⁻³	2.07 x 10 ⁻²	0.90	2.90
23	3.34	6.67 x 10 ⁻³	2.22 x 10 ⁻²	1.00	3.00
24	3.67	6.45 x 10 ⁻³	2.37 x 10 ⁻²	1.10	3.10
25	4.00	6.25 x 10 ⁻³	2.50 x 10 ⁻²	1.20	3.20
26	4.34	6.06 x 10 ⁻³	2.63 x 10 ⁻²	1.30	3.30
27	4.67	5.88 x 10 ⁻³	2.75 x 10 ⁻²	1.40	3.40
28	5.00	5.71 x 10 ⁻³	2.86 x 10 ⁻²	1.50	3.50
29	5.34	5.56 x 10 ⁻³	2.96 x 10 ⁻²	1.60	3.60

Table 2.14 The concentration of dihydrogenphosphate ion that used in copper ion complexation studies with ligand L in the presence of an anion and final ratios of guest:host

Point	Cu^{2+}/L	$[\text{L}+\text{H}_2\text{PO}_4^-]$ mM	$[\text{Cu}^{2+}]$ mM	V of M (mL)	V total (mL)
1	0.00	1.00×10^{-2}	0	0	2.00
2	0.07	9.90×10^{-3}	6.60×10^{-4}	0.02	2.02
3	0.13	9.80×10^{-3}	1.31×10^{-3}	0.04	2.04
4	0.20	9.71×10^{-3}	1.94×10^{-3}	0.06	2.06
5	0.27	9.62×10^{-3}	2.57×10^{-3}	0.08	2.08
6	0.33	9.52×10^{-3}	3.18×10^{-3}	0.10	2.10
7	0.40	9.43×10^{-3}	3.78×10^{-3}	0.12	2.12
8	0.47	9.35×10^{-3}	4.36×10^{-3}	0.14	2.14
9	0.53	9.26×10^{-3}	4.94×10^{-3}	0.16	2.16
10	0.60	9.17×10^{-3}	5.51×10^{-3}	0.18	2.18
11	0.67	9.09×10^{-3}	6.06×10^{-3}	0.20	2.20
12	0.80	8.93×10^{-3}	7.15×10^{-3}	0.24	2.24
13	0.93	8.77×10^{-3}	8.19×10^{-3}	0.28	2.28
14	1.07	8.62×10^{-3}	9.20×10^{-3}	0.32	2.32
15	1.20	8.47×10^{-3}	1.02×10^{-2}	0.36	2.36
16	1.33	8.33×10^{-3}	1.11×10^{-2}	0.40	2.40
17	1.60	8.06×10^{-3}	1.29×10^{-2}	0.48	2.48
18	1.87	7.81×10^{-3}	1.46×10^{-2}	0.56	2.56
19	2.13	7.58×10^{-3}	1.61×10^{-2}	0.64	2.64
20	2.40	7.35×10^{-3}	1.77×10^{-2}	0.72	2.72
21	2.67	7.14×10^{-3}	1.91×10^{-2}	0.80	2.80
22	3.00	6.90×10^{-3}	2.07×10^{-2}	0.90	2.90
23	3.34	6.67×10^{-3}	2.22×10^{-2}	1.00	3.00
24	3.67	6.45×10^{-3}	2.37×10^{-2}	1.10	3.10
25	4.00	6.25×10^{-3}	2.50×10^{-2}	1.20	3.20
26	4.34	6.06×10^{-3}	2.63×10^{-2}	1.30	3.30
27	4.67	5.88×10^{-3}	2.75×10^{-2}	1.40	3.40
28	5.00	5.71×10^{-3}	2.86×10^{-2}	1.50	3.50
29	5.34	5.56×10^{-3}	2.96×10^{-2}	1.60	3.60

CHAPTER III

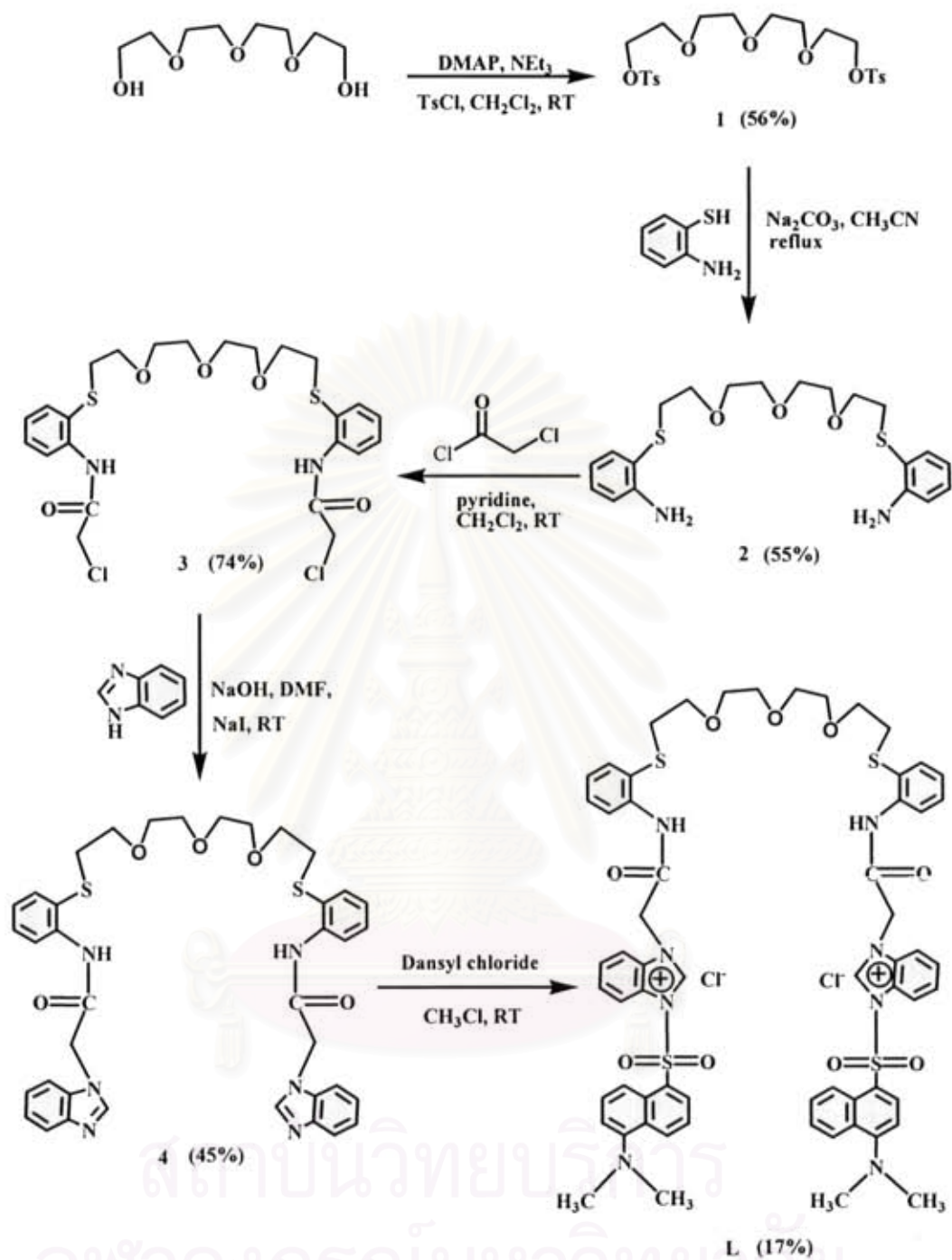
RESULTS AND DISCUSSION

3.1 Design concept

It is known that polyethylene glycol, tetraethylene glycol dimethyl ether (glyme) and their ethers are one of the most versatile building blocks. Receptors and sensory units (chromophores and fluorophores) can be attached to both of their terminals. Consequently, these systems are an interest of utilization for recognition of analytes in the applications of molecular switches, molecular sensors, molecular gates, and etc.

On the basic of this strategy. We placed thiophenol moieties for binding transition metals and amide group and imidazolium salt for binding anion at both of podand terminals. That expected for making in bifunctional receptor allosteric switch or/and molecular gate. Because of a highly flexible of acyclic crown ether, we used their utilization for change the structure from linear crown ether to pseudocyclic crown ether upon complexation with metal ion. According to the desired property, suitable amide and imidazole moieties should be preorganized in the system for binding anion using hydrogen bonding interaction and electrostatic force $[(C-H)^+ \cdots X^-]$. Furthermore, the dansyl (dimethylaminonaphthalene sulfonyl) group was chosen as the fluorophore because it is very sensitive to solvent polarity and it has widely used for fluorescent labeling amines. [44-45]

Therefore, ligand **L** was synthesized by attaching 2-aminothiophenol and benzimidazole moieties at both terminals of the podand and studied the complexation by 1H - NMR, UV-Vis and fluorescent spectroscopy. The synthetic pathway is shown in Scheme 3.1.



Scheme 3.1 Synthesis pathway of acyclic thiacrown ether derivatives L

3.2 Synthesis and characterization of acyclic thiacyclic crown ether derivatives containing imidazolium moieties (L)

In order to improve the yields of ligand **L**, many bases, solvents system and different reaction conditions were tried. The synthesis of acyclic thiacyclic crown ether derivatives containing imidazolium moieties **L** was carried out by the nucleophilic substitution reaction in various conditions.

The synthetic pathway was started by tosylation of tetraethylene glycol and toluene-4-sulfonyl chloride in the presence of triethylamine as base and catalytic amount of DMAP. After purification by column chromatography using 10% ethyl acetate in dichloromethane as eluent, the tetraethylene glycol ditosylate was obtained as colorless oil in 56% yield. The $^1\text{H-NMR}$ spectrum showed the characteristic peaks of tosyl groups as singlet of the methyl protons (ArCH_3) at 2.359 ppm, two doublets of the aromatic proton (ArH) at 7.716 and 7.270 ppm and the bridging glycolic protons ($\text{OCH}_2\text{CH}_2\text{O}$) appeared at 4.083-3.606 ppm.

The tetraethylene glycol ditosylate (**1**) was reacted with 2-aminothiophenol using 5 equiv. of anhydrous sodium carbonate as base in acetonitrile under nitrogen atmosphere. Unfortunately, no desired product was obtained. Probably, two protons on thiol should be deprotonated by refluxing between base and 2-aminothiophenol before adding the tetraethylene glycol ditosylate, resulting in the 1,8-Bis(aminothiophenol) tetraethylene glycol (**2**). The desired product was purified by column chromatography using dichloromethane until 15% ethyl acetate as eluent, to gain 55% yield as the yellow oil of compound **2**. Since compound **2** containing the aromatic amine may be easy to be decomposed, it should be done for the next step immediately. The $^1\text{H-NMR}$ data of determined **2** displayed the absence of the doublets of aromatic protons and methyl protons of toluenesulfonyl (Tos) at 7.716 and 7.270 ppm and at 2.359 ppm, respectively. Additionally, two doublets and two triplets of aromatic protons of 2-aminothiophenol moieties were found at 7.391-6.672 ppm. The bridging glycolic protons moved to upfield shift at 3.577-2.933 ppm.

The primary amine **2** was then transformed to amide using chloroacetyl chloride in the presence of pyridine as base in dichloromethane under nitrogen atmosphere at room temperature for 4 h. The reaction temperature was cooled down and kept to 0 °C while the solution of chloroacetyl chloride in dichloromethane was slowly dropped to avoid a vigorous reaction. The color of the mixture was changed

from light yellow to purple. The amide derivative **3** was obtained as a gray liquid in 74 % yields after treatment with 3 M hydrochloric acid to get rid of residue base and extraction with dichloromethane. $^1\text{H-NMR}$ data of compound **3** showed a singlet signal of *NH* protons at 9.723 ppm corresponding to amide protons. Interestingly, two doublets and two triplets of aromatic protons of 2-aminothiophenol moieties were assigned by downfield shift to 8.397-7.107 ppm affecting by an electron withdrawing group of carbonyl parts. Moreover, the appearance of singlet assignment of ClCH_2CO at 4.250 ppm in the spectrum supported the structure of compound **3**.

Nucleophilic substitution of **3** was achieved using the reaction between benzimidazole and sodium hydroxide as base in DMF. In order to deprotonate *NH* protons of benzimidazole, sodium hydroxide was left stirring in DMF for 0.5 h. prior to add the solution of compound **3** in DMF. The reaction was carried out under nitrogen atmosphere for 2 days. Compound **4** was obtained as a yellow solid in 45% yields after purification by column chromatography using ethyl acetate until 10% methanol as eluent. $^1\text{H-NMR}$ spectrum of compound **4** was assigned a singlet signal of *NH* protons of amide group and *NCHN* of benzimidazole at 8.875 and 8.052 ppm, respectively. The range of aromatic protons (7-10 ppm) of compound **4** showed a significant difference from those of compound **3** in an attribution to aromatic protons of benzimidazole part. Furthermore, $^1\text{H-NMR}$ spectrum of **4** exhibited three signals of $\text{CH}_2\text{OCH}_2\text{CH}_2\text{O}$ of tetraethylene glycol at 3.448, 3.394 and 3.200 ppm with the different *J*-coupling constants which indicated that the ethylene bridge protons were in the different environments possibly caused by the steric hindrance of benzimidazolium derivatives.

Finally, the final product containing imidazolium salt was accomplished by the coupling reaction with dansyl chloride as fluorophore. The addition 2.2 equiv. of dansyl chloride solution into compound **4** in chloroform under nitrogen atmosphere at room temperature provided the fluorescent molecule **L**. Obviously, the reaction should be carried out under dark condition because dansyl groups were sensitive to light. The color change of solution was observed from light yellow to bright green, when checked the reaction in UV- lamp, indicating the product as a fluorescent compound. Compound **L** bearing chloride as counter anions was achieved as a bright green solid in 17% yield after purification by column chromatography using ethyl acetate as eluent. The $^1\text{H-NMR}$ spectrum depicted in Figure 3.1 displayed both downfield shifts of a singlet signal of *NH* protons and singlet signal of C^+-H of

benzimidazole at 10.832 and 9.101 ppm, respectively. Possibly, these events occurred because $C^+ \cdots H$ proton formed the hydrogen bonding with chloride ion and dansyl was the electron acceptor. Consequently, protons at NH amide proton and C^+-H of benzimidazole existed at low electron density. Aromatic protons of dansyl groups also exhibited at 8.570 and 7.454 ppm and additionally, the methyl protons of dansyl groups appeared at 2.872 ppm. MALDI-TOF mass spectrum in Figure 3.2 confirmed the structure of **L** observed by an intense peak at m/z 1266.77 corresponding to the mass of **L** having dansyl fluorophore and chloride counter anions.

In addition, IR spectrum (Figure 3.3) of **L** exhibited an absorption bands of NH stretching at 3444.48 cm^{-1} , amide $C=O$ stretching at 1672.94 cm^{-1} , aromatic $C=C$ stretching at 1578.30 cm^{-1} and dansyl $S=O$ stretching at 1338.5 and 1143.99 cm^{-1} . According to all results, the obtained product has a structure in agreement with the structure of **L**.

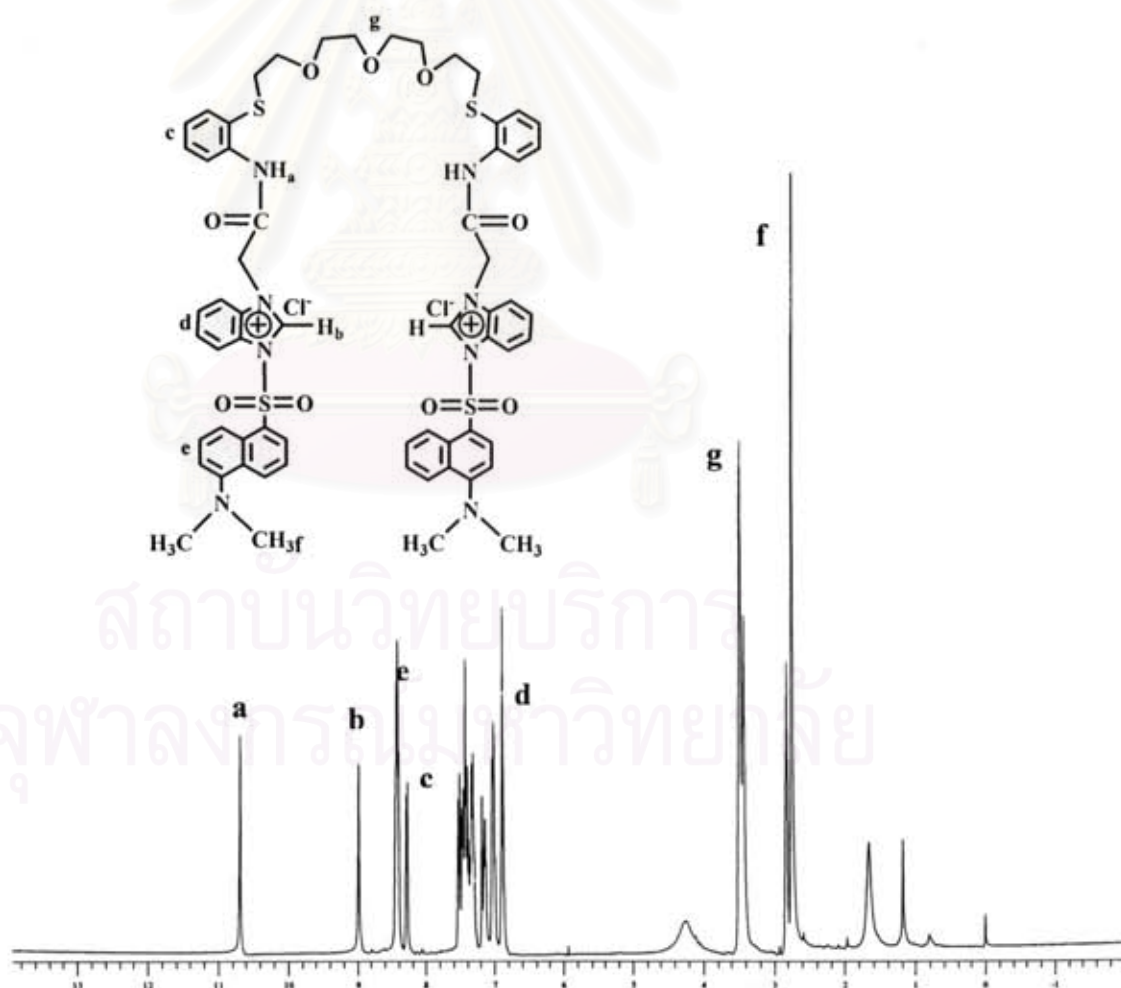


Figure 3.1 The 1H -NMR spectrum of acyclic thiacycrown ether containing imidazolium and dansyl fluorophore (**L**)

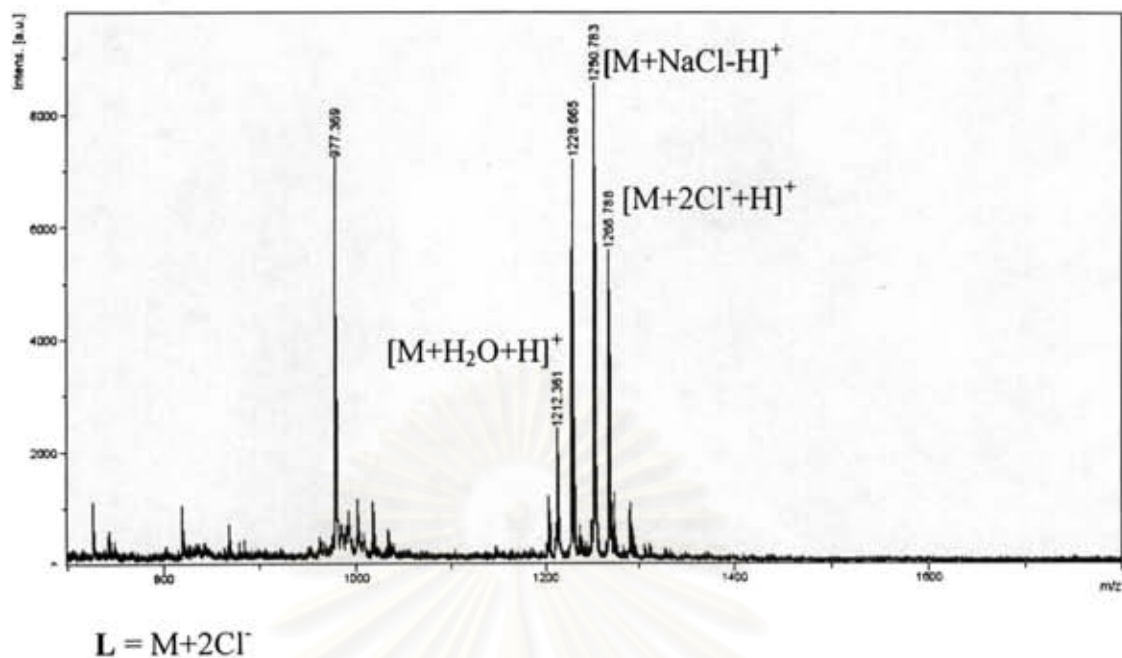


Figure 3.2 MALDI-TOF mass spectrum of L

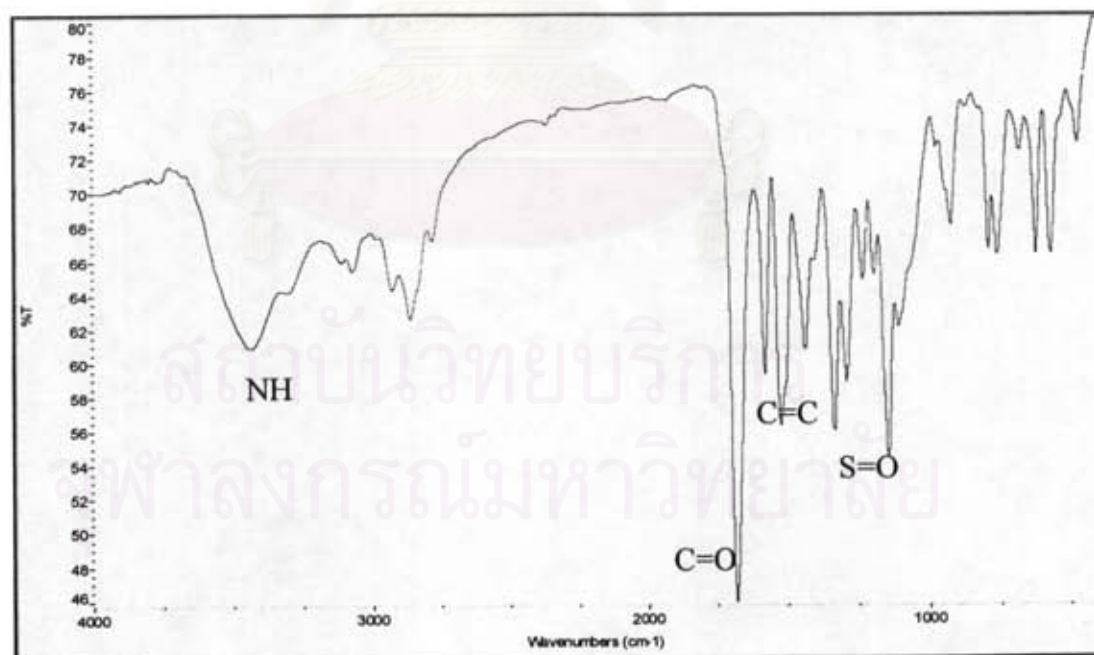


Figure 3.3 IR spectrum of L

3.3 The complexation studies of ligand L

Ligand L also contains two sulfur and two nitrogen donor atoms at the end of tetraethylene glycol part, which can chelate metal ions into their cavities. Both of them were used to study their binding ability towards transition metal ions. Furthermore, ligand L has amide NH groups and imidazolium moieties designed as anion binding sites *via* hydrogen bonding and electrostatic interactions. Thus, we studied the binding properties of ligand L and both cations and anions by $^1\text{H-NMR}$, UV-Vis and fluorescent techniques.

Ligand L was designed using dansyl groups as fluorophores. Therefore, we employed fluorescence titration to investigate the basicity and complexation abilities of L.

The initial experiment to evaluate the potential of ligand L as ditopic receptor and to validate reasoning began with the $^1\text{H-NMR}$ spectroscopy. Moreover, we, firstly, studied the effect of the structural change and the effect of anion toward cations binding ability by $^1\text{H-NMR}$ spectroscopy.

3.3.1 Anion complexation studies

3.3.1.1 Anion complexation studies by $^1\text{H-NMR}$ spectroscopy

Preliminary binding studies of complexation between ligand L and various anions such as F^- , H_2PO_4^- , CH_3CO_2^- and $\text{C}_6\text{H}_5\text{CO}_2^-$ were determined by $^1\text{H-NMR}$ spectroscopy. To reduce the effect of ion pair, tetrabutylammonium should be used as counter cations. For this purpose, ligand L was titrated with tetrabutylammonium salt of various anions to evaluate binding properties. $^1\text{H-NMR}$ spectrum was found that the NH amide protons disappeared after adding various anions caused by deprotonation process. Because anions mentioned above are basic so they can abstract protons on the NH amide groups observed by disappearance of these protons in $^1\text{H-NMR}$ spectra as showed in Figure 3.4.

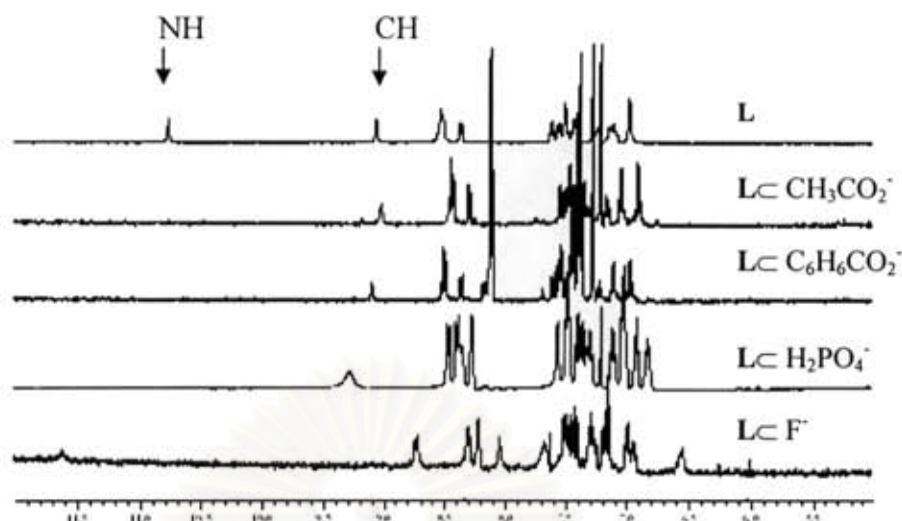


Figure 3.4 ^1H -NMR spectra (400 MHz) of L toward various anions

The selectivity is investigated by properties of anion such as charge, size, pH, solvation, geometry, basicity and the types of interactions depending on the binding site of ligand. ^1H -NMR titrations studied were carried out in the presence and absence of anions.

The signal of C(2)H protons of benzimidazole ($\text{C}^+\text{-H}$) showed a downfield shift. Presumably, C(2)H protons could bind to an anion using hydrogen bonding interaction and the complementary of electrostatic interaction ($\text{C}^+\text{-H}\cdots\text{X}^-$). [46] Because C(2)H acts as an acidic proton which has a potential to form hydrogen bonding, therefore, the charge transfers from the lone pair electron density or π -electron of proton acceptor to the anti bonding of proton donor bond.[47-48] Unlike the fluoride case, the disappearance of C(2)H protons ($\text{C}^+\text{-H}$) of ligand was monitored. The charge per size of fluoride ion is strong enough to induce the deprotonation process toward C(2)H protons. Interestingly, changes in aromatic protons of ligand were significantly observed, especially in the case of fluoride anion. The chemical shifts of ligand L and their induced chemical shifts on the formation of complexes with various anions were listed in Table 3.1

Table 3.1 $^1\text{H-NMR}$ chemical shift (ppm) for ligand **L** (in CDCl_3) in the absence and presence of anions

$^1\text{H-NMR}$ in species	Free L	Presence of F^-	Presence of H_2PO_4^-	Presence of CH_3CO_2^-	Presence of $\text{C}_6\text{H}_6\text{CO}_2^-$
NH_a	10.77	*	*	*	*
$\text{CH}_b, (\text{C}^+-\text{H})$ benzimidazole	9.05	*	9.27	9.00	9.08
H_c , dansyl	8.52, 8.52	ND	8.46, 8.44	8.45	8.51
H_c , aminothiophenol	8.37, 8.35	8.24, 8.22	8.27, 8.25	8.29, 8.27	8.36, 8.34

* disappearance of peak

ND = not determined

All spectra were recorded on Bruker DRX 400 MHz nuclear resonance spectrometers.

The Job's plots analysis were evaluated to determine binding stoichiometry of $\text{L} \subset \text{H}_2\text{PO}_4^-$ using $^1\text{H-NMR}$ titration of ligand **L** with increasing concentration of H_2PO_4^- in CD_3CN . In the spectra of $^1\text{H-NMR}$ titrations, all of aromatic protons belonging to dansyl groups and aminothiophenol showed slightly upfield shifts upon addition of 0.1-4.0 equivalents of tetrabutylammonium anions. The rationalization may be due to the increase of electron density in phenyl ring by anion added. A Job's plot that exhibits the symmetrical curve and a maximum point at 0.5 mole fraction in all case of anions indicates that the stoichiometry of host and guest is 1:1 complex as showed in Figure 3.5.

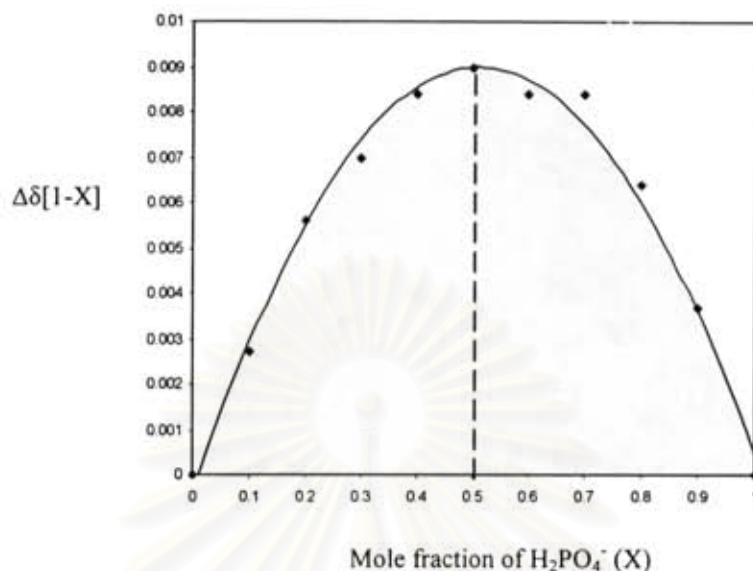


Figure 3.5 Job's plot of the complexation of $\text{L} \subset \text{H}_2\text{PO}_4^-$ was measured by the chemical shift of an aromatic dansyl proton.

3.3.1.2 Anion complexation studies by UV-Vis and fluorescence spectroscopy

In addition, to evaluate the potential of **L** and anions, we studied the binding properties by UV-Vis and fluorescence techniques. Ligand **L** contains the dansyl group as a fluorophore which is a powerful tool as the sensor for anions. The maximum absorption and emission band of ligand **L** displayed at 346 nm and 532 nm, respectively (spectra illustrated in Figure 3.6).

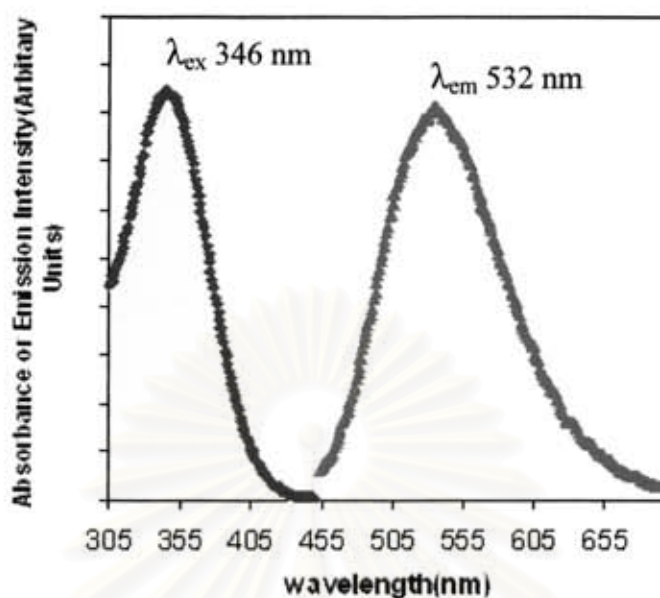


Figure 3.6 The absorption and the emission spectra of **L** in acetonitrile

Upon addition of anions such as F^- , $H_2PO_4^-$, $CH_3CO_2^-$ and $C_6H_5CO_2^-$ as tetrabutylammonium salt to **L** solution, the absorption spectra was induced to blue shift. It means that anion bounded to **L** destabilized the stability of ligand **L**. [49] In particular, the addition of two equivalents of $CH_3CO_2^-$, F^- and $H_2PO_4^-$ except for benzoate ion led not only a new shoulder peak valued at ca. 320 nm but also the color change from light green solution to colorless solution.

สถาบันวิทยบริการ
จุฬาลงกรณ์มหาวิทยาลัย

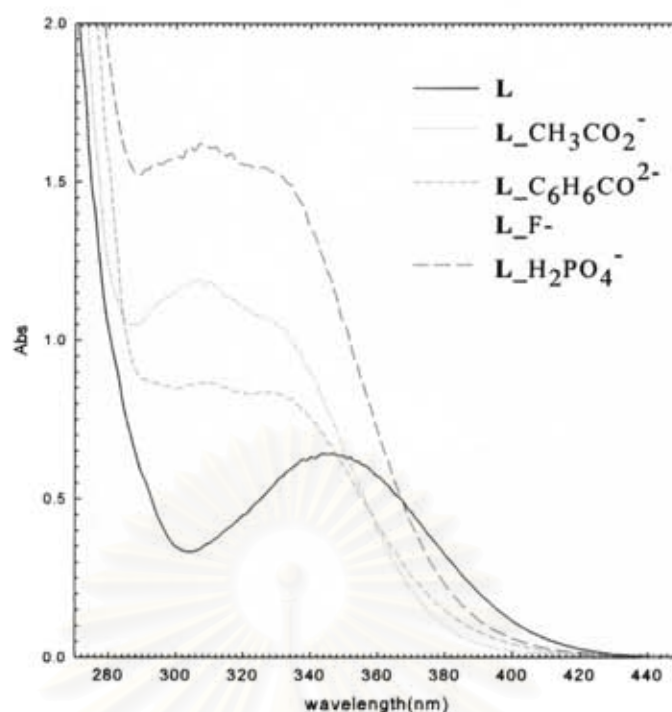


Figure 3.7 Absorption spectra (9×10^{-5} M) of **L** toward various anions in acetonitrile

The anion complexation abilities of ligand **L** with various anions such as dihydrogen phosphate, fluoride and acetate were investigated by the fluorometric titrations in acetonitrile. Figure 3.8-3.10 showed the change in emission spectra of fluoroionophore **L** (recorded in 0.01 M tetrabutylammonium hexafluorophosphate in acetonitrile and a concentration of **L** at 1×10^{-6} M) upon addition of anions (6.67×10^{-5} M in acetonitrile).

สถาบันวิทยบริการ
จุฬาลงกรณ์มหาวิทยาลัย

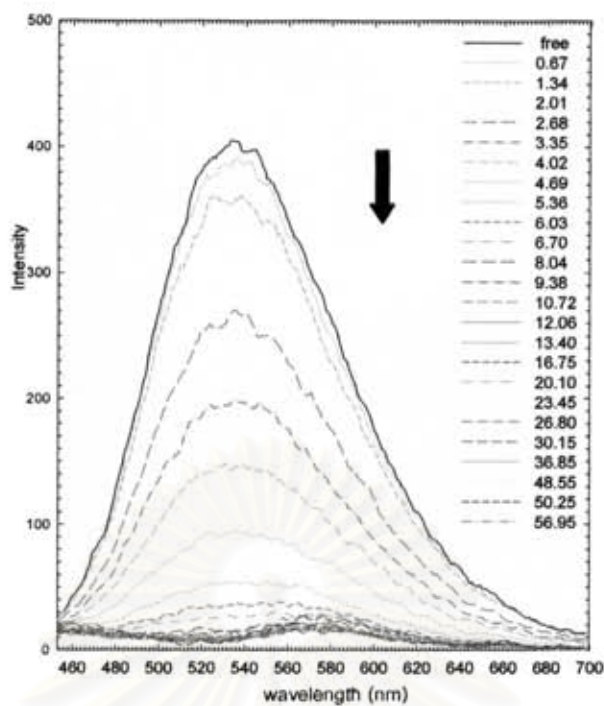


Figure 3.8 The fluorescence spectrum of L (1×10^{-6} M) in acetonitrile upon addition of increasing amounts of CH_3CO_2^- (6.67×10^{-5} M)

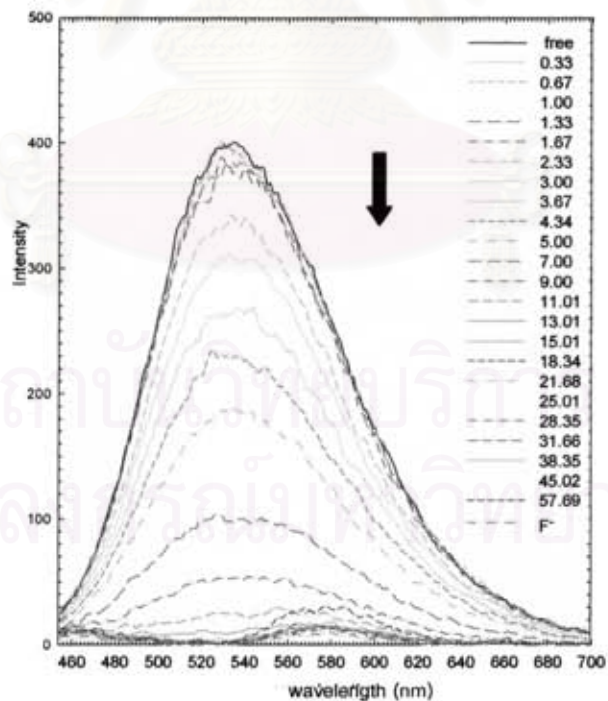


Figure 3.9 The fluorescence spectrum of L (1×10^{-6} M) in acetonitrile upon addition of increasing amounts of F^- (6.67×10^{-5} M)

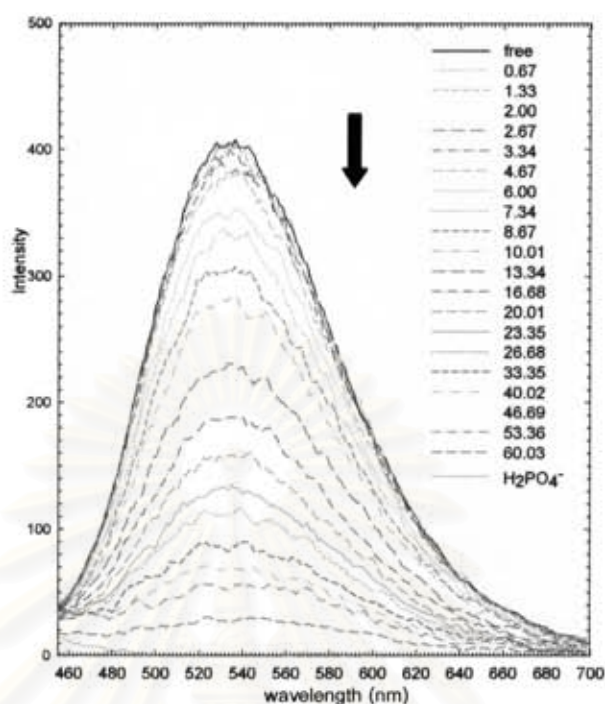


Figure 3.10 The fluorescence spectrum of **L** (1×10^{-6} M) in acetonitrile upon addition of increasing amounts of H_2PO_4^- (6.67×10^{-5} M)

Upon addition of anions, the emission band at 532 nm corresponding to dansyl group on unbound **L** was quenched significantly. Interestingly, the emission band maxima at 532 nm is quenched with the concomitant formation of a bathochromic shift at 580 nm with higher concentration of F^- and CH_3CO_2^- anions. It is possibly due to rapid charge transfer from anion to protons of amide group. [50] In contrast, the fluorescence quenching was observed in the case of adding H_2PO_4^- anion without a bathochromic shift. We proposed that a small bathochromic shift is due to the deprotonation on amide protons by a strong base such as F^- and CH_3CO_2^- . Previous $^1\text{H-NMR}$ data mentioned above, the disappearance of NH amide protons is an evidence for supporting the deprotonation process. From fluorescence behavior, it is possible that the fluorescence emission was quenched *via* PET mechanism. [48]

The fluorimetric titration was performed at least 2 times and the fluorescence intensity was recorded in Table 3.2. When $I_F^0 / (I_F - I_F^0)$ was plotted against the reciprocal of the anions concentration $[A]^{-1}$ (Figures 3.11-3.13), the stability constant is obtained from the ratio of intercept/slope. The log K values of complexes were collected in the Table 3.3.

Table 3.2 The fluorescence intensity of ligand L upon adding various anions

Titration		CH ₃ CO ₂ ⁻ 50 Equiv. (6.67x10 ⁻⁵ M)	F ⁻ 50 Equiv. (6.67x10 ⁻⁵ M)	H ₂ PO ₄ ⁻ 50 Equiv. (6.67x10 ⁻⁵ M)
1	I _F (a.u.)	390.80	263.92	394.86
	I _F - I _F ⁰ (a.u.)	-9.86	-136.60	-4.61
	I _F ⁰ / I _F - I _F ⁰	-40.64	-2.93	-86.64
2	I _F (a.u.)	383.90	226.80	400.49
	I _F - I _F ⁰ (a.u.)	-16.63	-164.50	-4.63
	I _F ⁰ / I _F - I _F ⁰	-24.08	-2.38	-87.45

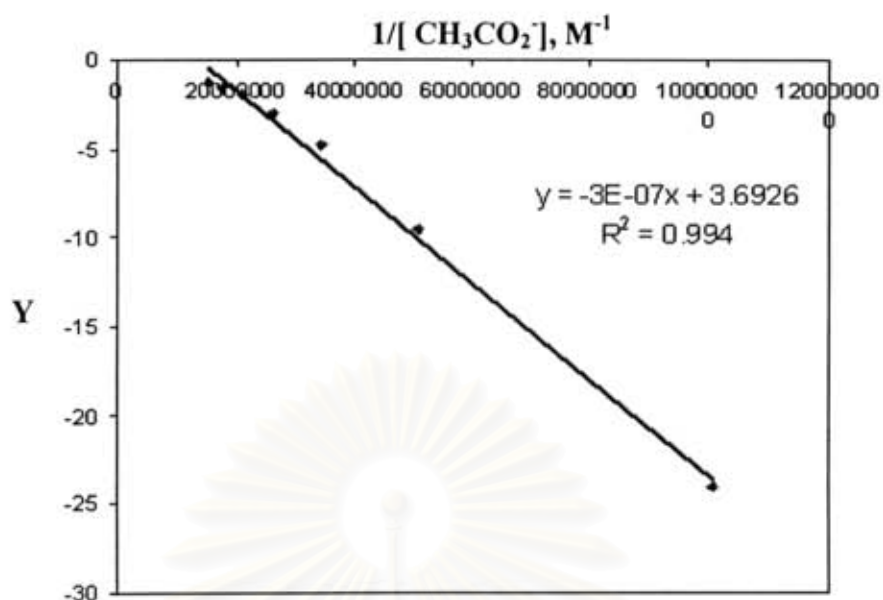


Figure 3.11 The linear plot between $Y = I_F^0 / (I_F - I_F^0)$ and $1/[\text{CH}_3\text{CO}_2^-]$ for the first fluorimetric titration

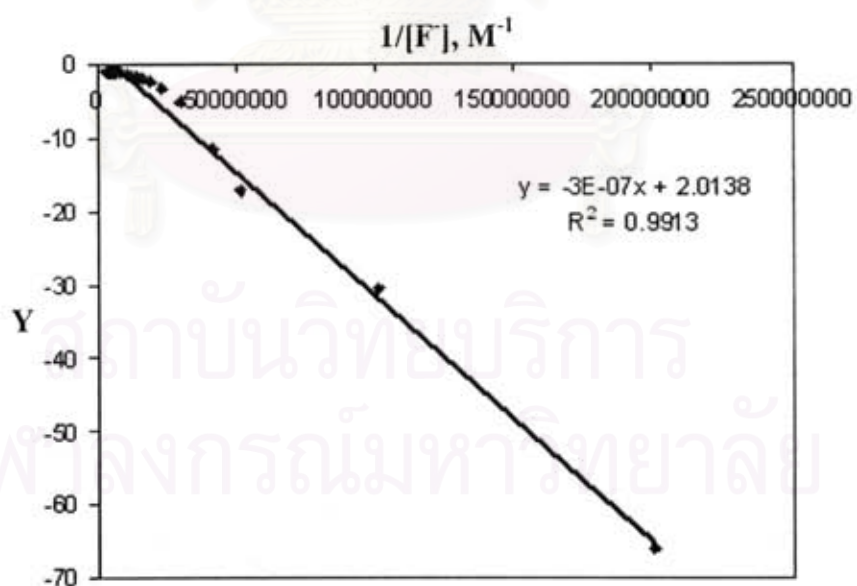


Figure 3.12 The linear plot between $Y = I_F^0 / (I_F - I_F^0)$ and $1/[\text{F}^-]$ for the first fluorimetric titration

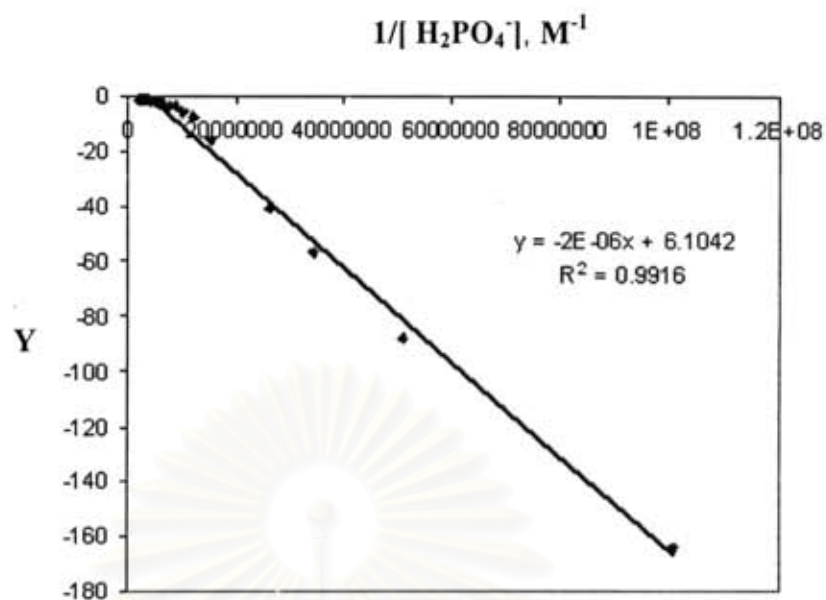


Figure 3.13 The linear plot between $Y = I_F^0 / (I_F - I_F^0)$ and $1/[H_2PO_4^-]$ for the first fluorimetric titration

Table 3.3 The stability constants of ligand L towards F^- , $H_2PO_4^-$ and $CH_3CO_2^-$

Anion	$CH_3CO_2^-$	F^-	$H_2PO_4^-$
Log K	7.09 ± 0.00	6.82 ± 0.01	6.48 ± 0.01

Considering the log K value of ligand **L** and anions, ligand **L** preferentially bound to all anions in the same trendancy. It means that ligand **L** has no selectivity for any anion. However, the small difference of log K value can give the binding affinities as follows: $\text{CH}_3\text{CO}_2^- > \text{F}^- > \text{H}_2\text{PO}_4^-$, which was in good agreement with the basicity of anions.[51] Hence among the examined anions, the interaction of **L** and CH_3CO_2^- is higher than that of **L** and other anions, possibly because of the suitable size and multiple binding sites of CH_3CO_2^- . [52]

According to all previous data, it was assumed that the structure of free ligand **L** exists a flexible chain. Consequently, the electron cannot transfer to HOMO of fluorophore. The excited electron can go back to ground state and emit light. After binding with anion, they induced aggregation and planarization of free ligand **L** as the fold structure. [50] Therefore, the fluorescence emission was quenched in the planar aggregated form. The selectivity is governed by basicity of anion and the interaction is subjected to hydrogen bonding and electrostatic interactions in terms of NH amide proton and $(\text{C-H})^+ \cdots \text{X}^-$. Hence, a conformation change of ligand **L** was induced during complexation of an anion *via* hydrogen bonding with the aid of intramolecular π - π interactions. The possible structure of anion complex with ligand **L** before and after the addition of anion is depicted in Figure 3.14. [53]

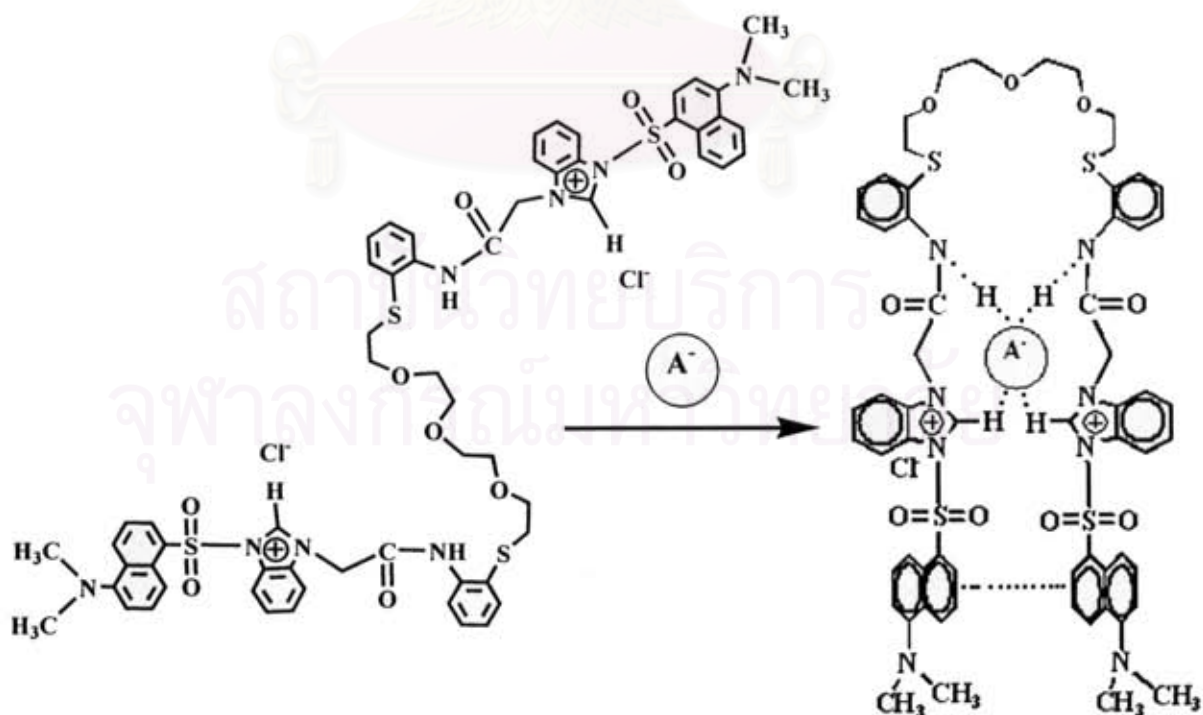


Figure 3.14 The proposed structure of ligand **L** induced by anion

3.3.2 Cation complexation studies

3.3.2.1 Nature of the complexes between ligand L with transition metals

Ligand **L** contains ethylene glycol linkages, which have oxygen and sulfur donor atoms for binding transition metal ions like crown ether. Thus the complexation studies of ligand **L** with transition metal ions were investigated for searching the suitable transition metal ions. Furthermore, we would like to study the effect of anions towards cation binding for ligand **L**.

Preliminary studies, UV-Vis technique is utilized for exploring the suitable transition metal to ligand **L**.

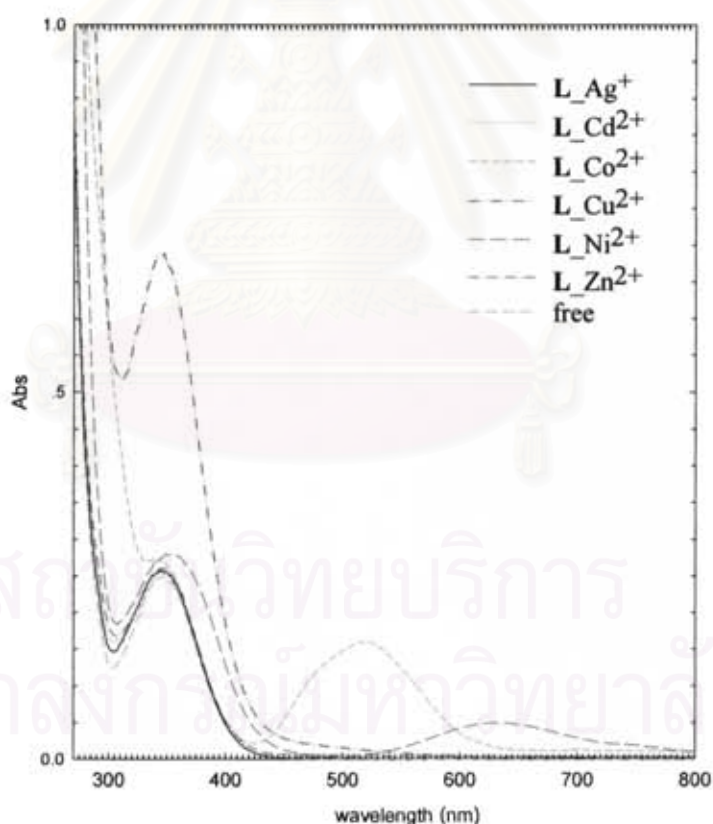


Figure 3.15 Absorption spectra (9×10^{-5} M) of **L** toward various cations in acetonitrile

Figure 3.15 showed absorption spectra of ligand **L** with various cations under the same condition for each cation. The presence of Cu^{2+} ion resulted in the large hypochromic (blue) shift with a concomitant color change from colorless to yellow solution. [29] However, no significant color changes were observed upon addition of excess amounts of Co^{2+} , Cd^{2+} , Zn^{2+} , Ni^{2+} and Ag^+ ions, indicating that only Cu^{2+} ion is able to form a strong coordination through the donor atoms of **L**.

The cation complexation abilities of ligand **L** with Cu^{2+} ion was focused on studying using the fluorometric titrations. The fluorescence spectra of ligand **L** in Figure 3.16 was performed the change in emission intensity with a gradual increase of Cu^{2+} solution. All experiments of fluorometric titrations were carried out in 0.01 M tetrabutylammonium hexafluorophosphate as supporting electrolyte. The emission spectrum of the complex of **L** and Cu^{2+} ion undergoes not only a fluorescence quenching but also with a concomitant of small bathochromic shift ca. 580 nm.

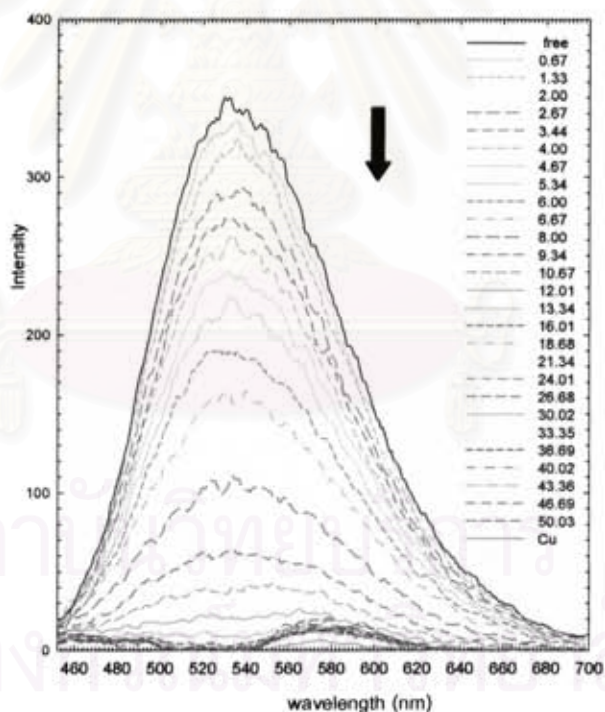


Figure 3.16 The fluorescence spectrum of **L** (1×10^{-6} M) in acetonitrile upon addition of increasing amounts of Cu^{2+} (6.67×10^{-5} M)

The fluorescence quenching behavior underwent a PET mechanism which was described that electron configuration of Cu^{2+} as d^9 was stabilized by obtaining the electron at excited state of ligand. Consequently, the excited electron could not transfer to ground state resulting in quenching fluorescent intensity. [54]

The fluorimetric titration was performed at least twice and the fluorescence intensity was recorded in Table 3.4. When $I_F^0 / (I_F - I_F^0)$ was plotted against the reciprocal of the cation concentration $[M]^{-1}$ (Figures 3.17), the stability constant is obtained from the ratio of intercept/slope (Table A13 in appendices).

Table 3.4 The fluorescence intensity of ligand L upon adding of Cu^{2+}

Titration	I_F (a.u.)	$I_F - I_F^0$ (a.u.)	$I_F^0 / I_F - I_F^0$
1	40.15	-299.33	-1.13
2	66.32	-256.46	-1.25

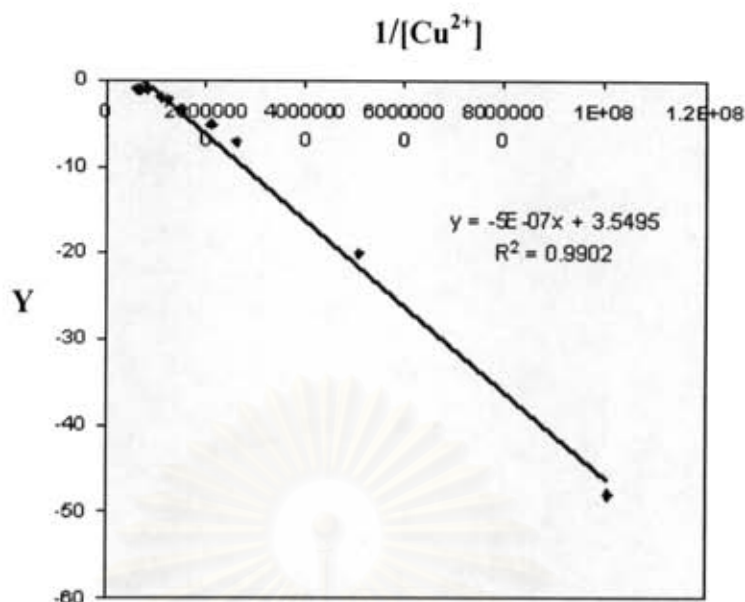


Figure 3.17 The linear plot between $Y = I_F^0 / (I_F - I_F^0)$ and $1/[Cu^{2+}]$ for the first fluorimetric titration

The stability constant of **L** and Cu^{2+} ion give a high $\log K$ values ($\log K = 6.82 \pm 0.04$) indicating that ligand **L** bound to Cu^{2+} ion effectively. [55] According to the structure of ligand **L**, it consists of two sulfur and three oxygen as donor atoms. It is not doubtably credible that Cu^{2+} ion was chelated strongly with all donor atoms. Therefore, Cu^{2+} ion preferentially bind to ligand **L** using soft and hard base donor atoms referred to hard-soft acid base theory. [56]

The conformation of ligand **L** was converted from the linear polyethylene glycol to pseudocyclic crown ether induced by transition metal ion as showed in Figure 3.18.

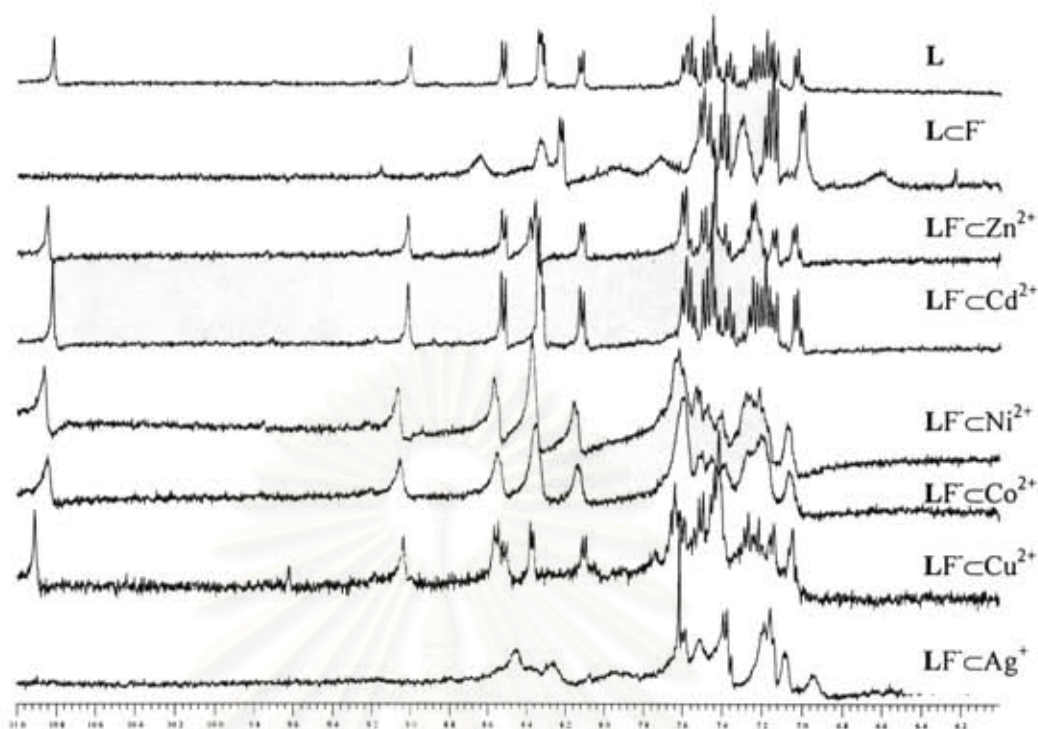


Figure 3.19 $^1\text{H-NMR}$ spectra (400 MHz) of LCF^- with various transition metals in CD_3CN

Since ligand L can bind to Cu^{2+} ion effectively as mentioned above, even through $^1\text{H-NMR}$ spectrum of LCF^- and Cu^{2+} is similar to that of unbound L . Therefore, it is an interest of studying the effect of anions toward the binding abilities of Ag^+ and Cu^{2+} ion to ligand L .

Before studying the effect of anions toward cation binding properties, the complexation of Ag^+ ion and unbound L was measured by fluorescence technique. It was found that the intensity of fluorescence changes slightly upon gradual increase of Ag^+ ion shown in Figure 3.20.

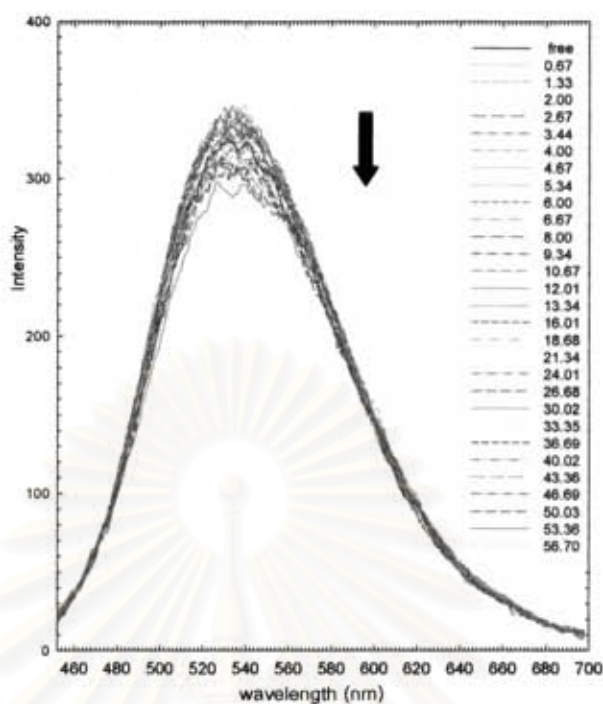


Figure 3.20 The fluorescence spectrum of L (1×10^{-6} M) in acetonitrile upon addition of increasing amounts of Ag^+ (6.67×10^{-5} M)

Unlike in the case of Cu^{2+} ion, the fluorescence was quenched significantly. These results give an agreement with the results in the previous topic. Additionally, types of anions might influent on the cation binding properties. Therefore, we pay attention on studying the cation binding properties in the presence of various anions such as CH_3CO_2^- , F^- and H_2PO_4^- .

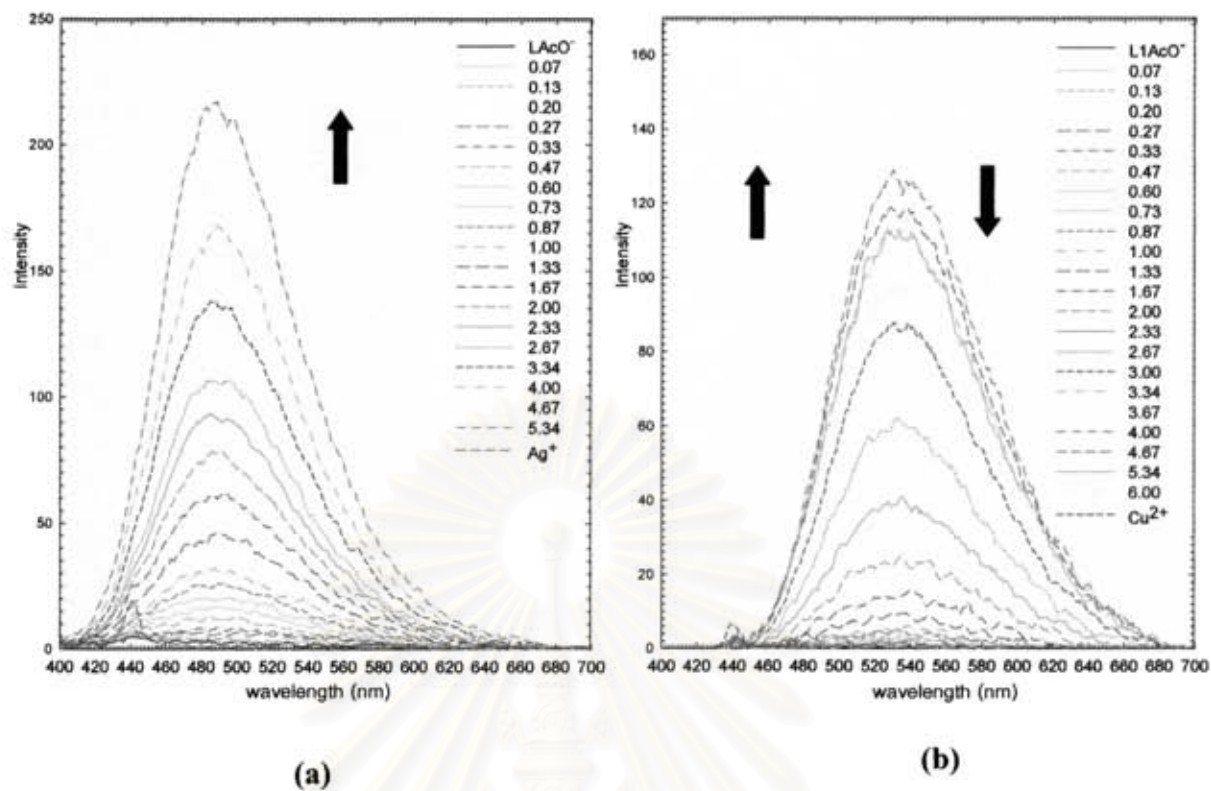


Figure 3.21 The fluorescence spectra of $LcCH_3CO_2^-$ (1×10^{-5} M) in acetonitrile upon addition of increasing amounts of cation (a) Ag^+ and (b) Cu^{2+} (6.67×10^{-5} M)

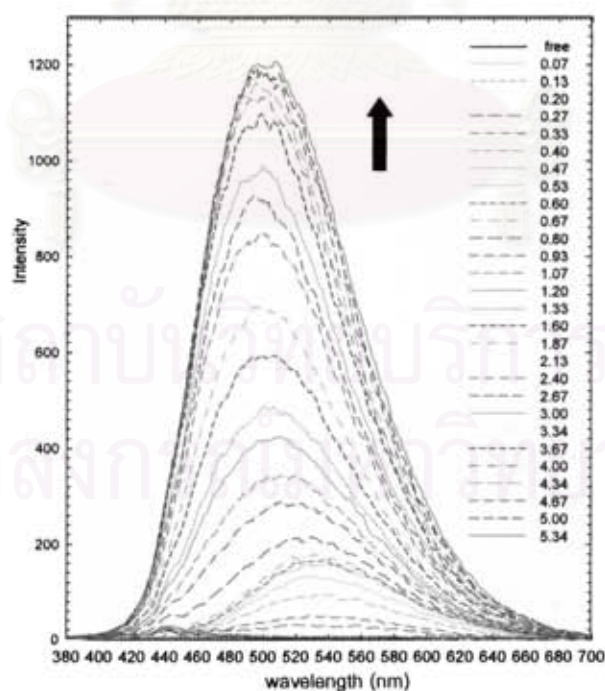


Figure 3.22 The fluorescence spectrum of LcF^- (1×10^{-5} M) in acetonitrile upon addition of increasing amounts of Ag^+ (6.67×10^{-5} M)

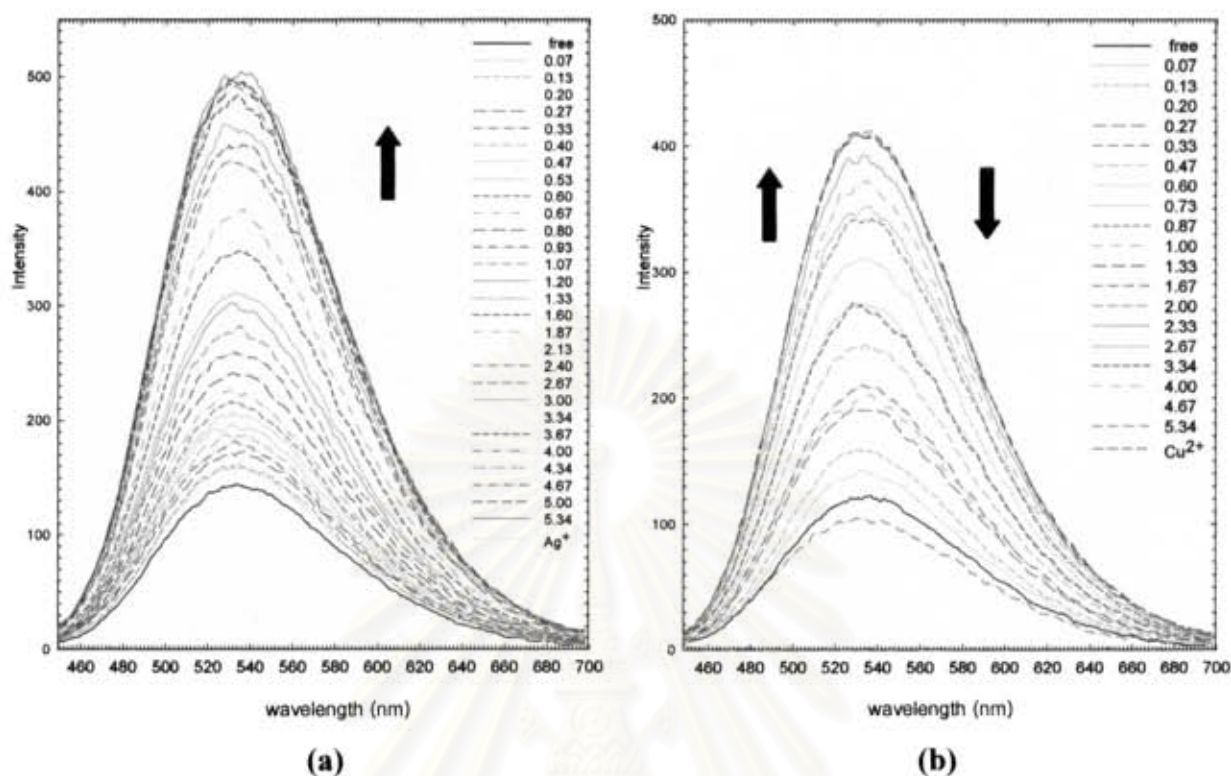


Figure 3.23 The fluorescence spectra of $L-C_2H_2PO_4^-$ (1×10^{-5} M) in acetonitrile upon addition of increasing amounts of cation (a) Ag^+ and (b) Cu^{2+} (6.67×10^{-5} M)

The fluorimetric titration was performed 2 times and the stability constants were calculated similarly to the studies of cation and anion complexation. In all cases, we used the concentration of anions and transition metal ions in the presence of 5 equivalents. In preparation, the mixture of ligand and 5 equivalents of anion is named as L^- anion. After that, cation solution was added gradually into the solution of L^- anion until 5 equivalents of cation solution. Figures 3.21- 3.23 show the spectrum changes of L^- anion with Ag^+ and Cu^{2+} ions.

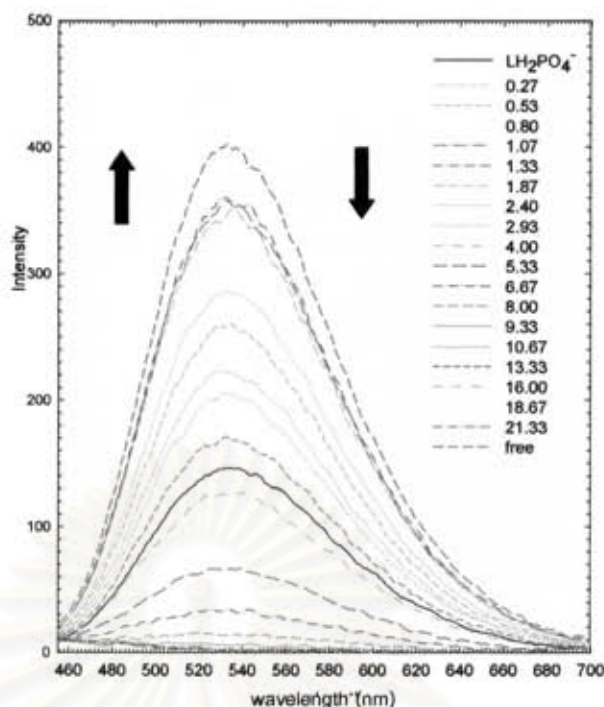


Figure 3.24 The fluorescence spectrum of $L\text{C}\text{H}_2\text{PO}_4^-$ (10^{-5} M) in acetonitrile upon addition of increasing amounts of Cu^{2+} (2.67×10^{-4} M)

Considering the emission spectrum of ligand **L** and anions (such as CH_3CO_2^- and F^-) with Ag^+ , the fluorescence intensity enhances significantly upon addition of increment of Ag^+ ion and the emission maxima existed at ca. 480 nm for $L\text{C}\text{CH}_3\text{CO}_2^-$ with Ag^+ and 500 nm for $L\text{C}\text{F}^-$ with Ag^+ .

The maximum emission band of unbound **L** shows the characteristic peak at 532 nm. Thus, Ag^+ ion could bind to ligand **L** in the presence of CH_3CO_2^- and F^- ion in terms of ion-pair inclusion. Compared to the case of Cu^{2+} ion, the fluorescence intensity was enhanced upon addition of Cu^{2+} and the emission maxima of the complexes ca. 532 nm is the same as that of the characteristic peak of unbound **L**. When, the Cu^{2+} ion was added over 5 equivalents into $L\text{C}$ anion, the fluorescence intensity was quenched similarly to the binding of **L** and Cu^{2+} ion. Presumably, the Cu^{2+} ion takes the anions (CH_3CO_2^- and H_2PO_4^-) off and forms as the complexation of copper acetate or copper dihydrogenphosphate. Unfortunately, the complexation between $L\text{C}\text{F}^-$ and Cu^{2+} ion could not be performed because of the disappearance of fluorescent intensity of $L\text{C}\text{F}^-$ and Cu^{2+} ion. Figure 3.24 is an evidence to support the previous reason. $L\text{C}\text{H}_2\text{PO}_4^-$ was titrated with 20 equiv of Cu^{2+} ion resulting in the quenching of fluorescence spectrum. This implied that Cu^{2+} ion could not bind well

with ligand **L** in the presence of anions and stability constants of the complexes of $L\text{-anion}/\text{Cu}^{2+}$ ion could not be calculated by analysis of the emission spectra. The complexation of ligand **L** with Cu^{2+} ion in the presence of anions was probably inhibited by the ion pairing effect of Cu^{2+} ion and anions.

The plot of $I_F^0 / (I_F - I_F^0)$ against the reciprocal of the silver ion concentration $[\text{Ag}^+]^{-1}$ shown in Figures 3.25-3.27 and the stability constants of $L\text{-anion}$ with Ag^+ ion were collected in the Table 3.5.

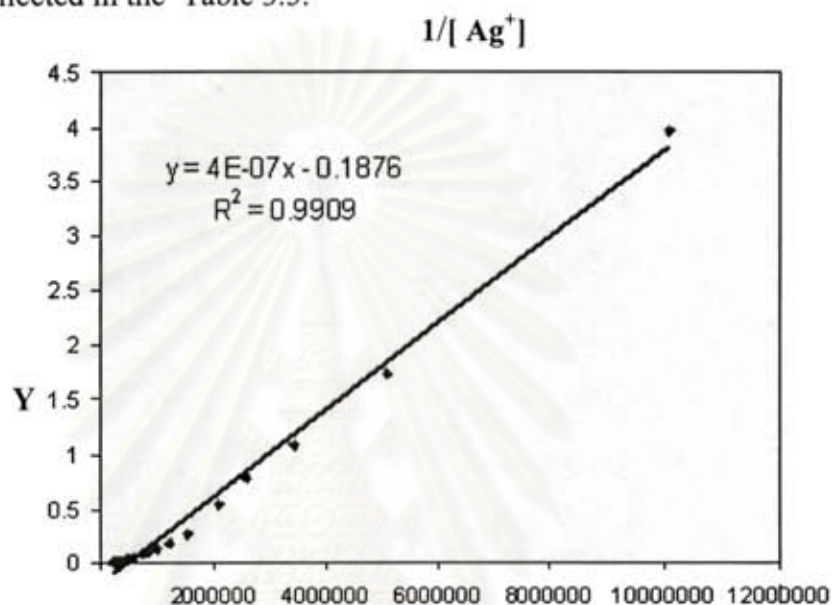


Figure 3.25 The linear plot between $Y = I_F^0 / (I_F - I_F^0)$ and $1/[\text{Ag}^+]$ for the first fluorimetric titration of $L\text{-CH}_3\text{CO}_2^-/\text{Ag}^+$

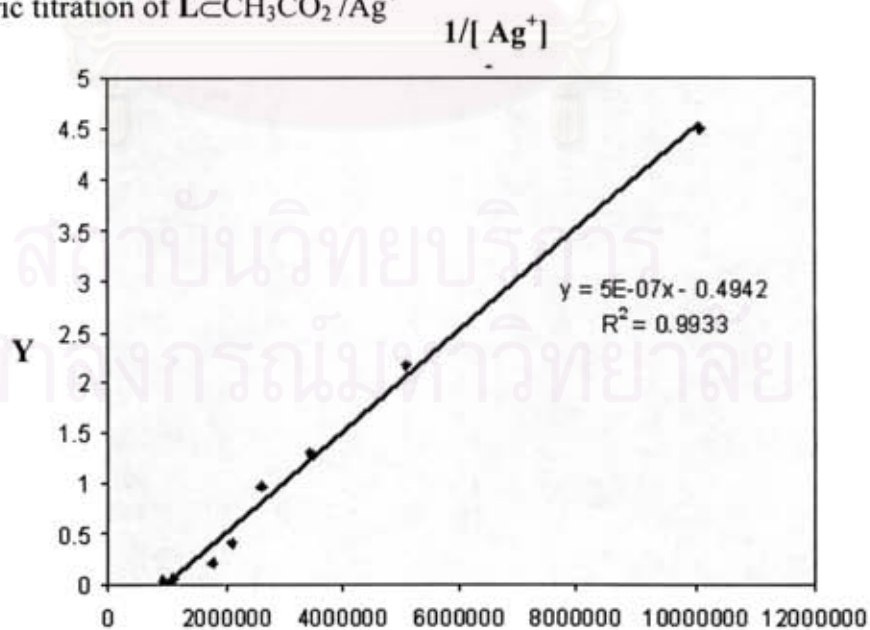


Figure 3.26 The linear plot between $Y = I_F^0 / (I_F - I_F^0)$ and $1/[\text{Ag}^+]$ for the first fluorimetric titration of $L\text{-F}^-/\text{Ag}^+$

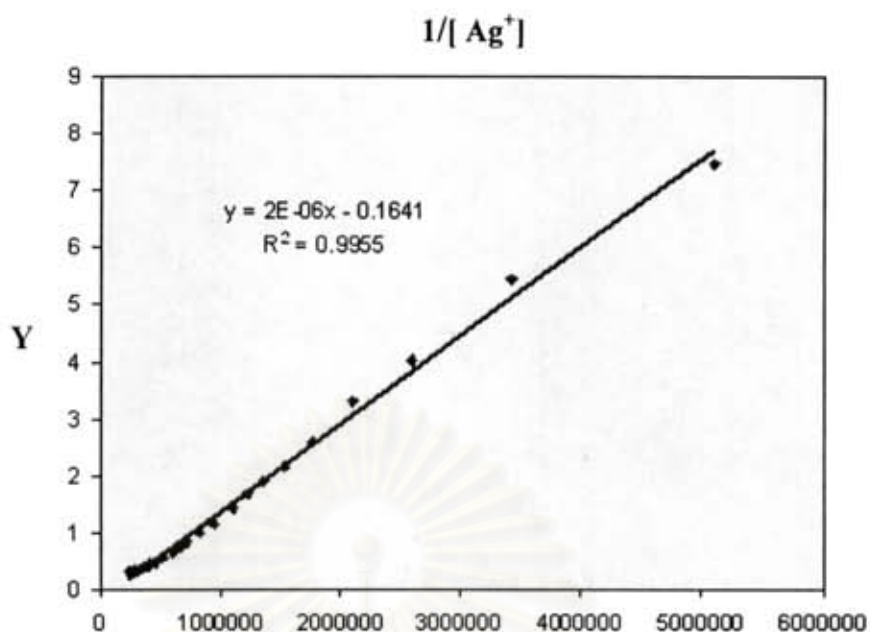


Figure 3.27 The linear plot between $Y = I_F^0 / (I_F - I_F^0)$ and $1/[Ag^+]$ for the first fluorimetric titration of $LCH_2PO_4^-/Ag^+$

Table 3.5 The stability constants of ligand L^- anion towards Ag^+

Titration	Log K $L^-CH_3CO_2^-$	Log K L^-F^-	Log K $L^-CH_2PO_4^-$
Ag^+	average = 5.68 ± 0.01	average = 6.00 ± 0.01	average = 4.93 ± 0.03

In all cases of adding Ag^+ ion, the enhancement of fluorescent intensity was observed and the order of binding affinity is $\text{F}^- \sim \text{CH}_3\text{CO}_2^- > \text{H}_2\text{PO}_4^-$. Possibly, the structure of ligand was preorganized to be pseudocyclic ring prior to bind with Ag^+ ion. F^- and CH_3CO_2^- ion give a high stability constant compared to H_2PO_4^- because F^- and CH_3CO_2^- have a suitable geometry to bound with ligand **L**. Consequently, both anions are appropriate to preorganize the structure of **L** to bind with Ag^+ ion effectively. [57] The evidence of complexation between $\text{L} \leftarrow \text{F}^-$ and Ag^+ ion was confirmed by MALDI-TOF mass spectrum which show the existence of the intense peak at $m/z = 1335.451$ corresponding on $[\text{M} + 2\text{F}^- + \text{Ag}^+ - 2\text{H}^+]^-$. The proposed structure of $\text{L} \leftarrow \text{anion}$ with Ag^+ ion was performed in Figure 3.29.

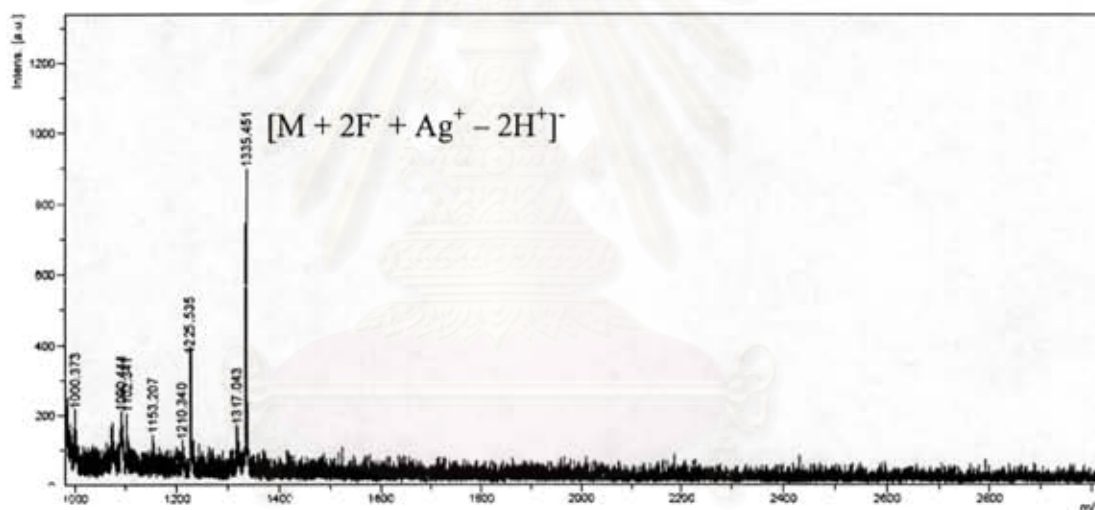


Figure 3.28 MALDI-TOF mass spectrum of $\text{L} \leftarrow \text{F}^- / \text{Ag}^+$ complexation

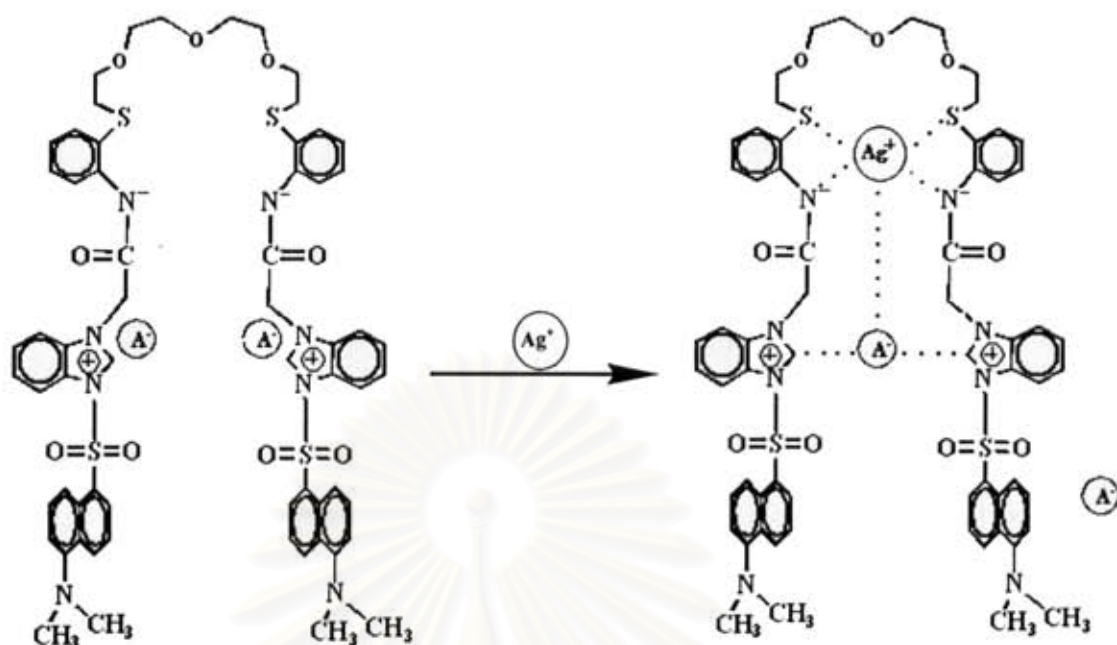


Figure 3.29 The proposed structure of L^-/Ag^+

Finally, the influences of the anion species toward Cu^{2+} and Ag^+ complexation with ligand **L** in the following:

1. Decreasing of copper binding ability of ligand **L** results from the rigid structure of anion complexes since Cu^{2+} ion preferred to bind to anion more than donor atom of oxyethylene glycol moiety.

2. Increasing of silver binding ability of ligand **L** was performed by the preorganization of structure **L** by anion to be the pseudocyclic ring for binding Ag^+ ion. It could diminish the ion pairing effect and induced Ag^+ ion to coordinate strongly with poly donor atoms and the behavior of **L** toward anion and Ag^+ ion is cooperative binding namely, a heteroditopic receptor.

CHAPTER IV

CONCLUSION

Polyethylene glycol derivatives containing imidazolium moieties and amide NH protons **L** was synthesized by reaction of tetraethylene glycol **2** with 2-aminothiophenol and benzimidazole, respectively. Finally, the nucleophilic substitution reaction of **4** and dimethylaminonaphthalene sulfonyl chloride (dansyl chloride) afforded as a light green product **L**. The absorption band of ligand existed at 346 nm and in the presence of various anions, this band moved to blue shift significantly. For fluorescence technique, the appearance of the emission band of free ligand showed at 532 nm. Upon the addition of anions, the quenching was observed. The stability constant of ligand **L** measured by fluorimetric titration in acetonitrile provided the small difference of log *K* values in case of F⁻, CH₃CO₂⁻ and H₂PO₄⁻. It means that **L** has no selectivity for any anion. In the case of cation complexation, ligand **L** was selective to copper ion. On the other hand, ligand **L** bound with anions has a high affinity to Ag⁺ ion. Therefore, it was concluded that anion effect toward Ag⁺ ion was accounted in positive allosteric effect.

Suggestion for future works:

1. Attempt to recrystallize the ligand **L** and their complexes with various ionic guests to gain the structure of synthetic receptor and its complexation in solid state.
2. Study on the complexation of alkali or alkali earth metals with ligand.
3. The possibility of using ligand **L** as a molecular device should be explored.

REFERENCES

- [1] Lippard, S. J. and Berg, A. *Principles of Bioinorganic Chemistry*. California: University Science Books, **1994**.
- [2] Cowan, J. A. *Inorganic Biochemistry: An introduction*. New York: VCH publisher, **1993**.
- [3] Elmidaoui, A.; Elhannouni, F.; Menkouchi, Sahli, L.; Chay, H.; Hafsi, E. M.; Largeteau, D. Pollution of nitrate in Moroccan ground water: removal by electro dialysis. *Desalination*, **2001**, *136*, 325-332.
- [4] Young, J. F.; Osborn, J. A.; Jardine, F. H.; Wilkinson, G. Hydride intermediates in homogeneous hydrogenation reactions of olefins and acetylenes using rhodium catalysts. *J. Chem. Commun.*, **1965**, 131-132.
- [5] Mcneil, J. H.; Yuen, V. G.; Hoveyda, H. R.; Orvig, C. Bis(maltolato) oxovanadium (IV) is a potent insulin mimic. *J. Med. Chem.*, **1992**, *35*, 1489-1491.
- [6] Frank Shaw III, C. Gold-based therapeutic agents. *Chem. Rev.*, **1999**, *99*, 2589-2600.
- [7] Koepf-Maier, P.; Koepf, H. Non-platinum group metal antitumor agents. History, current status, and perspectives. *Chem. Rev.*, **1987**, *87(5)*, 1137-1152.
- [8] Jamieson, E. R.; Lippard, S. J. Structure, recognition, and processing of Cisplatin -DNA adducts. *Chem. Rev.*, **1999**, *99(9)*, 2467-2498.
- [9] Renkawek, K.; Bosman, G. J.; Anion exchange proteins are a component of corpora amylacea in Alzheimer disease brain. *Neuroreport*, **1995**, *6*, 929-932.
- [10] Lehn, J. M. *Supramolecular Chemistry: Concepts and Perspectives*. Weinheim: VCH publisher, **1995**.
- [11] Lehn, J. M. in Proceeding of the Centenary of the Geneva Conference Organic Chemistry: Its Language and Its State of the Art (Kisakurek, M. V.(Ed.) Weinheim: VCH publisher, **1993**.
- [12] Vogtle, F. *Supramolecular Chemistry: An introduction*. Chichesters: John Wiley & Sons, **1991**.
- [13] Paul, D.; Gale, P. A.; Smith, D. K. *Supramolecular chemistry*. Oxford: Oxford university press, **1999**.

- [14] Jeong, K.; Park, T. Complexation and transport of zwitterionic Amino acids by an artificial receptor. *Bull Korean Chem. Soc.*, **1999**, *20*, 125-256.
- [15] Scheerder, J.; Duynhoven, J. P. M.; Engbersen, J. F. J.; Reinhoudt, D. N. Stabilization of NaX salts in chloroform by bifunctional receptors. *Angew. Chem. Int. Ed. Engl.*, **1996**, *10*, 35.
- [16] Beer, P. D.; Dent, S. W. Potassium cation induced switch in anion selectivity exhibited by heteroditopic ruthenium(II) and rhenium(I) bipyridyl bis(benzo-15-crown-5) ion pair receptors. *Chem. Commun.*, **1998**, *7*, 825-826.
- [17] Love, J. B.; Vere, J. M.; Glenney, M. W.; Blake, A. J.; Schroder, M. Ditopic azathioether macrocycles as hosts for transition metal salts. *Chem. Commun.*, **2001**, *24*, 2678-2679.
- [18] Mahoney, J. M.; Beatty, A. M.; Smith B. D. Selective Recognition of an Alkalide Halide Contact Ion-Pair. *J. Am. Chem. Soc.*, **2001**, *123*, 5847.
- [19] Nabeshima, T.; Inaba, Y.; Furakawa, N.; Hosoya, T.; Yano, Y. Artificial allosteric ionophores: reguration of ion recognition of polyethers bearing bipyridine moieties by copper(I). *Inorg. Chem.*, **1993**, *32*, 1407-1416.
- [20] Takeuchi, M.; Ikeda, M.; Sugasaki, A.; Shinkai, S. Molecular design of artificial molecular and ion recognition systems with allosteric guest responses. *Acc. Chem. Res.*, **2001**, *34*, 865-873.
- [21] Linton, B.; Hamilton, A. Formation of artificial receptors by metal-templated self-assembly. *Chem. Rev.*, **1997**, *97*, 1669-1680.
- [22] Abe, A. M. M.; Helaja, J.; Koskinen, A. M. P. Novel Crown ether and salen metal chelation driven molecular pincers. *Org. Lett.*, **2006**, *8*, 4537-4540.
- [23] Kovbasyuk, L.; Kramer, R. Allosteric supramolecular receptors and catalysts. *Chem. Rev.*, **2004**, *104*, 3161-3187.
- [24] Sate, K.; Arap, S.; Yamagishi, T. A New Tripodal Anion Receptor with C-H-X⁻ Hydrogen Bonding. *Tetrahedron Lett.*, **1999**, *40*, 5219.
- [25] Mamta, C.; Shailesh, U.; and Pramod S. P. Anion recognition by bisimidazolium and bisbenzimidazolium cholapods. *Tetrahedron*, **2007**, *63*, 171.

- [26] Bargossi, C.; Fiorini, M. C.; Montalti, M.; Prodi, L.; Zaccheroni, N. Recent developments in transition metal ion detection by luminescent chemosensors. *Coord. Chem. Rev.*, **2000**, *208*, 17-32.
- [27] Löhr, H-G.; Vögtle, F. Chromo- and fluoroionophores a new class of dye reagents. *Acc. Chem. Res.*, **1985**, *18*, 65-72.
- [28] Ataman, D.; Akkaya, E. U. Selective chromogenic response via regioselective binding of cations: a novel approach in chemosensor design. *Tetrahedron Lett.*, **2002**, *43*, 3981-3983.
- [29] Lee, S. J.; Lee, S. S.; Jeong, Y.; Lee, J. Y.; Jung, J. H. Azobenzene coupled chromogenic receptors for the selective detection of copper(II) and its application as a chemosensor kit. *Tetrahedron. Lett.*, **2007**, *48*, 393-396.
- [30] Wu, F.; Hu, M.; Wu, Y.; Tan, X.; Zhao, Y.; Ji, Z. Fluoride-selective colorimetric sensor based on thiourea binding site and anthraquinone receptor. *spectrochimica acta partA*, **2006**, *65*, 633-637.
- [31] Valeur, B.; Leray, I. Design principles of fluorescent molecular sensors for cation recognition. *Coord. Chem. Rev.*, **2000**, *205*, 3-40.
- [32] Jiang, P.; Guo, Z. Fluorescent detection of zinc biological system: recent development on the design of chemosensors and biosensors. *Coord. Chem. Rev.*, **2004**, *248*, 205-229.
- [33] Bren, V. A. Fluorescent and photochromic chemosensors. *Russ. Chem. Res.*, **2001**, *70*, 1017-1036.
- [34] Bronson, R. T.; Montalti, M.; Prodi, L.; Zaccheroni, N.; Lamb, R. D.; Dally, N. K.; Izatt, R. M.; Bradshaw, J. S.; Savage, P. B. Original of on-off fluorescent behavior of 8-hydroxyquinoline containing chemosensors. *Tetrahedron*, **2004**, *60*, 11139-11144.
- [35] McCarrick, M.; Wu, B.; Harris, S. J.; Diamond, D.; Barrett, G.; McKervery, M. A. Novel chromogenic ligands for lithium and sodium based on calix[4]arene tetraesters. *J. Chem. Soc. Chem. Commun.*, **1992**, 1287-1289.
- [36] Valeur, V.; Leray, I. Design principles of fluorescent molecular sensors for cation recognition. *Coord. Chem. Rev.*, **2000**, *205*, 3-40.

- [37] Pearson, J. A.; Xiao, W. Fluorescent Photoinduced Electron Transfer (PET) Sensing Molecules with *p*-Phenylenediamine as Electron Donor. *J. Org. Chem.*, **2003**, *68*, 5361-5368.
- [38] McCarrick, M.; Wu, B.; Harris, S. J.; Diamond, D.; Barrett, G.; McKervey, M. A. Chromogenic ligands for lithium based on calix[4]arene tetraesters bearing nitrophenol residues. *J. Chem. Soc. Perkin. Trans.2*, **1993**, 1963-1968.
- [39] Jiang, P.; Guo, Z. Fluorescent detection of zinc in biological systems: recent development on the design of chemosensors and biosensors. *Coord. Chem. Rev.*, **2004**, *248*, 205-229.
- [40] Steed, J. W.; Atwood, J. L.; *Supramolecular Chemistry*. West Sussex: John Wiley & Sons, **2000**.
- [41] Fery-Forgues, S.; Le Bris, M-T.; Guetté, J-P.; Valeur, B. Ion-responsive fluorescent compounds. 1. effect of cation binding on photophysical properties of a benzoxazinone derivative linked to monoaza-15-crown-5. *J. Phys. Chem.*, **1988**, *92*, 6233-6237.
- [42] Bouson, J.; Valeur, B. Ion-responsive fluorescent compounds. 2. cation-steered intramolecular charge transfer in a crowned merocyanine. *J. Phys. Chem.*, **1988**, *93*, 3871-3876.
- [43] Bouson, J.; Pouget, J.; Valeur, B. Ion-responsive fluorescent compounds. 4. effect of cation binding on the photophysical properties of a coumarin linked to monoaza- and diaza-crown ethers. *J. Phys. Chem.*, **1993**, *97*, 4552-4557.
- [44] Bernard, V. *Molecular fluorescence Principle and Applications*. New York: Wiley-VCH, **2002**.
- [45] Lakowicz, J. R. *Principle of Fluorescent spectroscopy*. 2nd ed. New York: Kluwer Academic/ Plenum Publishers, **1999**.
- [46] Chahar, M.; Upreti, S.; Pandey, P. S. Anion recognition bisimidazolium and bisbenzimidazolium cholapods. *Tetrahedron*, **2007**, *63*, 171-176.
- [47] Alhashimy, N.; Brougham, D. J.; Howarth, J.; Farrell, A.; Quilty, B.; Nolan, K. Homochiral tripodal imidazolium receptors: structural and anion-receptor studies. *Tetrahedron Lett.*, **2007**, *48*, 125-128.

- [48] Miao, R.; Zheng, Q. Y.; Chen, C. F.; Huang, Z. T. A novel calyx[4]arene fluorescent receptor for selective recognition of acetate anion. *Tetrahedron Lett.*, **2005**, *46*, 2155-2158.
- [49] Ajayaghosh, A. Chemistry of Squaraine-Derived materials: near-IR dyes, low band gap systems, and cation sensor. *Acc. Chem. Res.*, **2005**, *38*(6), 449-459.
- [50] Singh, N. J.; Jun, E. J.; Chellappan, K.; Thangadurai, D., Chandran, R. P.; Hwang, I.; Yoon, J.; Kim, K. S. Quinoline-imidazolium receptors for unique sensing of pyrophosphate and acetate by charge transfer. *Org. Lett.*, **2007**, *9*, 485.
- [51] Wu, F.; Hu, M.; Wu, Y.; Tan, X.; Zhao, Y.; Ji, Z. Fluoride-selective colorimetric sensor based on thiourea binding site and anthraquinone receptor. *spectrochimica acta partA*, **2006**, *65*, 633-637.
- [52] Maeda, H.; Ito, Y. BF₂ complex of fluorinated dipyrrolyldiketone: A new class of efficient receptor for acetate anions. *Inorg. Chem.*, **2006**, *45*, 8205-8210.
- [53] Martı́nez-Mañez, R.; Fe'lix, S. Fluorogenic and Chromogenic Chemosensors and Reagents for Anions. *Chem. Rev.*, **2003**, *103*, 4419-4476.
- [54] Arunkumar, E.; Ajayaghosh, A.; Daub, J. Selective Calcium Ion Sensing with a Bichromophoric Squaraine Foldamer. *J. AM. Chem. Soc.*, **2005**, *127*, 3156.
- [55] Mutsuo, K.J. A Long-Wavelength Fluorescent Chemodosimeter Selective for Cu(II) Ion in Water. *Chem. Commun.*, **1975**, 326.
- [56] Weng, Y.; Teng, Y.; Yue, F.; Zhong, Y.; Ye, B. A new selective fluorescent chemosensor for Cu (II) ion based on zinc porphyrin-dipyridylamino. *Inor. Chem. Commun.*, **2007**, *10*, 443-446.
- [57] Deetz, M. J.; Smith, B. D. Heteroditopic ruthenium(II) bipyridyl receptor with adjacent saccharide and phosphate binding sites. *Tetrahedral Lett.*, **1998**, *39*, 6841.



APPENDICES

สถาบันวิทยบริการ
จุฬาลงกรณ์มหาวิทยาลัย

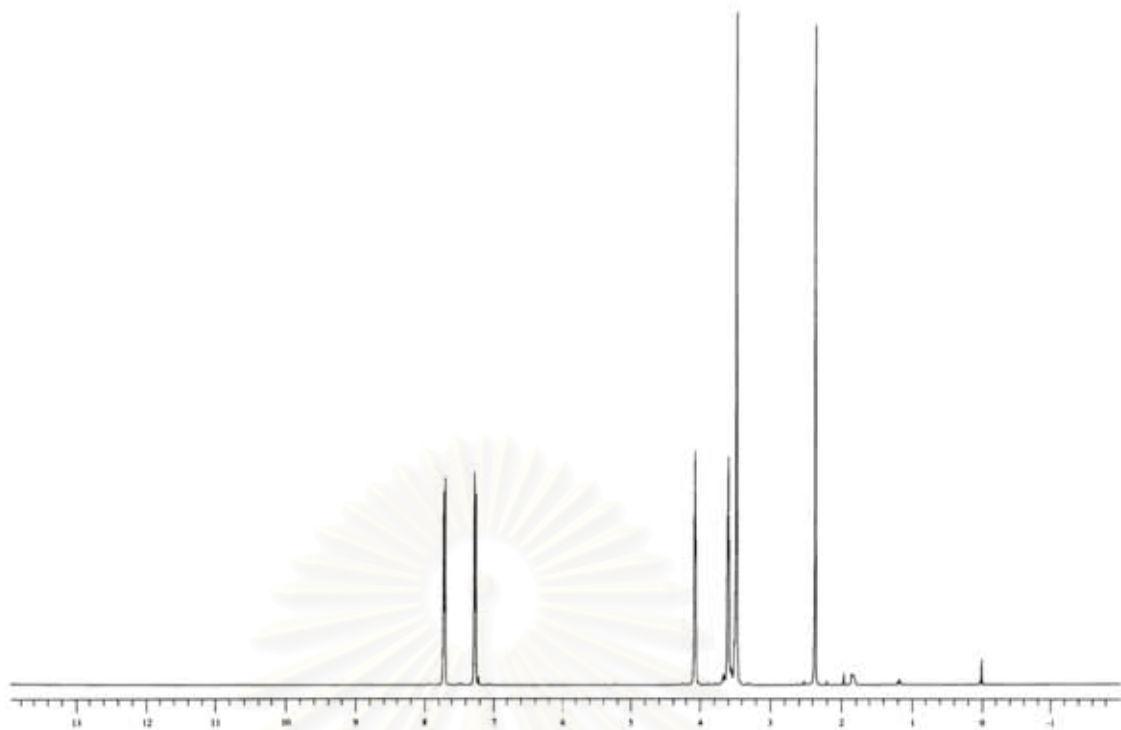


Figure A.1 The ¹H-NMR spectrum of tetraethylene glycol ditosylate (1) in CD₃Cl with 400 MHz

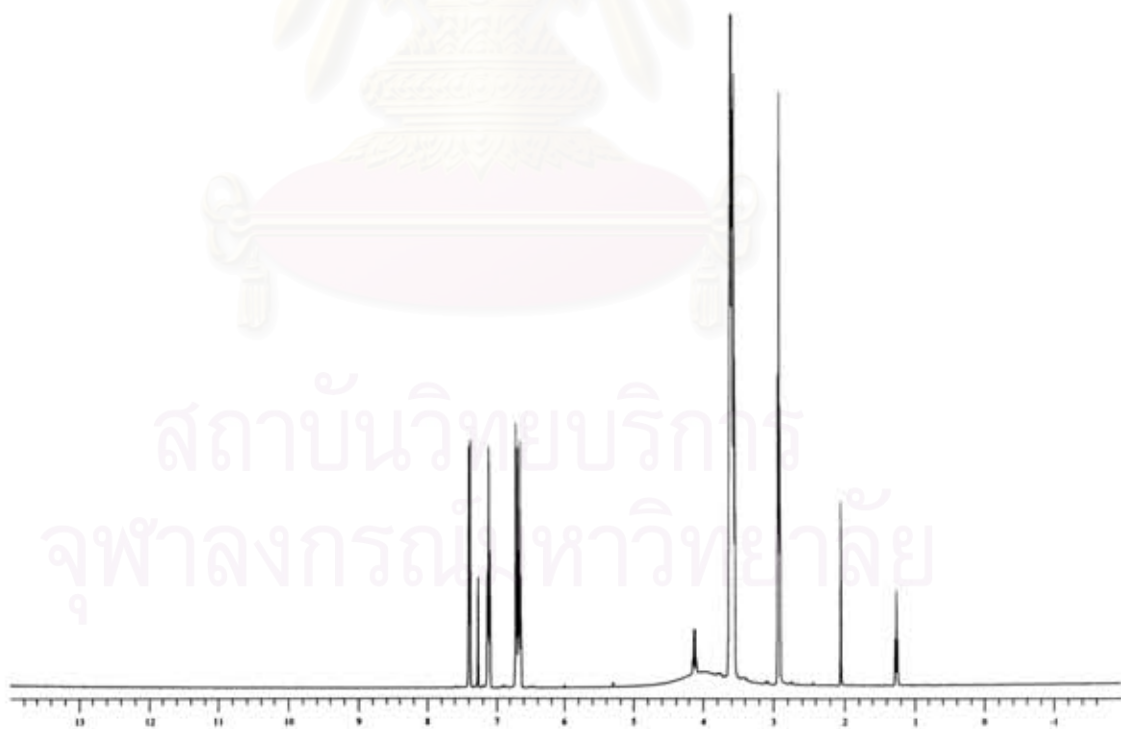


Figure A.2 The ¹H-NMR spectrum of 1,8-Bis(aminothiophenol) tetraethylene glycol (2) in CD₃Cl with 400 MHz

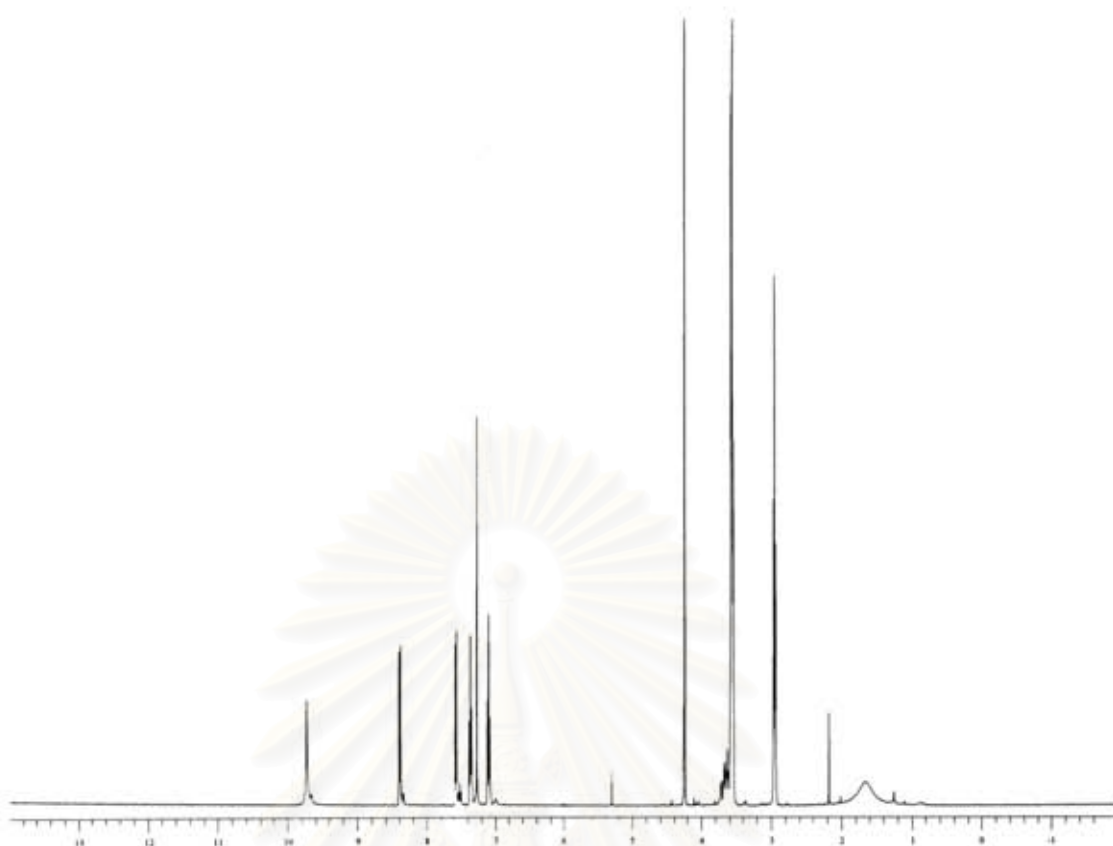


Figure A.3 The ^1H -NMR spectrum of 1,8-Bis(2-chloromethylamide) tetraethylene glycol (**3**) in CD_3Cl with 400 MHz

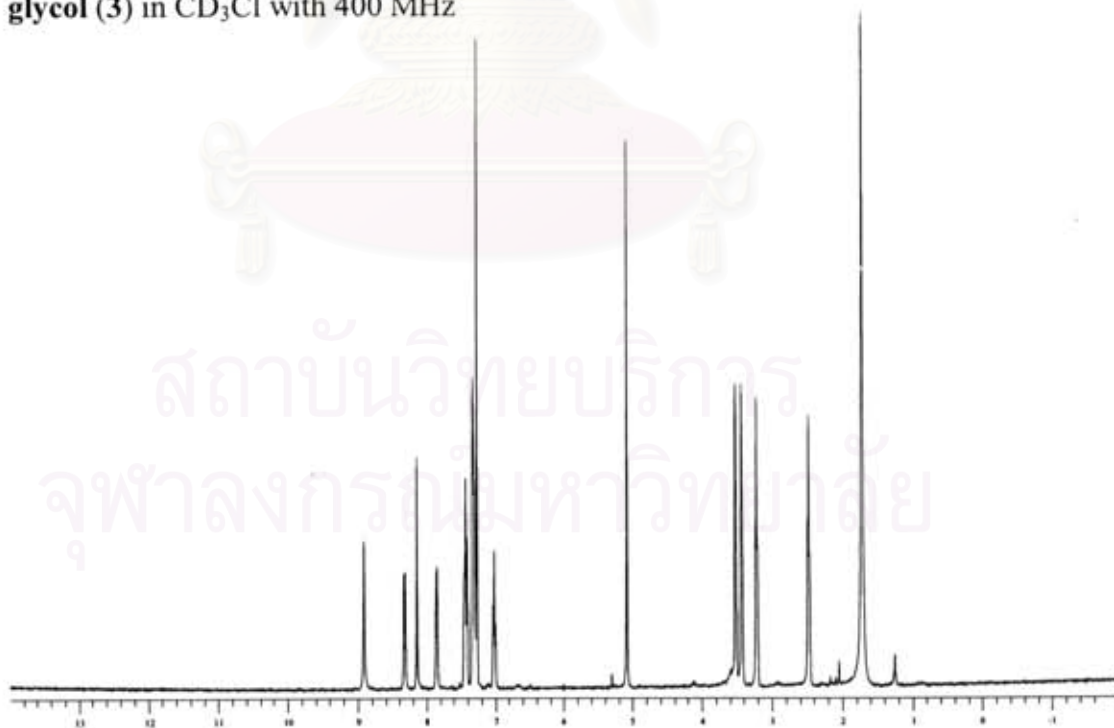


Figure A.4 The ^1H -NMR spectrum of 1,8-Bis(2-methylbenzimidazolium) tetraethylene glycol (**4**) in CD_3Cl with 400 MHz

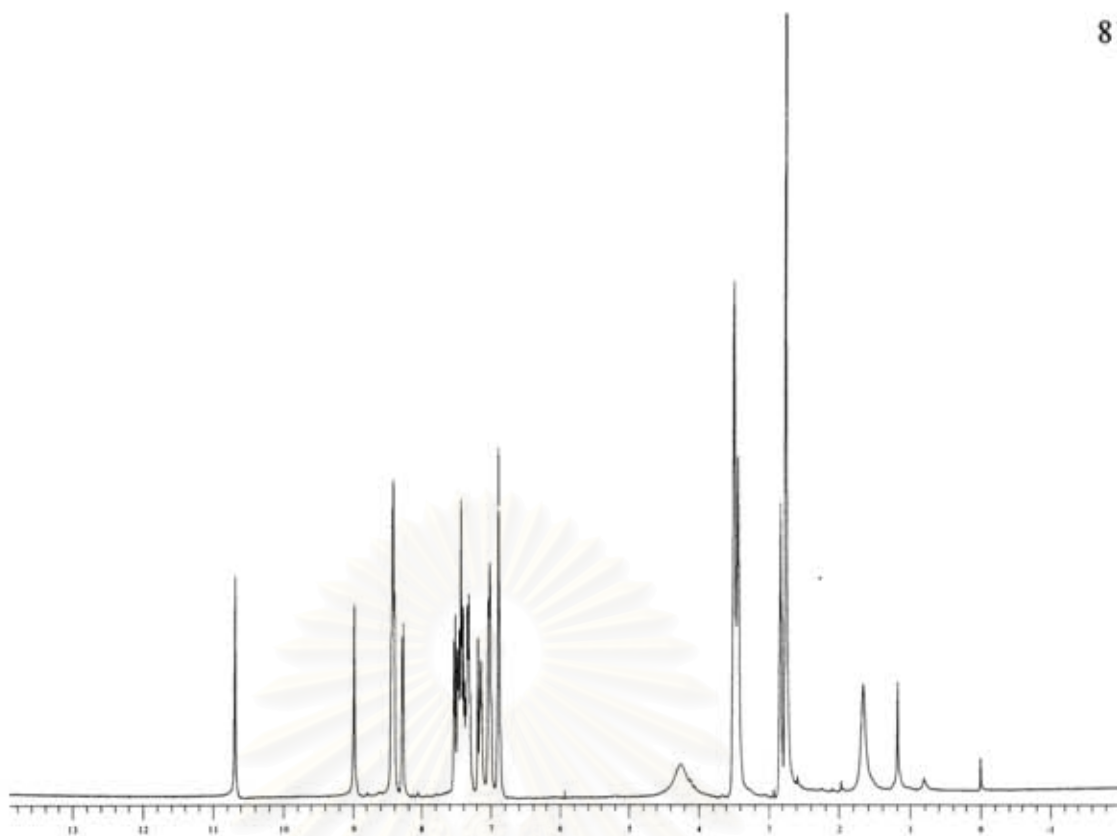


Figure A.5 The ^1H -NMR spectrum of acyclic thiacycrown ether containing imidazolium and dansyl fluorophore (L) in CDCl_3 with 400 MHz

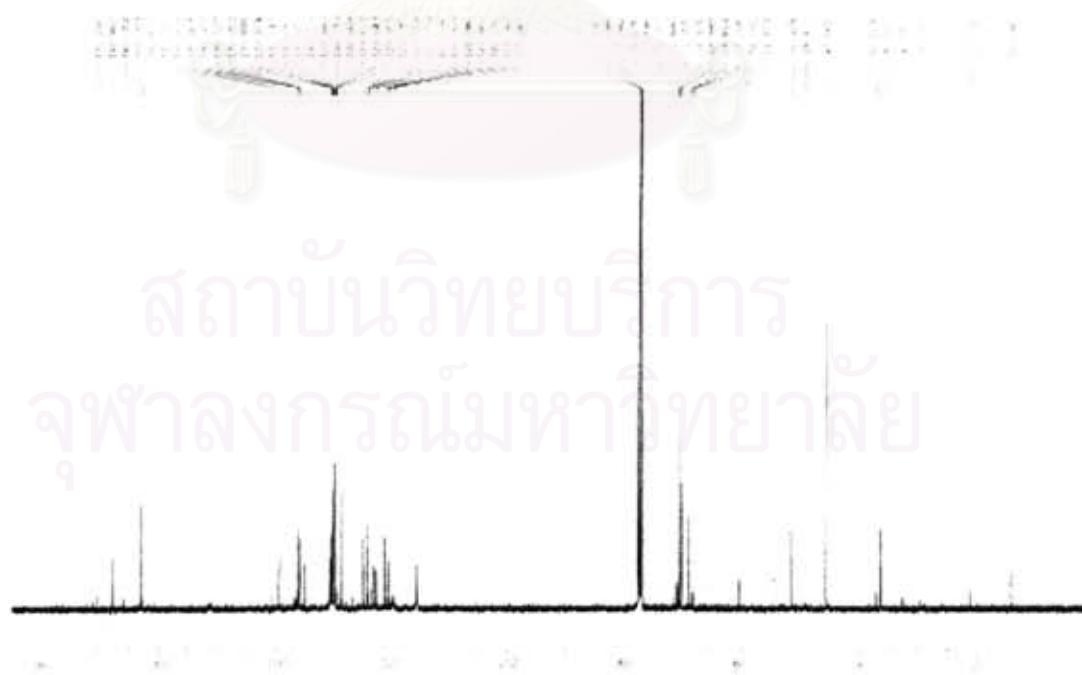


Figure A.6 The ^{13}C -NMR spectrum of acyclic thiacycrown ether containing imidazolium and dansyl fluorophore (L) in CDCl_3 with 400 MHz

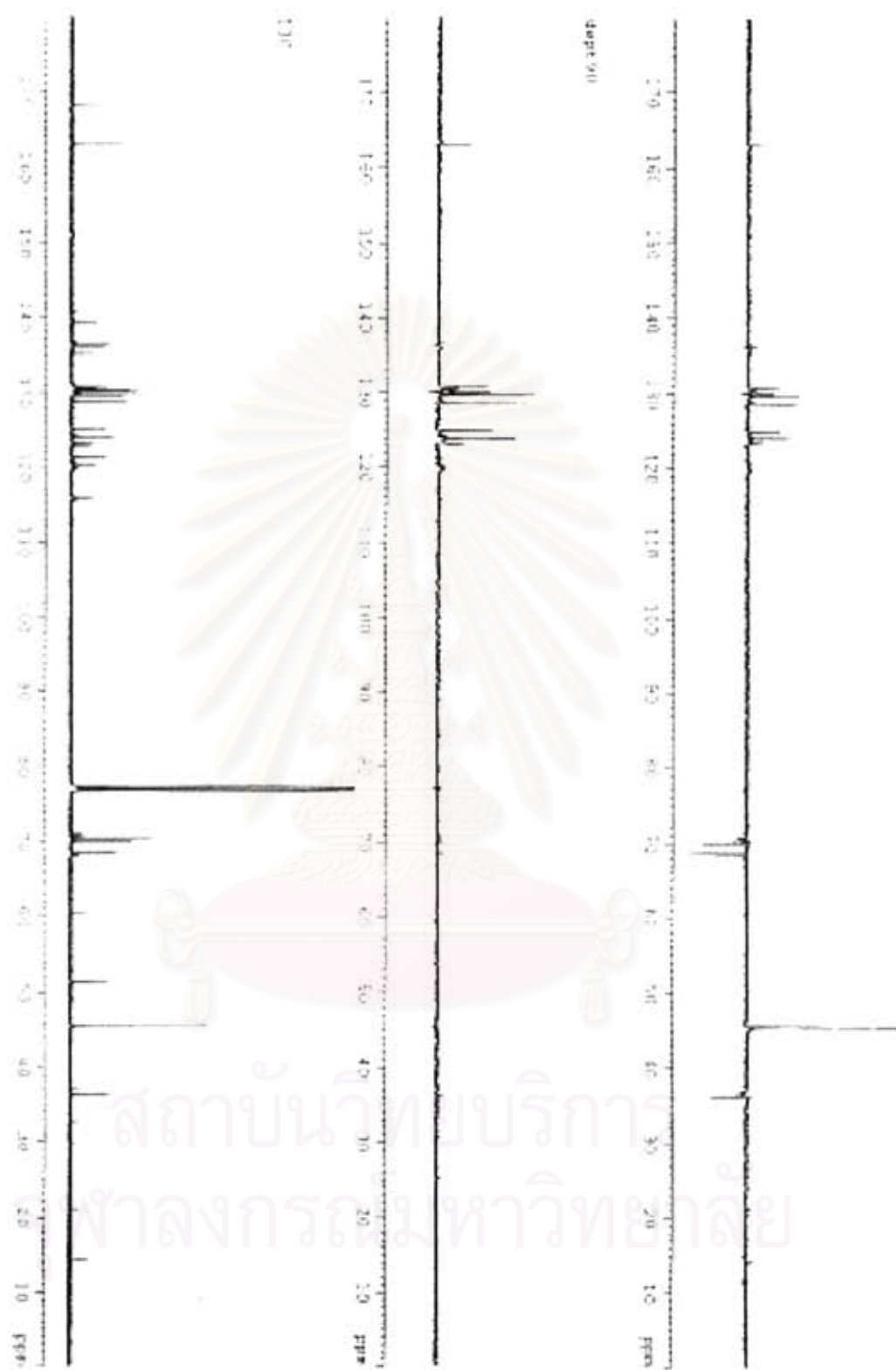


Figure A.7 DEPT 135 and DEPT 90 of acyclic thiacrown ether containing imidazolium and dansyl fluorophore (L) in CDCl₃ with 400 MHz



Figure A.8 ^1H - ^1H COSY of acyclic thiacycrown ether containing imidazolium and dansyl fluorophore (**L**) in CDCl_3 with 400 MHz

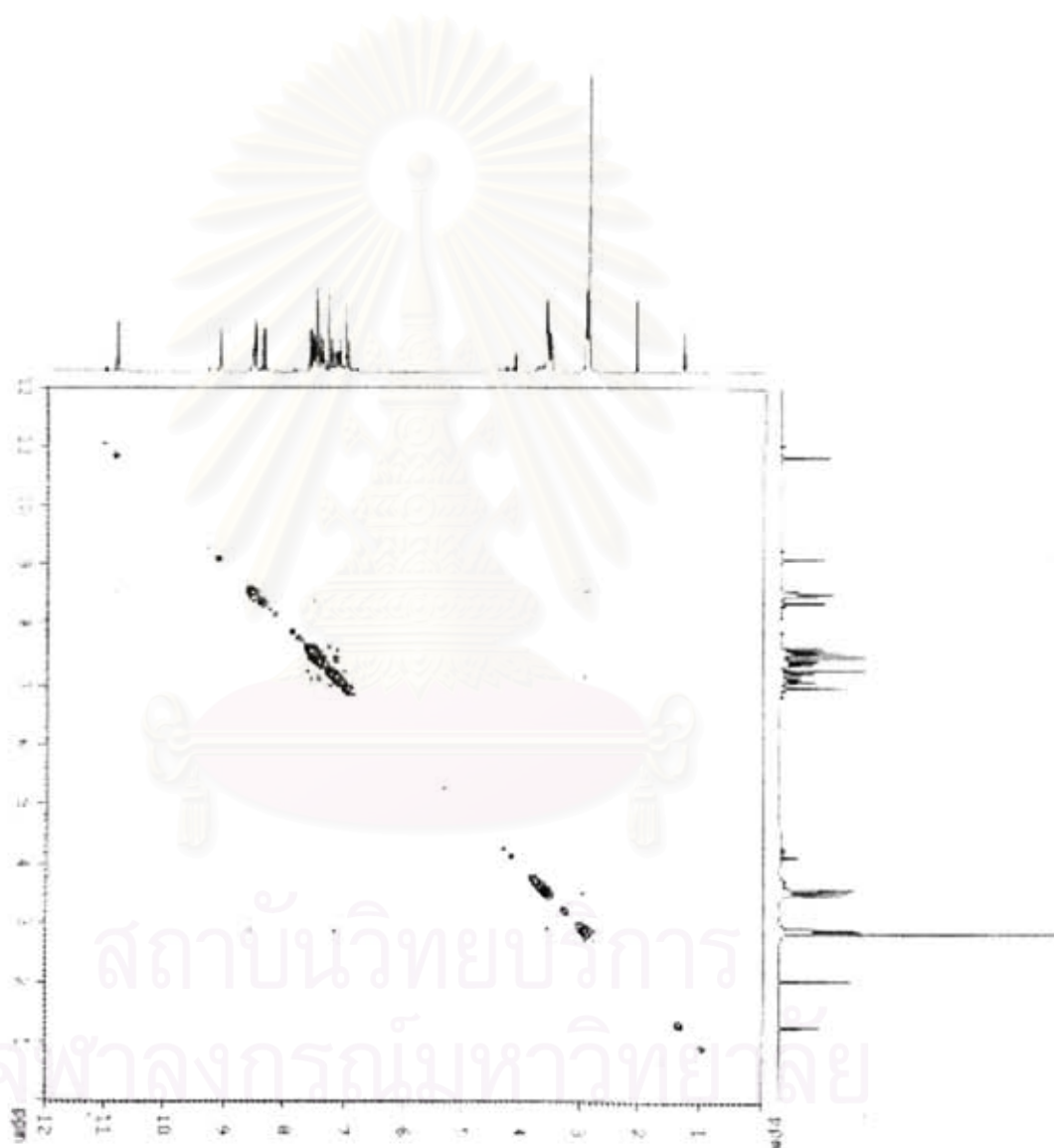


Figure A.9 ^1H - ^1H NOESY of acyclic thiacycrown ether containing imidazolium and dansyl fluorophore (L) in CDCl_3 with 400 MHz

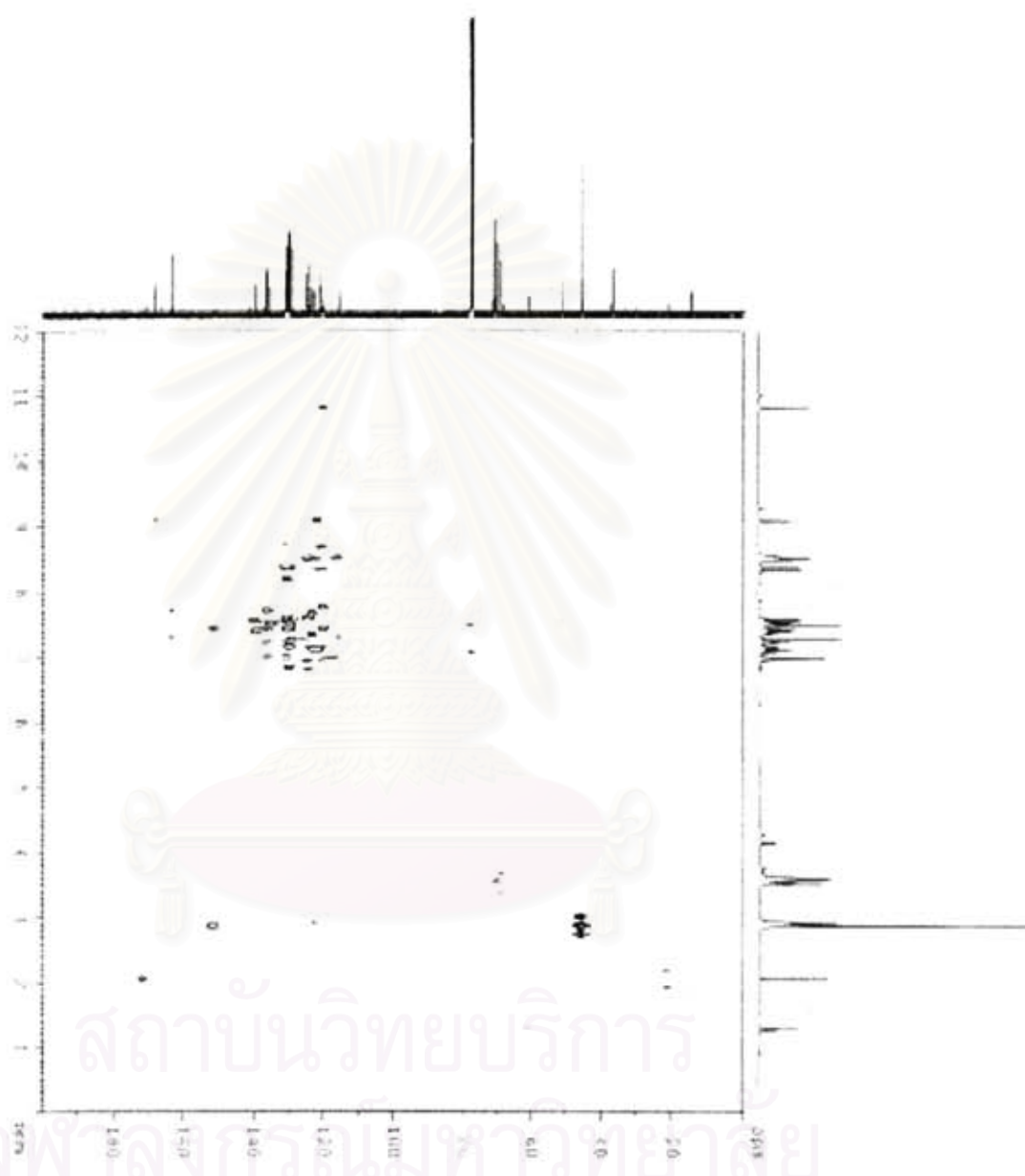


Figure A.10 HMBC of acyclic thiacrown ether containing imidazolium and dansyl fluorophore (L) in CDCl₃ with 400 MHz

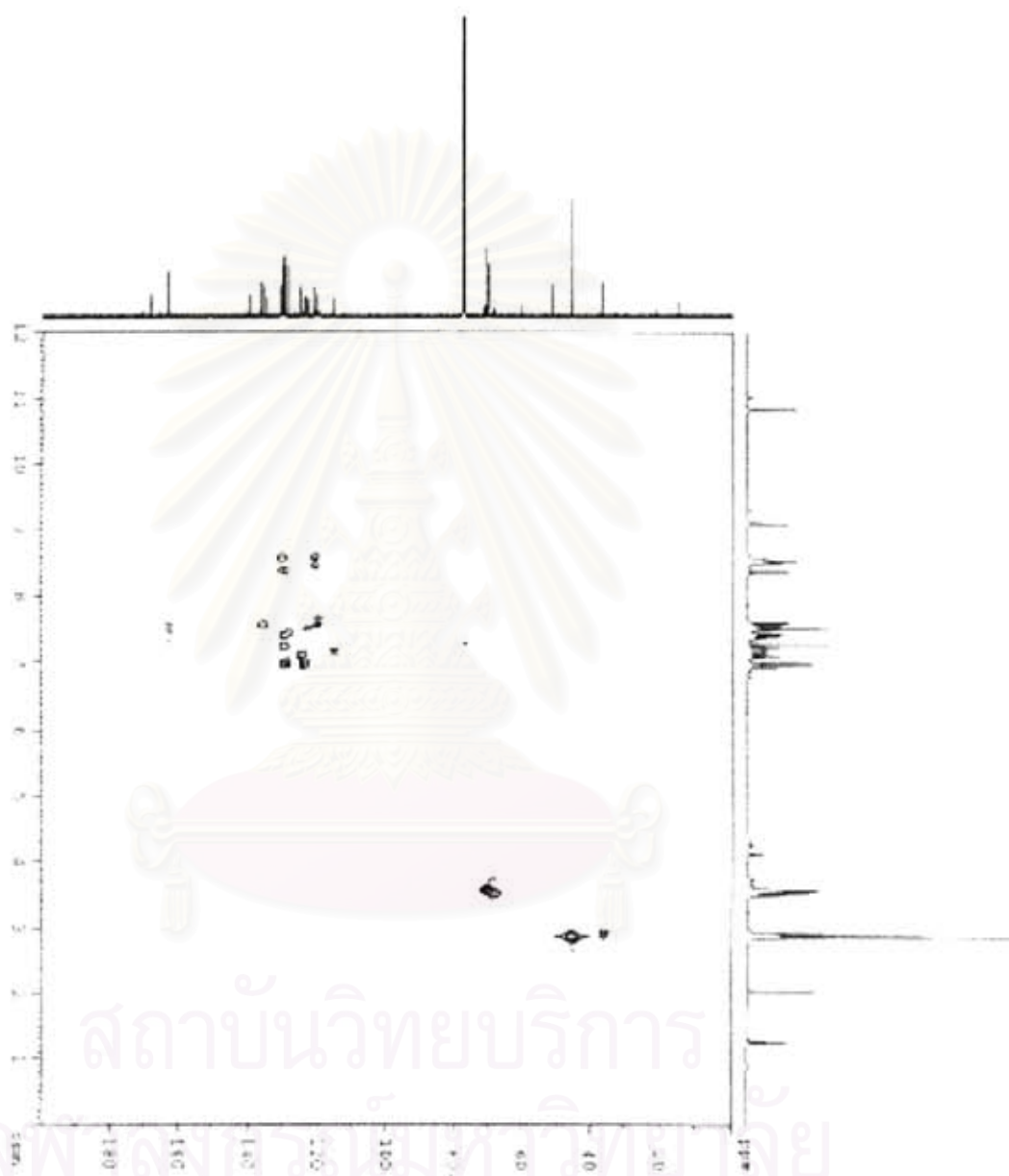


Figure A.11 HMQC of acyclic thiacrown ether containing imidazolium and dansyl fluorophore (L) in CDCl_3 with 400 MHz

Table A.1 The stability constants of ligand L towards F⁻, H₂PO₄⁻ and CH₃CO₂⁻

Titration		Intercept	slope	R ²	Log K	Average stability constant
CH ₃ CO ₂ ⁻	1	4.9590	-4.00 x 10 ⁻⁷	0.9901	7.09	7.09 ± 0.00
	2	3.6926	-3.00 x 10 ⁻⁷	0.9940	7.09	
F ⁻	1	2.5612	-4.00 x 10 ⁻⁷	0.9910	6.81	6.82 ± 0.01
	2	2.0138	-3.00 x 10 ⁻⁷	0.9913	6.83	
H ₂ PO ₄ ⁻	1	5.9235	-2.00 x 10 ⁻⁶	0.9913	6.47	6.475 ± 0.01
	2	6.1042	-2.00 x 10 ⁻⁶	0.9916	6.48	

Table A.2 The stability constants of ligand L towards Cu²⁺

Titration		Intercept	slope	R ²	Log K	Average stability constant
Cu ²⁺	1	3.5495	-5.00 x 10 ⁻⁷	0.9902	6.85	6.82 ± 0.04
	2	5.0312	-8.00 x 10 ⁻⁷	0.9923	6.79	

Table A.3 The stability constants of ligand L⁻anion towards Ag⁺

Titration		Log K L ⁻ CH ₃ CO ₂ ⁻	Log K L ⁻ F ⁻	Log K L ⁻ H ₂ PO ₄ ⁻
Ag ⁺	1	5.67	6.00	4.95
	2	5.69	5.99	4.91
		average = 5.68±0.01	average = 6.00±0.01	average = 4.93±0.03

สถาบันวิทยบริการ
จุฬาลงกรณ์มหาวิทยาลัย

VITA

Miss Sornkrit Marbumrung was born on May 3, 1980 in Nakhonratchasima, Thailand. She received her Bachelor's degree of Science in Chemistry from Kasetsart University in 2004. Since 2005, she has been a graduate student at the Department of Chemistry, Chulalongkorn University and become a member of Supramolecular Chemistry Research Unit under the supervision of Assistant Professor Dr. Boosyarat Tomapatanaget and Associate Professor Dr. Thawatchai Tuntulani. She finished her Master's degree of Science in the academic year 2006.



สถาบันวิทยบริการ
จุฬาลงกรณ์มหาวิทยาลัย